UNCLASSIFIED

AD NUMBER
ADB024249
LIMITATION CHANGES

TO:

Approved for public release; distribution is unlimited.

FROM:

Distribution authorized to U.S. Gov't. agencies only; Test and Evaluation; AUG 1977. Other requests shall be referred to Air Force Weapons Lab., Kirtland AFB, NM 87117.

AUTHORITY
AFWL ltr 29 Apr 1985

THIS PAGE IS UNCLASSIFIED

AD <u>B024249</u>

AUTHORITY: <u>AFWL 7tr, 29 Apr 85</u>

AFWL-TR-77-90

AFWL-TR-77-90

②

ADB024249

DEVELOPMENT AND EVALUATION OF A TRIAXIAL INTERFACE STRESS TRANSDUCER.

Stephen F. Pickett

University of New Mexico
Albuquerque, NM 87131

AFWL, SBIE

Aug 77

104 p.

TR-77-90,
AD-E 200 072

Final Report,

F29601-76-C-0015

Distribution limited to US Government agencies only because
of test and evaluation of military systems/equipment (Aug 77).
Other requests for this document must be referred to AFWL
(DED-I), Kirtland AFB, NM 87117.

This research was sponsored by the Defense Nuclear Agency
under Subtask L11CAX5X352, Work Unit 52, Work Unit Title:
"Development of Field Instrumentation."

Prepared for
Director
DEFENSE NUCLEAR AGENCY
Washington, DC 20305

DDC
RECEIVED
JAN 19 1978
B

AIR FORCE WEAPONS LABORATORY
Air Force Systems Command
Kirtland Air Force Base, NM 87117

256 050

AFWL-TR-77-90

This final report was prepared by the University of New Mexico, Albuquerque, New Mexico, under Contract F29601-76-C-0015, Job Order WDNS0318 with the Air Force Weapons Laboratory, Kirtland Air Force Base, New Mexico. Santos J. Ayala, (DED-I) is the Project Officer-in-Charge.

When US Government drawings, specifications, or other data are used for any purpose other than a definitely related Government procurement operation, the Government thereby incurs no responsibility nor any obligation whatsoever, the fact that the Government may have formulated, furnished, or in any way supplied the said drawings, specifications, or other data is not to be regarded by impli- cation or otherwise as in any manner licensing the holder or any other person or corporation or conveying any rights or permission to manufacture or sell any patented invention that may in any way be related thereto.

This technical report has been reviewed and is approved for publication.

SANTOS J. AYALA,
Project Officer

FOR THE COMMANDER

RUDOLPH V. MATALUCCI, Lt Col, USAF
Chief, Development Branch

FRANK J. LEECH, Lt Col, USAF
Chief, Civil Engrg Rsch Division

REPORT DOCUMENTATION PAGE		READ INSTRUCTIONS BEFORE COMPLETING FORM
1. REPORT NUMBER AFWL-TR-77-90	2. GOVT ACCESSION NO.	3. RECIPIENT'S CATALOG NUMBER
4. TITLE *(and Subtitle)* DEVELOPMENT AND EVALUATION OF A TRIAXIAL INTERFACE STRESS TRANSDUCER		5. TYPE OF REPORT & PERIOD COVERED Final Report
		6. PERFORMING ORG. REPORT NUMBER
7. AUTHOR(s) Stephen F. Pickett		8. CONTRACT OR GRANT NUMBER(s) F29601-76-C-0015
9. PERFORMING ORGANIZATION NAME AND ADDRESS University of New Mexico Albuquerque, NM 87117		10. PROGRAM ELEMENT, PROJECT, TASK AREA & WORK UNIT NUMBERS Program Element: 62710H JON: WDNS0318
11. CONTROLLING OFFICE NAME AND ADDRESS Director Defense Nuclear Agency Washington, D. C. 20305		12. REPORT DATE August 1977
		13. NUMBER OF PAGES 106
14. MONITORING AGENCY NAME & ADDRESS*(if different from Controlling Office)* Air Force Weapons Laboratory Kirtland Air Force Base, NM 87117		15. SECURITY CLASS. *(of this report)* UNCLASSIFIED
		15a. DECLASSIFICATION/DOWNGRADING SCHEDULE

16. DISTRIBUTION STATEMENT *(of this Report)*

Distribution limited to US Government agencies only because of test and evaluation of military systems/equipment (Aug 77). Other requests for this document must be referred to AFWL (DED-I), Kirtland AFB, NM 87117.

17. DISTRIBUTION STATEMENT *(of the abstract entered in Block 20, if different from Report)*

18. SUPPLEMENTARY NOTES

19. KEY WORDS *(Continue on reverse side if necessary and identify by block number)*

Stress	Interface Stress
Shear Stress	Structure/Media Interface Stress
Transducers	

20. ABSTRACT *(Continue on reverse side if necessary and identify by block number)*

A dual bending beam dynamic triaxial interface stress transducer was designed and built. Cross-axis sensitivities and unwanted input sensitivities were quite low. Both static and dynamic testing were performed to determine transducer response in an actual sand/concrete interface environment. Results showed that the shear-gage response followed the inferred shear response in trend, with outputs typically 65 percent of the inferred shear.

CONTENTS

ILLUSTRATIONS

TABLES

SECTION 1
INTRODUCTION

BACKGROUND

Shear-stress loading on certain types of structures is a very important con-
tribution to structural response and ultimate structural failure. In turn,
structural response to shear loading is an important design factor in new de-
signs for certain Air Force structures, as well as a useful analytical variable
to predict the response of existing strategic structures with regard to struc-
ture and internally housed equipment survivability.

In the past, simple Coulomb friction models were used in structural response
codes which yielded or inferred predictions for structure/media interface shear
loading based on interface friction coefficients, normal stress, and structure/
media relative motions. Simple static tests were used to determine friction
coefficients for structure/media interfaces of interest; however, actual dy-
namic testing indicated that the model was entirely inadequate. Typical fric-
tion coefficients were found to be in the neighborhood of 0.5, based on static
laboratory testing; however, results from actual testing indicated that fric-
tion coefficients of about 0.05 were required to bring the Coulomb friction
model into the realm of actual loading. Because of this discrepancy a new,
extremely complex, shear-loading code was developed to better predict the in-
terface shear-loading contribution to structural response (ref. 1).

In order to determine the adequacy of the new code and to find what code changes
were necessary in analytical predictions, an actual measurement of dynamic shear
stress was needed and thus the requirement for a shear-stress transducer was es-
tablished. Although transducers for static shear stress were available, there
appeared to be none with dynamic capabilities--in particular, insensitivity to

---

1. Huck, Peter J., et al., *Dynamic Response of Soil/Concrete Interfaces at
   High Pressure*, AFWL-TR-73-264, Air Force Weapons Laboratory, Kirtland Air
   Force Base, New Mexico, April 1974.

acceleration. With such a device, electrical analogs of shear stress at selected points of interest on structure/media interfaces could be obtained. As with other types of measurements, i.e., velocity, acceleration, displacement, blast pressure, soil stress, and interface normal stress, data from actual testing of numerous structure/media interface configurations could be used to refine and perfect the analytical prediction codes.

An interface shear gage was developed and partially evaluated. The gage was fielded in the HARD PAN I Test Series[*] with apparent success and evaluated in the laboratory to check case sensitivity, axis interaction, dynamic acceleration sensitivity, and ring frequency. A static calibration fixture was developed and is in use, but to insure confidence in the data obtained, a dynamic calibration fixture and method were developed and used for evaluation.

OBJECTIVE

The objective of this research effort was to continue the evaluation of the interface shear gage developed previously. This transducer was originally designed to measure two orthogonal shear-stress vectors in the structure/media interface plane; however, a later modification allowed the basic primary element to be used for normal stress; thus, the transducer provides a measurement of three mutually orthogonal dynamic stress vector time histories. Target objectives included the following:

(1)	Range	2000-psi shear stress (two axes) 3000-psi normal stress (one axis)
(2)	Useable Frequency Range	dc to 500 Hz or higher
(3)	Mounting Requirements	3-in. thick wall or greater (gage may protrude into interior structure)
(4)	Shear-Axis Sensitivity to Normal Stress	No greater than 5 percent apparent shear stress at 1000-psi normal stress
(5)	Normal-Axis Sensitivity to Shear Stress	No greater than 5 percent apparent normal stress at 1000-psi shear stress
(6)	Acceleration Sensitivity (all axes)	Shear: 0.02 psi/g or better Normal: 0.03 psi/g or better

---

[*] The Hard Pan Test Series was composed of structure/media interaction test events conducted by the Air Force Weapons Laboratory (AFWL) at Trading Post, Kansas.

(7) The force-collecting surface of the
     transducer shall be 1 in. in diameter
     and shall be textured to match as
     nearly as possible the coefficient
     of friction of the structure.

In addition to these design and specification objectives, the following exper-
imental and analytical objectives were undertaken:

(1) Determine stress sensitivities and develop a
     calibration procedure.

(2) Determine unwanted input sensitivities experimentally.

(3) Conduct both static and dynamic shear tests in a
     true structure/sand interface condition.

(4) Provide manufacturing drawings, performance data,
     calibration and installation instructions and data
     interpretation instructions to AFWL for production
     and utilization of the transducer.

(5) Investigate data-processing methods to provide for fre-
     quency response and cross-axis sensitivity corrections.

SCOPE

After initial conception of a bending-beam, shear-stress transducer, dynamic
requirements were studied and a design for a modified dual bending-beam stress
transducer was modeled to determine transducer shear-stress response, as well
as sensitivities to unwanted inputs. Although the model was highly idealized,
it did appear that unwanted sensitivities would be low enough to make the de-
sign practical. A prototype transducer was then built.

A calibration device was built, and the transducer was tested for scale factor,
linearity, and unwanted sensitivities.

A shear test fixture, as well as an alternate shear measuring technique, was
designed, developed, and modified to allow both static and dynamic shear tests
to be performed, and comparisons were made between the transducer output and
the inferred shear output.

5

SECTION 2
PRINCIPLE OF OPERATION

To meet the initial requirements of a single axis of shear measurement, it was determined that a bending beam properly strain-gaged with a force-collecting surface flush with the structure would respond linearly to applied shear stress.

When a vertical shear stress, σ_s, is applied to the effective force-collecting area, A, a load, $\sigma_s A$, is applied to the free end of the cantilever beam. The resulting bending moment at points a and a' (fig. 1) is (assuming simplified beam theory)

$$M_x = \sigma_s A(\ell-x)$$

where

M_x = bending moment

ℓ = total length of beam

x = distance from fixed end of beam to points a and a'

and the strain at points a and a' is

$$\xi_{a,a'} = \frac{\pm\sigma_s A(\ell-x)c}{EI}$$

where c is the distance from the neutral axis to the surface of the beam at points a and a'. Thus, $\xi_{a,a'}$ is linearly proportional to σ_s when σ_s is the only applied force on the transducer. Unfortunately, for this simple design, vertical shear stress will not be the only force input in field situations in which a vertical shear stress analog is required; the following inputs will also contribute to the strain at points a and a':

(1) normal (axial) stress

(2) horizontal shear stress[*]

(3) horizontal acceleration[*]

(4) vertical acceleration

(5) axial acceleration

(6) angular acceleration

---

[*] Ideally, horizontal shear stress and acceleration will not affect $\xi_{a,a'}$ if a and a' are on the horizontal bending neutral axis.
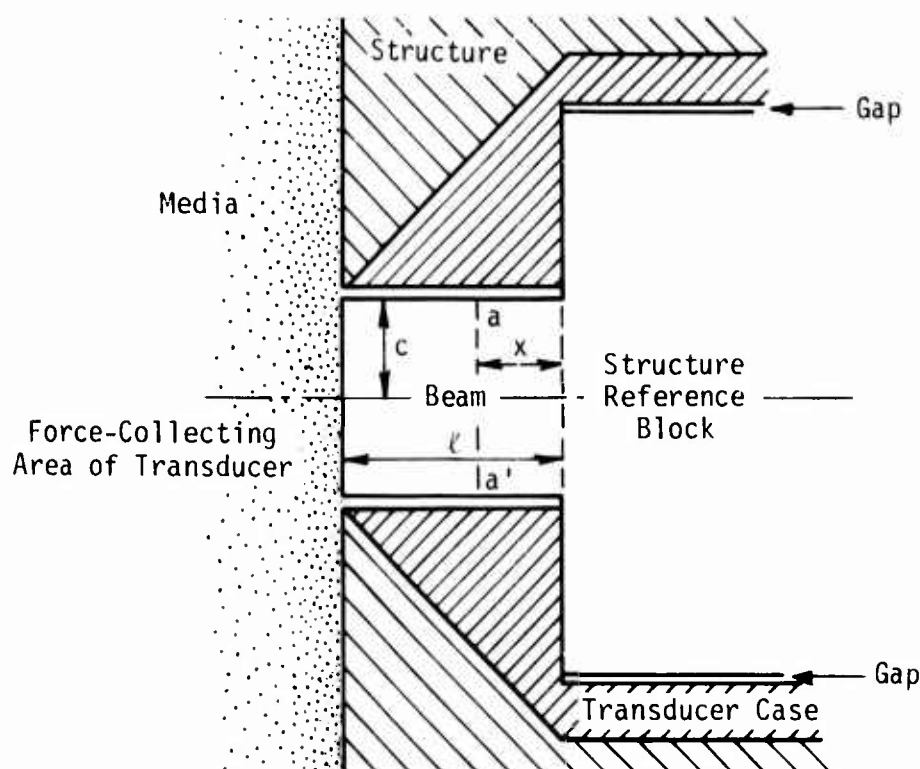
Figure 1. Basic Shear-Stress Transducer Beam

By adding a dummy beam as shown in figure 2 and properly interconnecting strain gages, these effects, except angular acceleration, can be effectively cancelled. With P-type piezoresistive strain gages located at points a, a', b, and b', a voltage analog of shear stress is produced by the circuit shown in figure 3.

When the primary element experiences downward vertical acceleration, $R_{a'}$ and $R_{b'}$ increase the resistance equally, while R_b and R_a decrease the resistance equally; thus, bridge balance is maintained. When horizontal acceleration is experienced in the major axis of the primary element, R_a and $R_{a'}$ increase the resistance equally, while R_b and $R_{b'}$ decrease the resistance equally, and again bridge balance is maintained. If normal stress is experienced, R_b and $R_{b'}$ do not change, while R_a and $R_{a'}$ decrease equally and thus cause no bridge upset. Horizontal shear stress and acceleration in the horizontal shear-stress axis cause little or no change in any of the gage resistances if the gages are properly located on the neutral axis of the beam. The horizontal shear axis is gaged in the same manner as the vertical axis, and it performs in the same manner. The normal-stress axis presently uses only the active beam gaged as
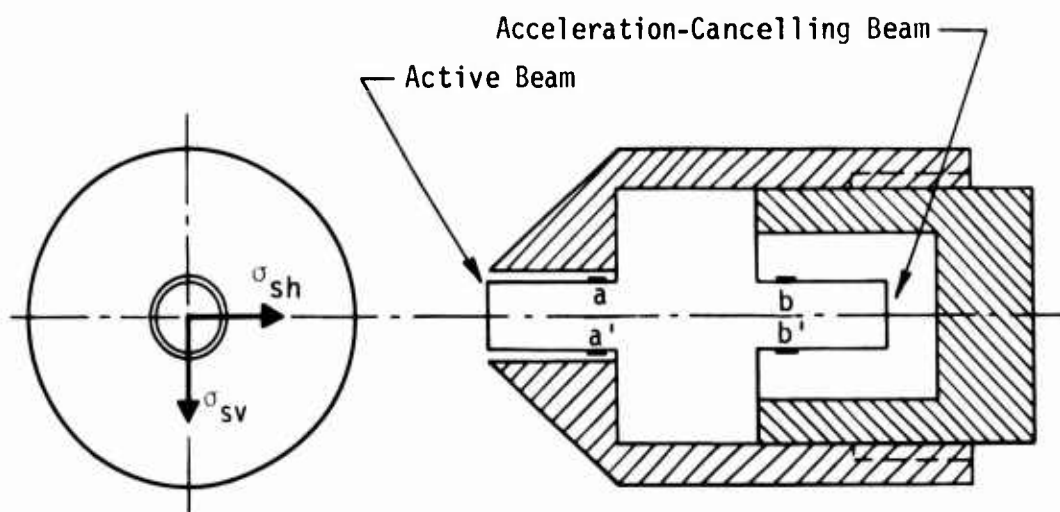
7

Figure 2.   Total Primary Element Showing Active and
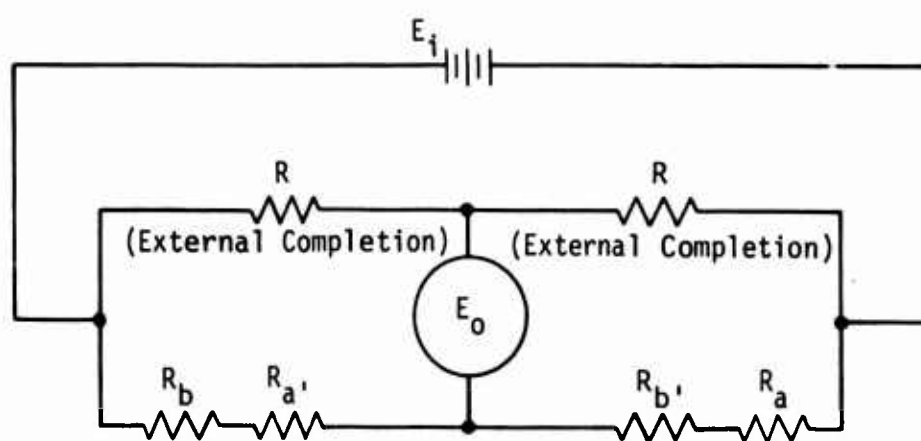Acceleration-Cancelling Beams

Figure 3.   Electrical Circuit for Shear-Axis Bridge

a load cell much like the WAM gage (ref. 2). (Although this normal-stress bridge appears to perform well, it is felt that substantial improvement can be made by using both beams to eliminate acceleration sensitivity.) With these three independent bridges, the primary element of the dual beam is capable of providing voltage analogs of three mutually orthogonal interface stress vectors.

2. Pickett, Stephen F., *Development and Evaluation of Measurement Systems for Blast-Induced Motions in Buried Structures*, AFWL-TR-73-230, Air Force Weapons Laboratory, Kirtland Air Force Base, New Mexico, April 1974.

9

SECTION 3
DEVELOPMENT

INITIAL DESIGN

Three initial design triaxial stress transducers (fig. 4) were built. These transducers demonstrated that the shear-stress axes outputs were indeed linear with beam bending moment equivalent to 2000 psi shear on the force-collecting area and that cross-axis sensitivity was low. However, this transducer exhibited an extremely low tympanic resonance of 1100 to 1200 Hz because of the disk-like collecting elements which were used to match the overall beam stiffness with concrete stiffness.

INTERMEDIATE DESIGN

The second triaxial stress transducer of which six were built is shown in figure 5. This design incorporated a significant size reduction and the elimination of the disk collectors; the latter change provided a uniform cross-sectional area along the full length of the beams.

Initial testing of this transducer established that all three axes were linear with very little cross-axis sensitivity. In addition acceleration sensitivities were very low. Because of its size, this transducer was easy to handle and install compared to the initial transducer. While this transducer was being evaluated for unwanted sensitivity, careful attention was focused on the size of the force-collecting area. Although it was agreed by the Civil Engineering Research Facility (CERF), AFWL, and AFWL consultants that the small size and the maneuverability in field installation were desirable features, it was felt by some that the force-collecting area should be increased in order to minimize anomalies caused by large particles of media. Although not all were in agreement on this, the concensus opinion was that it would be better to have a 1-in. diameter beam to increase the force-collecting area by 300 percent. All agreed that the 1-in. diameter would not be harmful, and thus the requirement for a third design was established.
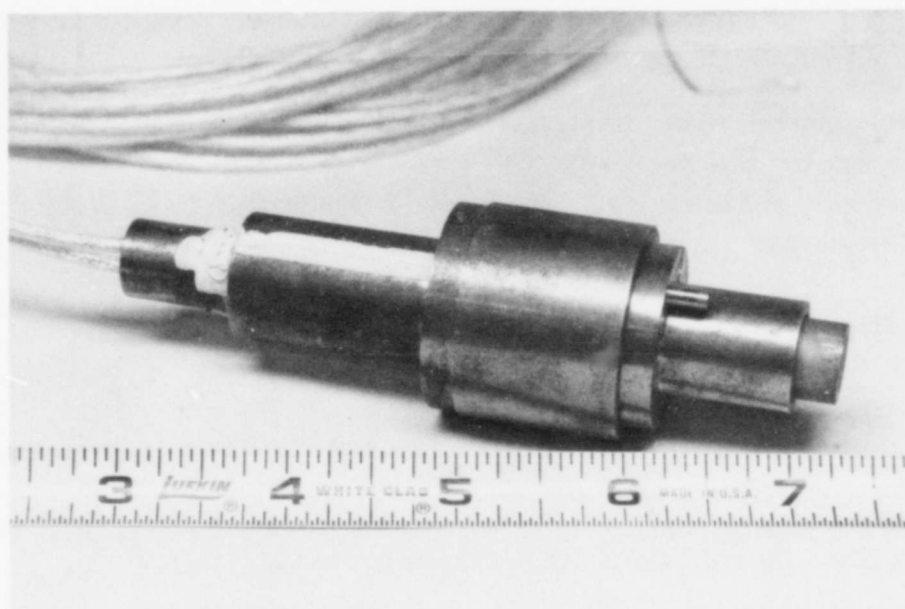
Figure 4.   Initial Triaxial Stress Transducer

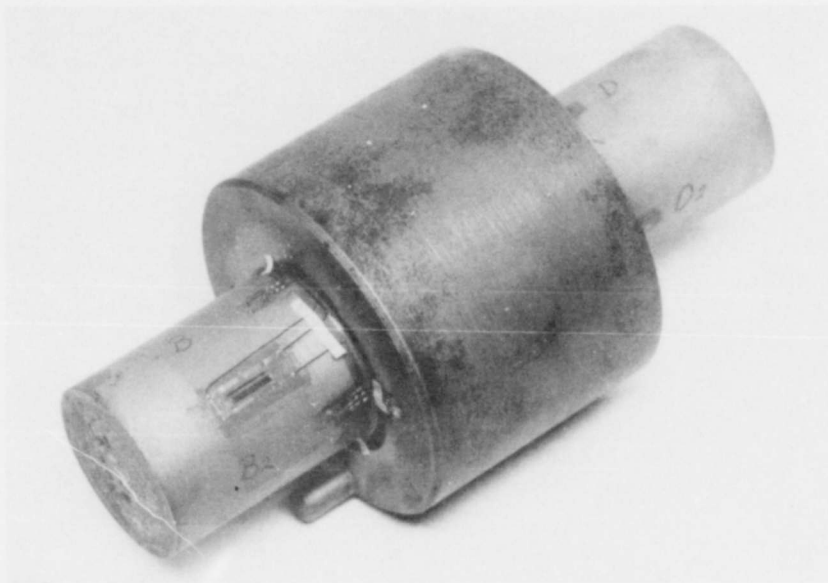Figure 5.   Intermediate Triaxial Stress Transducer

11

Figure 6. Final Triaxial Stress Transducer (Primary Element)

FINAL DESIGN

The final triaxial stress transducer developed is shown in figure 6. Engineer-
ing drawings for this transducer are contained in appendix A. All transducer
parts are made of Ledloy 130, although any suitable steel could probably be
used. Assembly of the transducer is covered in detail in appendix B.

Description

The primary element is made from a single piece of cylindrical stock. The two
opposing beams are separated by a 2-in. diameter, 1.5-in. thick structure refer-
ence block, which has a dowel pin on the active beam side for axial alignment
purposes and four threaded holes on the dummy beam side for attachment of the
protection sleeve. Two holes through the reference block allow passage for
the interconnecting wires between the active- and dummy-side strain gages.

The normal-axis gages are Kulite Type M(9) E-GP350-500 with a gage factor of 265 $\pm$ 5 percent and a resistance of 350 Ω $\pm$ 2 percent at 75°F. These gages are centered 0.650 in. from the end of the beam. The shear-axes gages are Kulite Type PEP350-090 with a gage factor of 130 $\pm$ 5 percent and a resistance of 350 Ω $\pm$ 2 percent at 75°F and are centered 1 in. from the end of the beam.

The sleeve provides a protective housing for the dummy beam as well as a termination point for internal circuitry attachment to external cables. It is attached to the primary element by four 4-40 screws.

The lock is used to secure the primary element in the case. (See appendix C.) Lead wires exit through a hole in the center of the lock and into the inside of the structure.

The case is a hollow cylinder tapered at the end and it must be placed in the structure form before the concrete is poured. (See appendix C.) Three 1/2-in. diameter 20 UNF tapped holes are located around the base for insertion of bolt-type concrete anchors. A dowel pin hole in the case mates with the dowel pin on the primary element to ensure desired case/sensitive-axis alignment.

Strain Gage Location

Since strain-gage location is important in order to achieve the desired balancing effect, a special device for correctly locating the gages was built (appendix B). From the equation in section 2 it is easy to see the effects of errors in locating the strain gages. The ℓ-x term by design should be 1.00 in.; this leaves 0.250 in. between the center of the strain gage and the supported end of the beam. This was felt to be necessary in order to avoid the unpredictable boundary strain effects near the supported end of the beam. If ℓ-x varies between the active and dummy beams, an undesired strain differential occurs and acceleration cancellation is jeopardized. Variation of the nominal resistance of the strain gage and of the gage factor also affects acceleration cancellation, but there is no way to control these variations.

Material Geometry

As indicated in the engineering drawings (appendix A) there is a number of tight tolerances on the primary element. This is to insure a good match between beam deflections (active and dummy) during shear-axes accelerations.

Calculated Sensitivities

With a simplified mathematical model of the primary element, various combinations of wanted and unwanted sensitivities were evaluated for unwanted sensitivity output contributions. These effects were found to be less than 1 percent of the true applied shear at combined unwanted input levels of 2000g acceleration, 2000-psi normal stress, and 2000-psi cross-axis shear stress. Based on this, it was felt that this design would have an excellent chance of meeting the unwanted sensitivity specification requirements.

The unwanted sensitivities appeared to be low for both a full-bridge and a half-bridge arrangement for shear, but the half bridge was slightly favored. The only possible problem with the half-bridge system is that the higher transducer source impedance could reduce the upper frequency response limits of the total system to an unacceptably low level when long lines are used.

Surface Texture Matching

Rather than determine static and dynamic coefficients of friction for both a Ledloy 130/sand interface and a typical structure/sand interface, a texturing scheme was devised to make the transducer active surface of concrete, except for a necessary small retaining annulus.

Several texture-retaining designs were tested with applied soil-stress (20-40 dry Ottawa sand) levels to 8000 psi and applied beam g-levels to 10,000g to determine which design would maintain the best surface integrity under these conditions. All designs appeared to work very well; however, the design chosen exhibited virtually no texture shrinkage (permanent compression) with the 8000-psi, soil-stress load.

14

A cup was cut in each end of the beam and four threaded holes were made in the bottom of each cup to allow 6-32 screws to be used as reinforcement for an epoxy/grout mix which was placed in the cups. (See primary element drawing in appendix A and texturing procedures in appendix B.)

The concrete insert material was Embeco 630 nonshrink grout with Epocast 530 epoxy and 9816 hardener. This was placed on both the active and dummy beam in an effort to maintain beam balance.

SECTION 4
CALIBRATION

A modified case mounted on pillow blocks (fig. 7) was used to calibrate the transducer. With this device, a known bending moment could be applied to each of the shear axes by a calibrated kip machine. To calibrate the normal axis, the encased primary element was removed and repositioned for kip machine loading in the normal axis only.

Although the calibration device worked well and showed that the shear axes outputs were linear with applied moment and that the normal axis output was linear with applied load, it was decided to test the load sensitivity of the case by applying a kip machine load to the case; i.e., the case was squeezed. At load levels up to 50 kips, the transducer outputs were 154 psi equivalent shear stress (worst case) and 187 psi equivalent normal stress (worst case). These were considered to be unreasonably high; the cause was not determined. However, after increasing the clearance between the structure reference block and the case (fig. 1), the problem cleared up (21 psi equivalent shear stress, worst case; 47 psi equivalent normal stress, worst case). Three separate primary elements were tested in each of three cases both before and after this modification.
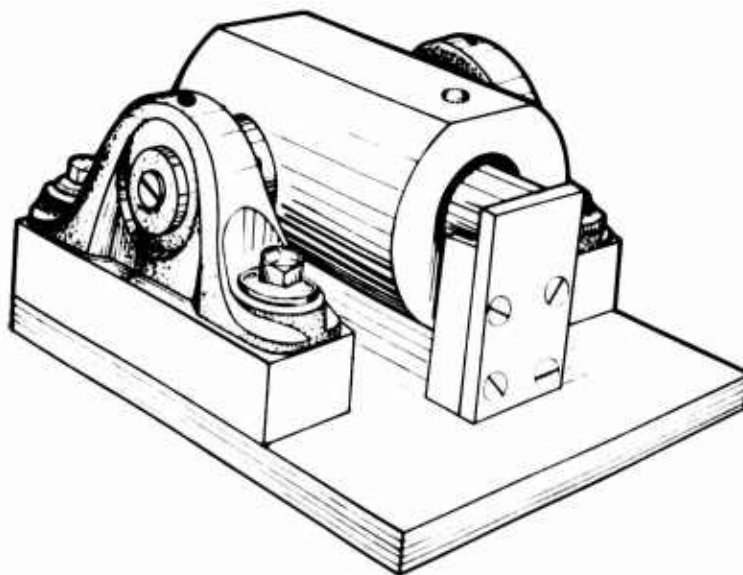
Figure 7. Calibration Fixture

16

SECTION 5
LABORATORY TESTING

CROSS-AXIS STRESS SENSITIVITY

Cross-axis stress sensitivities were evaluated in the calibration fixture
(fig. 7). Three transducers were used in this test series, and the following
tests were performed on each unit:

(1) A bending moment equivalent to a 2000-psi shear stress
      was applied to the vertical shear-stress axis and the
      outputs of the two remaining stress axes were monitored.

(2) A bending moment equivalent to a 2000-psi shear stress
      was applied to the horizontal shear-stress axis and the
      outputs of the two remaining stress axes were monitored.

(3) A normal load equivalent to a 2000-psi normal stress was
      applied to the normal axis, and the outputs of the two
      remaining stress axes were monitored.

Cross-axis normal loading resulted in 31.6- to 62.15-psi equivalent shear
stress (1.5 to 3.1 percent of cross-axis loading). Cross-axis shear loading
resulted in 14.7- to 57.6-psi equivalent shear stress on the unloaded shear
axis (0.7 to 2.88 percent of cross-axis loading) and 200- to 320-psi equivalent
normal stress (10 to 16 percent of cross-axis loading).

Shear-axis sensitivities were well within the desired specifications; however,
the normal-axis sensitivities were extremely high. Before speculating on the
cause of this, it should be pointed out that a number of the triaxial trans-
ducers built for the HARD PAN Events were tested in this same manner and the
results from these tests showed that the normal axis was consistently less
cross-axis stress sensitive than the shear axes. These data were not logged
or recorded nor was it required for the HARD PAN Events. The tests were per-
formed merely from curiosity and were easy to do during the normal calibration
procedure; i.e., while the axis calibrated was being plotted on an X-Y record-
er, millivolt outputs of the other two conditioned axes were monitored. Of
eight transducers monitored in this fashion, all but one exhibited about the

17

same shear-axis response to cross-axis loading as found during cross-axis testing of the three experimental transducers. The remaining transducer exhibited virtually no cross-axis sensitivity on one shear axis with applied normal loading. For all eight transducers, normal-axis sensitivity to shear loading was in the range of 30 to 70 percent of the shear-axis sensitivity to cross-axis shear loading.

After the transducers were built for HARD PAN, it was decided jointly by CERF and AFWL to build and test three new prototypes employing the same features used on the HARD PAN transducers (primarily changes in the glass backing used on the shear-axis strain gages to reduce hysteresis). Three older prototypes had previously been tested for unwanted input sensitivities only.

There was an adequate supply of shear-axis strain gages left after satisfying HARD PAN requirements; however, the available normal-axis strain gages were not considered to be of high quality, primarily because of matrix skew (fig. 8). These gages were used anyway, and this could well be the reason for the poor normal-axis performance in cross-axis stress and acceleration sensitivity, linearity, and repeatability.

Figure 8. Typical Normal-Axis Strain Gages Used in
Prototype Transducers

ACCELERATION SENSITIVITY

The three prototype transducers were evaluated for stress-axis acceleration
sensitivity. In this experiment, the CERF drop tower was used to impart inputs
of 225 to 3300 g to all three transducer axes. The transducer case, containing
the transducer, was placed on top of two layers of blotter pad which rested on
the dropping mass platform. The case was fastened in place with bookbinder's
tape and the entire drop platform was raised approximately 30 in. for 2200g to
3000g drops. After being released and dropping the 30 in., the drop platform
was arrested by the drop table. Four 4 by 4 in. precompressed styrofoam pads
were used to cushion the drop and tailor the acceleration pulse. The condi-
tioned stress outputs, as well as an acceleration output from an Endevco 2264-
5000 accelerometer (used to sense vertical acceleration), were amplified through
Astrodata 141 amplifiers and recorded on an Ampex CP100 tape deck running at
60 in/sec. Wideband FM recording was used (108 kHz center frequency ± 40 per-
cent deviation with 20 kHz response). Results are shown in table 1.

The wide variance in g drop levels occurred because of difficulties in restrain-
ing angular acceleration and because many of the acceleration inputs contained
significant energy at and above the transducer resonant frequency (12 kHz). In
an effort to minimize these effects numerous drops at various g-levels were
made. In spite of these efforts there were still some sensitivity contribu-
tions from ringing and angular acceleration.

STATIC-SHEAR SENSITIVITY

In order to check the shear response of the transducer in an actual shear envi-
ronment a special fixture which allowed the transducer to be subjected to both
static and dynamic vertical shear-stress inputs was built (fig. 9). Included in
this fixture was a means of inferring vertical shear stresses. This inferred
shear was necessary to evaluate the shear response of the transducer. The central
part of this fixture is cylindrical with a 6-in. diameter and consists of the
cased transducer embedded in a 6-in. diameter by 6-in. long concrete cylinder.
Load cells at the top and bottom of the concrete cylinder separate the sample
cylinder from the metal cylinder extensions. A surgical rubber tubular bladder

19

Table 1. Acceleration Sensitivity Test Data

	Vertical Shear-Axis Drop	Horizontal Shear-Axis Drop	Normal-Axis Drop
Transducer SN 07			
g-Level, g	528	3300*	1221
Vertical Shear Sensitivity, psi/g	0.01388	0.085	0.030
Horizontal Shear Sensitivity, psi/g	0.01440	0.0809	0.0417
Normal Sensitivity, psi/g	0.120	0.2033	0.2444
Transducer SN 08			
g-Level, g	226	265	396
Vertical Shear Sensitivity, psi/g	0.0196	0.010	0.0089
Horizontal Shear Sensitivity, psi/g	0.00787	0.02518	0.01123
Normal Sensitivity, psi/g	0.01962	0.150	0.02239
Transducer SN 16			
g-Level, g	3080**	396	409
Vertical Shear Sensitivity, psi/g	0.098	0.000	0.0223
Horizontal Shear Sensitivity, psi/g	0.032	0.0059	0.0113
Normal Sensitivity, psi/g	0.119	0.0297	0.0793

*Discontinuities in output noted.
**Acceleration had extremely fast rise time and a large level of high-frequency ringing.

20
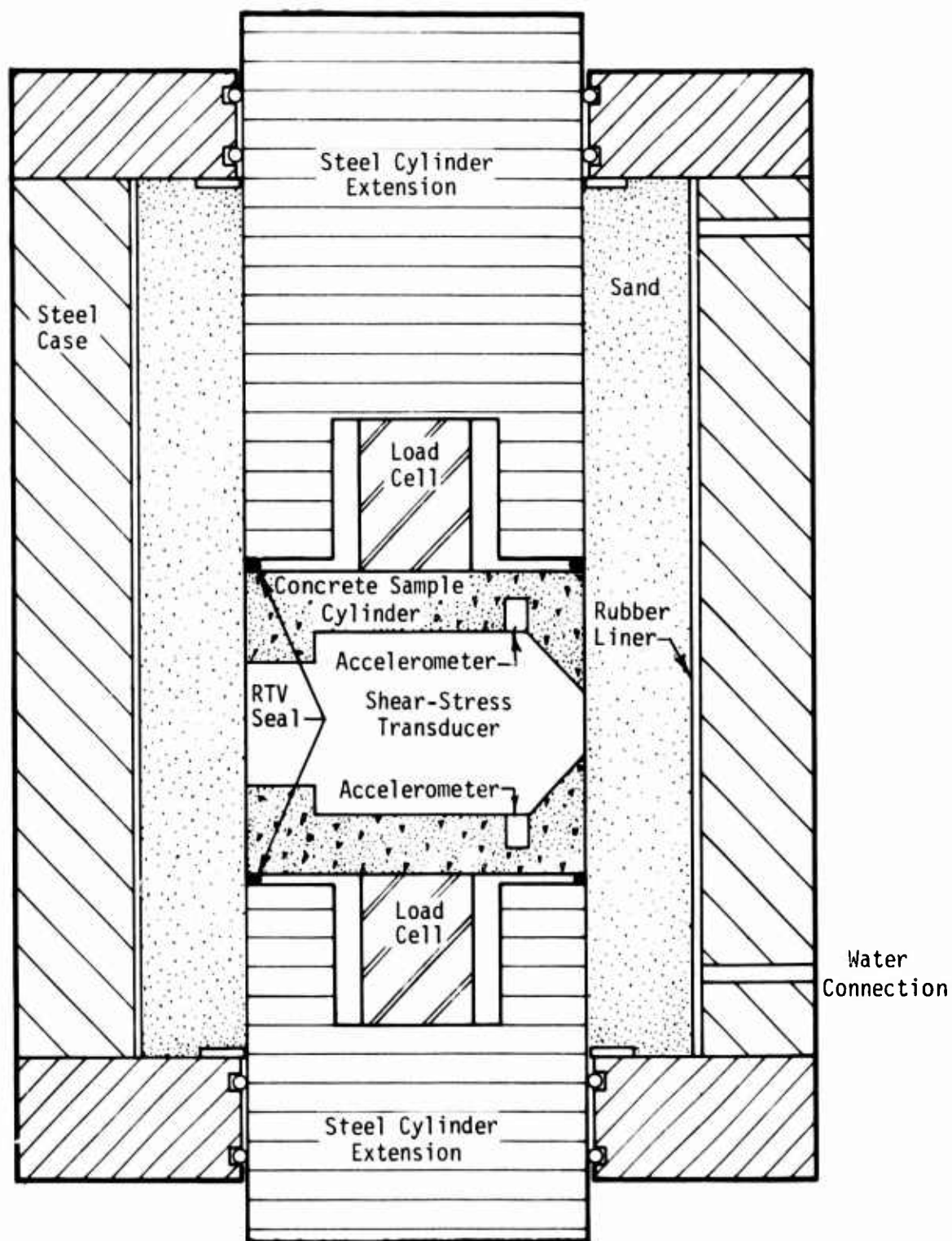
Figure 9. Shear-Stress Test Fixture

is used in conjunction with a hydraulic pump to establish a normal stress
through 20-40 Ottawa sand against the central cylinder. Vertical load may
then be placed on the upper portion of the central cylinder to create ver-
tical shear stress on the sample interface surface.

This fixture is similar to the shear fixture used by Leonards (ref. 3) except
that external pressure is applied to the outside of the bladder as opposed to
evacuating the inside of the bladder. This allows higher normal interface
stresses to be imparted to the sample. Two accelerometers are mounted--one
above and one redundant accelerometer below the transducer case (fig. 10) in
the concrete sample section (fig. 11). The acceleration measurement when
scaled and summed properly with the load cell measurements are used to infer
average shear stress on the sample. The following force-balance equations
are employed:

$$F = ma$$

$$ma = F_u - F_L - F_s$$

or

$$F_s = F_u - F_L - ma$$

where

F_s = total shear force on concrete sample

F_u = upper load cell force

F_L = lower load cell force

 m = mass of sample

 a = acceleration of sample

Dividing both sides of the latter equation by the interface surface area of the
sample, A, gives

$$\frac{F_s}{A} = \sigma_s = \frac{F_u - F_L - ma}{A}$$

Thus, the average shear stress on the sample is inferred by the algebraic
weighted sum of the upper and lower load cell forces and sample acceleration.

---

3. Leonards, G. A., *Experimental Study of Static and Dynamic Friction Between
    Soil and Typical Construction Materials*, AFWL-TR-65-161, Air Force Weapons
    Laboratory, Kirtland Air Force Base, New Mexico, December 1965.
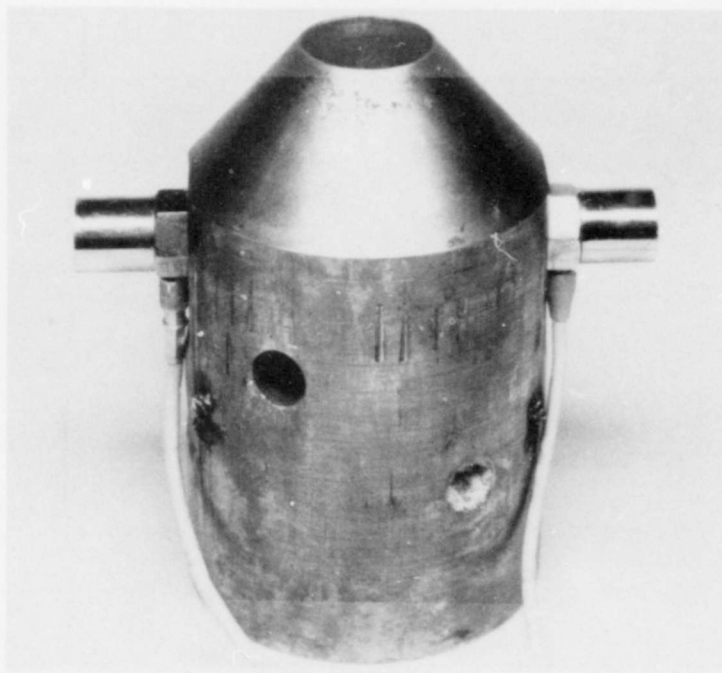
Figure 10. Transducer Case with Mounted Accelerometers

The following assumption must be made in order to use these data to evaluate shear-stress performance: the σ_s inferred by the three fixture transducers is the same as the σ_s encountered on the active surface of the transducer. There are a number of reasons why this may not be true:

(1) Differential load cell readings are subject to large common mode errors unless the lower load cell output is very nearly zero. For example, if the upper load is actually only 5 percent higher than the lower load and both cells are accurate to ± 5 percent of the reading, measured load differential is

$$F_u - F_L = [1.05(1 \pm 0.05) - (1 \pm 0.05)]F_L$$

This could yield implied load differentials with errors in the range of -105 to +305 percent. Fortunately this example represents a drastic case which was not encountered during testing. Typically, the lower load cell readings were about one-third to one-half the upper load cell readings; however, there is room for common mode errors.

23
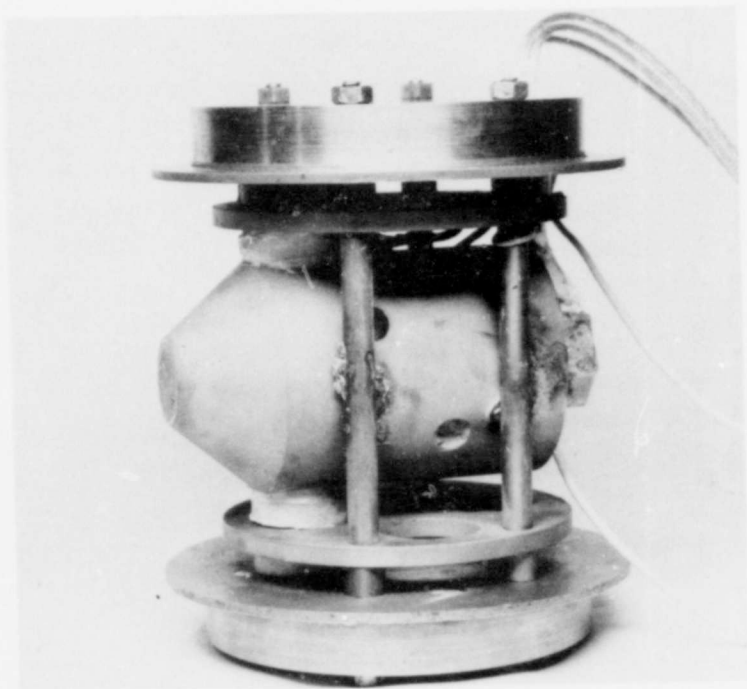
Figure 11. Concrete Sample Assembly

24

(2) If sand penetrates the RTV seal between either load
cell and the sample, load bridging can occur; i.e.,
the load cell will not see the total applied load
since the sand will transmit some of the load. This
obviously occurred on one series of static tests at
the lower load cell junction. Extremely high shear
stress was inferred because of pulverized sand in
the lower portion of the fixture.*

(3) Although the sample surface appears to have a relatively
uniform texture, the transducer force-collecting surface
represents a plane of osculation on the cylindrical sur-
face, i.e., a surface aberration which may cause a normal
stress and shear stress planar gradient at and around
the shear-stress, force-collecting surface (fig. 11).

The test specimen (shear transducer) was mounted in its steel housing and then
placed in a mold, into which concrete was poured. The transducer was placed
so that the sensing surface was even with the outside surface of the cylindri-
cal mold and the normal sensing axis was perpendicular to the longitudinal axis
of the concrete cylinder. After curing (approximately 7 days), the concrete
cylinder was removed from the mold, and the upper and lower load cells were
attached with the steel load-bearing cylinders. This test cylinder was then
placed inside the steel test fixture. The test fixture has a rubber bladder
inside so that water pressure may be applied to the sand surrounding the test
cylinder without saturating the sand. After placing the test cylinder inside
the test fixture, 20-40 Ottawa sand was rained around the test cylinder until
the fixture was filled to the top (fig. 12). The top plate was then installed
and torqued to 80 ft-lb on each of the eight bolts. The bottom plate had pre-
viously been installed in the same manner.

The test fixture was placed into a 300,000-lb capability Reihle Machine. All
instrumentation was hooked up and balanced, and outputs were connected to

_____
*In this test series the RTV seal was not used; only a small gap was used to
retard sand bridging. The RTV seal was used in subsequent testing and appeared,
upon post-test inspection, to eliminate load bridging.

Figure 12.   Shear-Stress Test Fixture Before Placement of Lid

assigned tape recorder channels and the X-Y plotter. Water pressure applied
to the test fixture compacted the sand around the inside of the test cylinder
and against the face of the shear transducer. Various loads were applied to
the top of the test cylinder; this caused a shear load on the face of the shear
transducer. Water pressure, as well as the load into the test cylinder, was
varied from test to test. Outputs from the shear-transducer sensors, as well
as the two load cells and the water-pressure sensor, were recorded on magnetic
tape. The outputs from the load cells were also recorded on an X-Y plotter so
that slippage occurring inside the test fixture could be seen.

Results of the static testing are shown in appendix D. Various pressure load-
ing and kip machine loading patterns were used. The normal-stress transducer,
which was not expected to perform properly, did agree in trend with the
hydraulic-pressure transducer but was typically about 30 percent higher. The
vertical shear-stress transducer outputs had the same pattern as the inferred
vertical shear stress with peaks about 70 percent of the inferred shear. Dur-
ing the last of this test series, peak outputs agreed more favorably, with

those from the vertical shear-stress transducer being slightly higher than those
of the inferred shear stress. No explanation can be offered for this. Both the
transducer vertical shear and the inferred vertical shear showed residuals when
the kip load was dropped, with the transducer vertical shear-stress residual in
excess of the inferred vertical shear stress. When the hydraulic load was re-
moved, however, both residuals disappeared. Apparent horizontal shear-stress
output was low; it ranged from 2 to 5 percent of the vertical shear stress.

DYNAMIC-SHEAR SENSITIVITY

Fixture preparation for the dynamic testing was identical to that for the
static testing, except the CERF drop tower was used to impart dynamic loads
to the sample column. The test fixture was placed under the impact machine
so that the weight would drop on top of the test cylinder load-bearing cylin-
der. Styrofoam discs and rubber pads were placed on top of the test cylinder
to reduce ringing in the test fixture and also to tailor the input shock wave-
form. The instrumentation was hooked up and checked out, and water pressure
was applied to the test fixture as in static testing. The weight was then
dropped on top of the test cylinder from various heights; this caused a shear
load to be applied to the shear transducer. A total of 21 tests were made
with different drop heights and water pressure combinations. Outputs from
all instrumentation were recorded on magnetic tape.

The dynamic test results are shown in appendix E. In the nine tests shown,
the initial normal stress is 14 to 26 percent higher than the hydraulic pres-
sure; vertical shear peak outputs are 42 to 77 percent of the inferred shear
peaks (average = 65 percent). The vertical shear and the inferred shear trends
are the same, with closer agreement toward the end of the transient interval.
Also, as in the static testing, apparent residuals appeared to be higher in the
vertical shear than in the inferred shear. Peak horizontal shear-stress outputs
averaged about 5.9 percent of the peak vertical shear-stress outputs. Peak ac-
celerations to peak vertical shear ratios were 1.6 to 4.8 (g/psi) with peak g-
inputs of 300g to 600g. Some obvious ring was apparent in both the vertical
and horizontal shear transducer outputs, but this ringing was not seen in the
normal-stress transducer output. This would indicate a bending ring mode

27

rather than an axial ring mode. Because of the ring, it is somewhat difficult
to appraise the acceleration sensitivity of the shear transducers, although it
appears that acceleration sensitivity may be contributing to transducer outputs,
especially in the early part of the shear transient. Peak data from the shear
transducer outputs were taken by fairing through the high-frequency ringing.

SECTION 6
SUMMARY OF TEST DATA

Test data findings and target objectives (requirements) are compared in the following summary:

(1) Range

Required: 2000-psi shear stress (two axes)
3000-psi normal stress (one axis)

Test Findings: Peak predicted stresses of 200 to 5000 psi can be handled on all axes.

(2) Useable Frequency Range

Required: dc to 500 Hz

Test Findings: dc to at least 2000 Hz

(3) Mounting Requirements

Required: 3-in. thick wall or greater

Test Findings: This requirement was met.

(4) Shear-Axis Sensitivity to Normal Stress

Required: No greater than 5 percent apparent shear stress at 1000-psi normal stress

Test Findings: Worst case was 3.1 percent.

(5) Normal-Axis Sensitivity

Required: No greater than 5 percent apparent normal stress at 1000-psi shear stress

Test Findings: Worst case was 16 percent. This requirement was met when data from HARD PAN transducers were taken into account.

(6) Acceleration Sensitivity (All Axes)

Required: Shear--0.02 psi/g or better
Normal--0.03 psi/g or better

Test Findings: Shear--0.0417 psi/g (worst case)
Normal--0.244 psi/g (worst case)

Note: The target objective is not met when worst-case test sensitivities are used; however, sensitivities other than worst case indicate satisfactory performance. The tests in which high-frequency ringing and output discontinuities occurred were not used for worst-case sensitivities.

(7) Shear-Axis Sensitivity to Cross-Axis Shear

    Required: No target objective established

    Test Findings: Worst case was 2.88 percent.

(8) Force-Collecting Surface

    Required: The force-collecting surface of the transducer shall be 1 in. in diameter and textured to match as nearly as possible the coefficient of friction of the structure.

    Test Findings: This requirement was met.

The vertical axis of the shear transducer in both static and dynamic testing exhibited a shear/time history quite similar in pattern and trend to the inferred shear.

During both dynamic and static testing, the peak vertical shear-stress output from the transducer was typically 65 to 70 percent of the inferred-shear peaks.

Residual (post-test) shear on the transducer appeared to be consistently higher than the inferred residuals, although both residuals dissappear when normal stress is relieved. The fact that a residual shear stress is indicated by both is not alarming and is probably due to locking of the test column against the upper and/or lower plate.

Cross-axis and acceleration sensitivities were adequately low and in most cases exceeded the target specifications.

Although the normal-stress gage did not perform well on the three test transducers, it does not mean that the normal-stress measurement cannot be made successfully. Indeed, during limited transducer testing for the HARD PAN Event, cross-axis and acceleration sensitivities were as good as, or better than, the shear-axis sensitivities.

SECTION 7
CONCLUSIONS AND RECOMMENDATIONS

CONCLUSIONS

During development and testing, the triaxial stress transducer met and exceeded nearly all target objectives. The triaxial transducer in its present configuration is recommended for field use, even though some improvements and additional experimental work would be beneficial.

Based on Ottowa sand test results and data from the HARD PAN Events, it appears that the device is capable of making good triaxial stress measurements in high g and high cross-axis stress environments. The bending moment calibration method can be employed along with the 0.65 registration factor to provide scale factors without an actual structure/media environment calibration if the structural surfaces have no pits, pockets, or other unusual surface anomalies. Calibration without actual interface shear stress input is roughly equivalent to 1g and 2g fallthrough calibrations, without actual velocity, performed on oil-damped pendulous velocity gages (ref. 4).

Since there was no established dynamic interface shear-stress standard before or during the development of the triaxial stress transducer, an actual structure/media inferred shear-stress method and apparatus were developed. These were used as a dynamic shear-stress standard for the triaxial stress transducer. Other methods were considered by both AFWL and CERF; but because of the requirement to evaluate the transducer in an actual structure/media environment, this method was considered superior to the others and a good dynamic shear-stress standard. The inferred shear measurement provides the average vertical shear stress seen by the entire sample area (100 in.^{2}); the transducer provides average shear seen by its force-collecting surface (less than 1 in.^{2}). This accounts for the differences seen in the two measurements.

---

4. Sonnenburg, Paul N., and Schulz, George, *Response Properties of an Orthogonal System of Pendulum-Type Velocity Gages*, AFWL-TR-73-31, Air Force Weapons Laboratory, Kirtland Air Force Base, New Mexico, June 1973.

31

RECOMMENDATIONS

Calibration Fixture

Although the dynamic shear-stress calibration fixture worked well, the follow-
ing improvements can be made:
  (1) Stiffer load cells should be made to allow higher shear-
       stress levels to be obtained and to decrease gap varia-
       tion between the sample cylinder and cylinder extensions.
  (2) The sample surface area should be decreased as much
       as possible to minimize shear gradient effects.
  (3) The transducer force-collecting surface should be machined
       (for laboratory testing purposes only) to match the sample
       surface contour. This would provide a more uniform cylin-
       drical sample surface and eliminate local shear gradients
       around the transducer force-collecting area. The same
       contouring procedure should be applied to both transducer
       beams to minimize beam imbalance.
  (4) It would probably be beneficial if the steel cylinder ex-
       tensions had concrete surfaces to further reduce shear
       gradients at the upper and lower boundaries of the sample.
       This could be accomplished by decreasing the diameter of
       the steel cylinders adjacent to the load cells and casting
       with concrete back up to the original diameter. A concrete
       anchoring system similar to the one used in the transducer
       beams should be employed.

Triaxial Stress Transducer

  (1) Ledloy was chosen for the transducer material because it
       is not attacked by concrete. Stainless steel (416 annealed)
       would probably have been a better choice. This material is
       easily machined, not attacked by concrete, and not oxidized
       like Ledloy. It is thus recommended that future transducers
       be made of this material. Although the oxide coat on the
       transducers presented no real problem, better bonding of
       the RTV seal could be achieved on stainless steel.

32

(2) The acceleration-cancelling beam used to reduce acceleration
    sensitivity on the shear-stress axes could also be used in a
    half-bridge configuration to reduce acceleration sensitivity
    on the normal-stress axis. It is recommended that this be
    evaluated for effectiveness.

(3) The necessary steel retaining annulus around the concrete
    force-collecting surface makes up over 30 percent of the
    total beam surface, and this is responsible in part for the
    shear underregistration. However, this area cannot be sub-
    stantially reduced without jeopardizing beam integrity. It
    would be adviseable to test a transducer without the concrete
    textured surface to determine the shear-force contribution
    from the steel force-collecting area. This information could
    be used to provide the effective force-collecting area for
    the shear axes of the transducer.

(4) The medium used in this investigation was Ottowa sand; however,
    tests should be performed in the calibration fixture with other
    media of interest to determine if transducer shear performance
    and shear scale factor are media biased.

(5) In field use, significant input components above 3 kHz should
    be avoided to eliminate the possibility of ringing. It is
    recommended that future studies include either vibration test-
    ing or transient-generated transfer functions to establish
    actual upper-frequency limitations.

(6) With the usable frequency range of the transducer being at
    least three times higher than the 500 Hz required, it is anti-
    cipated that data reconstruction techniques need not be em-
    ployed. However, if obvious output components above 3 kHz are
    seen in the data and if these are attributable to shear inputs,
    methods are available to extend the effective gage frequency
    passband. By characterizing the gage in the laboratory with
    known inputs of adequate high frequency content, relatively

simple reconstruction procedures can be used to correct the
voltage data analogs. In particular, the ratio of the known
input sample set fast Fourier transform to the input response
sample set fast Fourier transform multiplied appropriately by
the fast Fourier transform of the field data sample set in
question can be brought back corrected in the time domain with
an inverse fast Fourier transform operation. Time-domain
methods are also available for data reconstruction. For step-
input-related time-domain deconvolution, a laboratory-generated,
step-response sample set is required along with the field data
sample set to determine the corrected or reconstructed sample
set. With arbitrary input-related, time-domain deconvolution,
sample sets of any sufficiently known arbitrary input, gage
response to this input, and field data are used to generate a
reconstructed field data sample set. Other time-domain data-
reconstruction methods include impulse-invariant, step-invariant,
and ramp-invariant Z transform methods, which require a system
mathematical model (refs. 5, 6, 7).

(7) Cross-axis response correction can also be easily made if
cross-axis sensitivity scale factors are constant (which
appears to be the case for the triaxial stress transducers
tested). Correction then becomes a matter of solving three
simultaneous equations with three unknowns.

$$E_{ov} = \alpha\sigma_{sv} + \beta\sigma_{sh} + \gamma\sigma_n$$
$$E_{oh} = \alpha'\sigma_{sv} + \beta'\sigma_{sh} + \gamma'\sigma_n$$
$$E_{on} = \alpha''\sigma_{sv} + \beta''\sigma_{sh} + \gamma''\sigma_n$$

5. Schulz, George L., *Method of Transfer Function Calculation and Distorted
    Data Correction*, AFWL-TR-73-300, Air Force Weapons Laboratory, Kirtland Air
    Force Base, New Mexico, March 1975.

6. Pickett, Stephen F., *An Evaluation of Four Data Reconstruction Techniques
    Applied to Seismometer Data*, Masters Thesis, University of New Mexico,
    Albuquerque, New Mexico, December 1974.

7. Stearns, Samuel D., *Digital Signal Analysis*, Hayden Book Co., Inc.,
    Rochelle Park, New Jersey, 1975.

where

E_{ov} = vertical-axis output voltage

E_{oh} = horizontal-axis output voltage

E_{on} = normal-axis output voltage

σ_{sv} = vertical shear stress

σ_{sh} = horizontal shear stress

σ_n = normal stress

$$\left.\begin{array}{l} \alpha = E_{ov}/\sigma_{sv} \\ \alpha' = E_{oh}/\sigma_{sv} \\ \alpha'' = E_{on}/\sigma_{sv} \end{array}\right\} \quad \text{when } \sigma_{sh} = \sigma_n = 0$$

$$\left.\begin{array}{l} \beta = E_{ov}/\sigma_{sh} \\ \beta' = E_{oh}/\sigma_{sh} \\ \beta'' = E_{on}/\sigma_{sh} \end{array}\right\} \quad \text{when } \sigma_{sv} = \sigma_n = 0$$

$$\left.\begin{array}{l} \gamma = E_{ov}/\sigma_n \\ \gamma' = E_{oh}/\sigma_n \\ \gamma'' = E_{on}/\sigma_n \end{array}\right\} \quad \text{when } \sigma_{sv} = \sigma_{sh} = 0$$

$$\begin{bmatrix} \alpha & \beta & \gamma \\ \alpha' & \beta' & \gamma' \\ \alpha'' & \beta'' & \gamma'' \end{bmatrix} \begin{bmatrix} \sigma_{sv} \\ \sigma_{sh} \\ \sigma_n \end{bmatrix} = \begin{bmatrix} E_{ov} \\ E_{oh} \\ E_{on} \end{bmatrix}$$

$$\begin{bmatrix} \sigma_{sv} \\ \sigma_{sh} \\ \sigma_n \end{bmatrix} = \begin{bmatrix} \alpha & \beta & \gamma \\ \alpha' & \beta' & \gamma' \\ \alpha'' & \beta'' & \gamma'' \end{bmatrix}^{-1} \begin{bmatrix} E_{ov} \\ E_{oh} \\ E_{on} \end{bmatrix}$$

The solution becomes more complicated when cross-axis sensitivity scale factors are not constant, i.e., if cross-axis output is a nonlinear function of cross-axis input, and virtually impossible if the input/output relationship is multi-valued. Sonnenburg and Schulz addressed similar cross-axis sensitivity problems of an orthogonal system of pendulous velocity gages and developed a computer code for the solution of cross-axis sensitivities (ref. 4). Since cross-axis sensitivities are extremely low on the shear axes and can be made extremely low on the normal axis, it should not be necessary to employ cross-axis correction schemes on most field data.

REFERENCES

1. Huck, Peter J., et al., *Dynamic Response of Soil/Concrete Interfaces at High Pressure*, AFWL-TR-73-264, Air Force Weapons Laboratory, Kirtland Air Force Base, New Mexico, April 1974.

2. Pickett, Stephen F., *Development and Evaluation of Measurement Systems for Blast-Induced Motions in Buried Structures*, AFWL-TR-73-230, Air Force Weapons Laboratory, Kirtland Air Force Base, New Mexico, April 1974.

3. Leonards, G. A., *Experimental Study of Static and Dynamic Friction Between Soil and Typical Construction Materials*, AFWL-TR-65-161, Air Force Weapons Laboratory, Kirtland Air Force Base, New Mexico, December 1965.

4. Sonnenburg, Paul N., and Schulz, George, *Response Properties of an Orthogonal System of Pendulum-Type Velocity Gages*, AFWL-TR-73-31, Air Force Weapons Laboratory, Kirtland Air Force Base, New Mexico, June 1973.

5. Schulz, George L., *Method of Transfer Function Calculation and Distorted Data Correction*, AFWL-TR-73-300, Air Force Weapons Laboratory, Kirtland Air Force Base, New Mexico, March 1975.

6. Pickett, Stephen F., *An Evaluation of Four Data Reconstruction Techniques Applied to Seismometer Data*, Masters Thesis, University of New Mexico, Albuquerque, New Mexico, December 1974.

7. Stearns, Samuel D., *Digital Signal Analysis*, Hayden Book Co., Inc., Rochelle Park, New Jersey, 1975.

APPENDIX A

ENGINEERING DRAWINGS

Lock

Sleeve

Primary Element

Case

TRANSDUCER ASSEMBLY

38

0.125 Drill
Through Chamfer

1.985 Diameter

1.488
Diameter

45°

0.375 Drill
0.875 Deep

0.625
Diameter

Drill Through Countersink
for 4-40 Screw on 1.750
Circle (4 Places)

0.125 Drill Through
Chamfer on 1.00
Circle (2 Places)

0.625

1.500 Bore
0.625 Deep

1.250

0.750

1.375

1.500

2.500
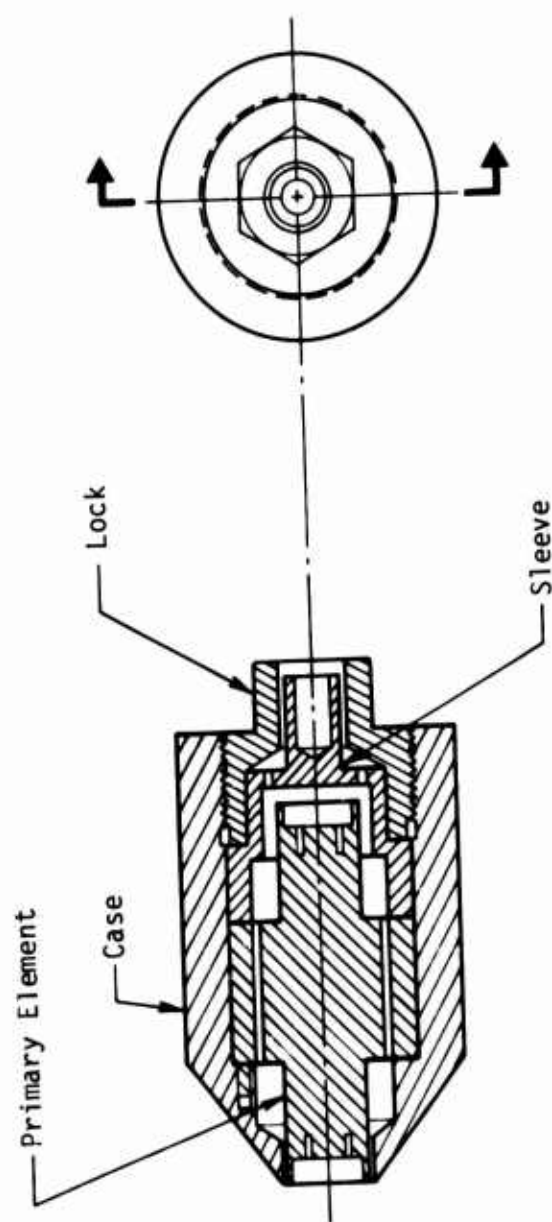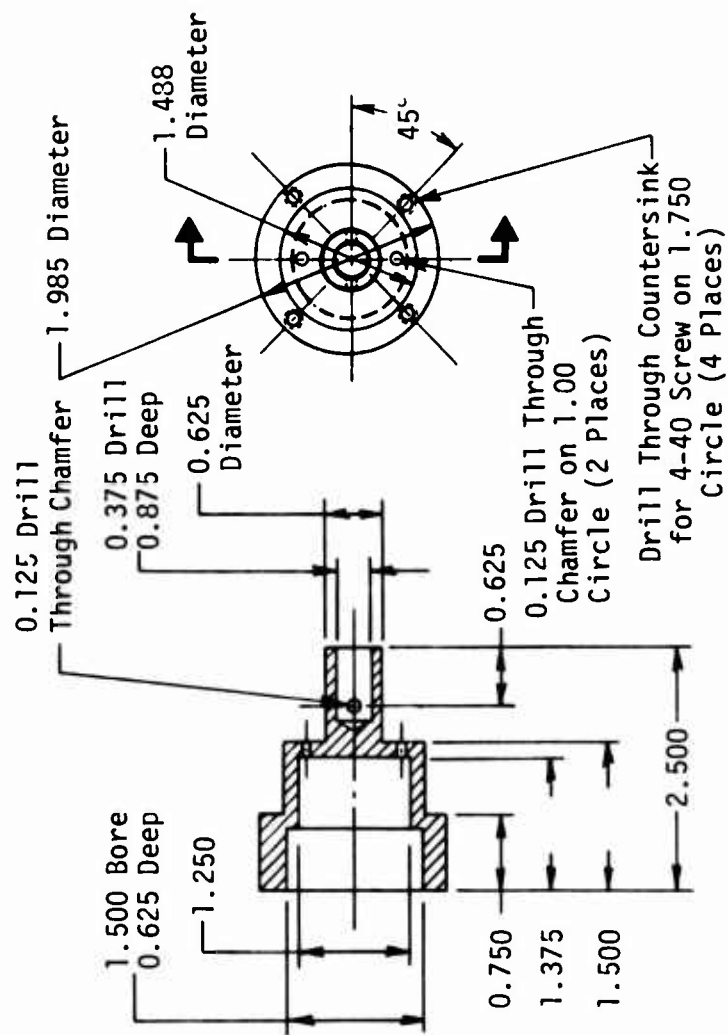
Note: All dimensions are in inches.

SLEEVE

39

Drill and Tap for 4-40
(4 Places) 0.375 Deep
on 1.750 Diameter Circle

0.125 Drill Through
Chamfer (2 Places)
on 1.375 Diameter Circle

45°

0.1875 x 0.750 Dowel Pin

1.000** Diameter

1.250*

4.000

2.000* Diameter

0.875*   0.250 **

0.375 **   0.250 **

0.800** Diameter

1.250**

Chamfer

0.500 ± 0.001 Diameter
90 ± 1° Apart
(4 Places)
Drill and Tap
6-32
Both Ends

* ±0.001   ** ±0.005
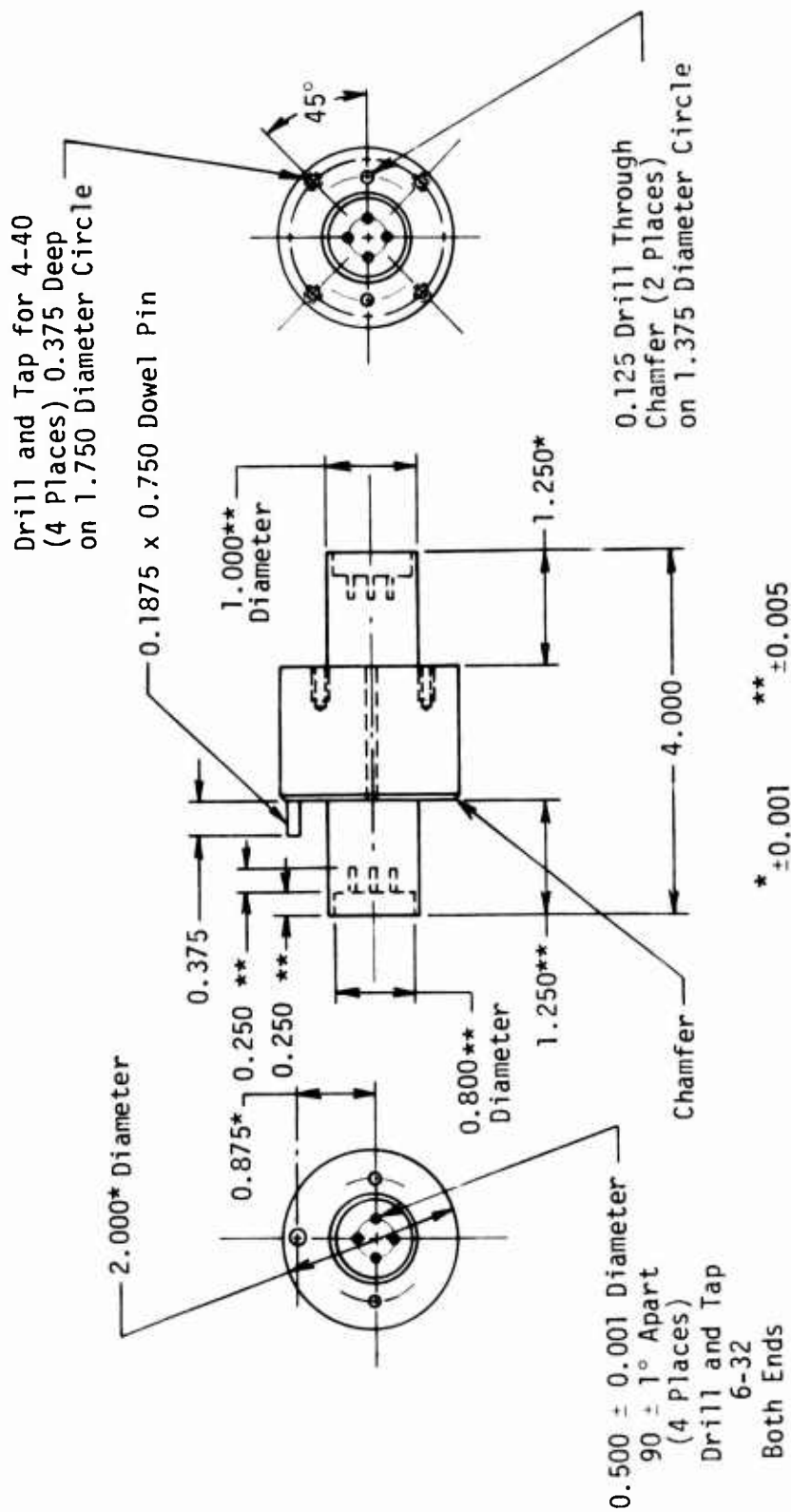
Note: All dimensions are in inches.

PRIMARY ELEMENT

40

0.1885**-Diameter Hole,
0.500 Deep

1.500
Diameter

3.000 Diameter

2.125 12 UN-2B

0.875*

Drill & Tap
0.500 in 20 UNF
(3 Places)

2.010
2.013
Diameter

40°

1.250

4.750

1.034
1.036
Diameter

0.625

1.250**

2.250

* ±0.001   ** ±0.005

Note: All dimensions are in inches.

CASE

41

0.1875 x 0.750 Dowel Pin
Can Drill Through

0.375

0.750 16UNF-2A

0.875
± 0.001

0.500

0.500

2.000

3.000

3.500

2.001
1.999 Diameter

Slot:
0.025 Wide x 0.020 Deep
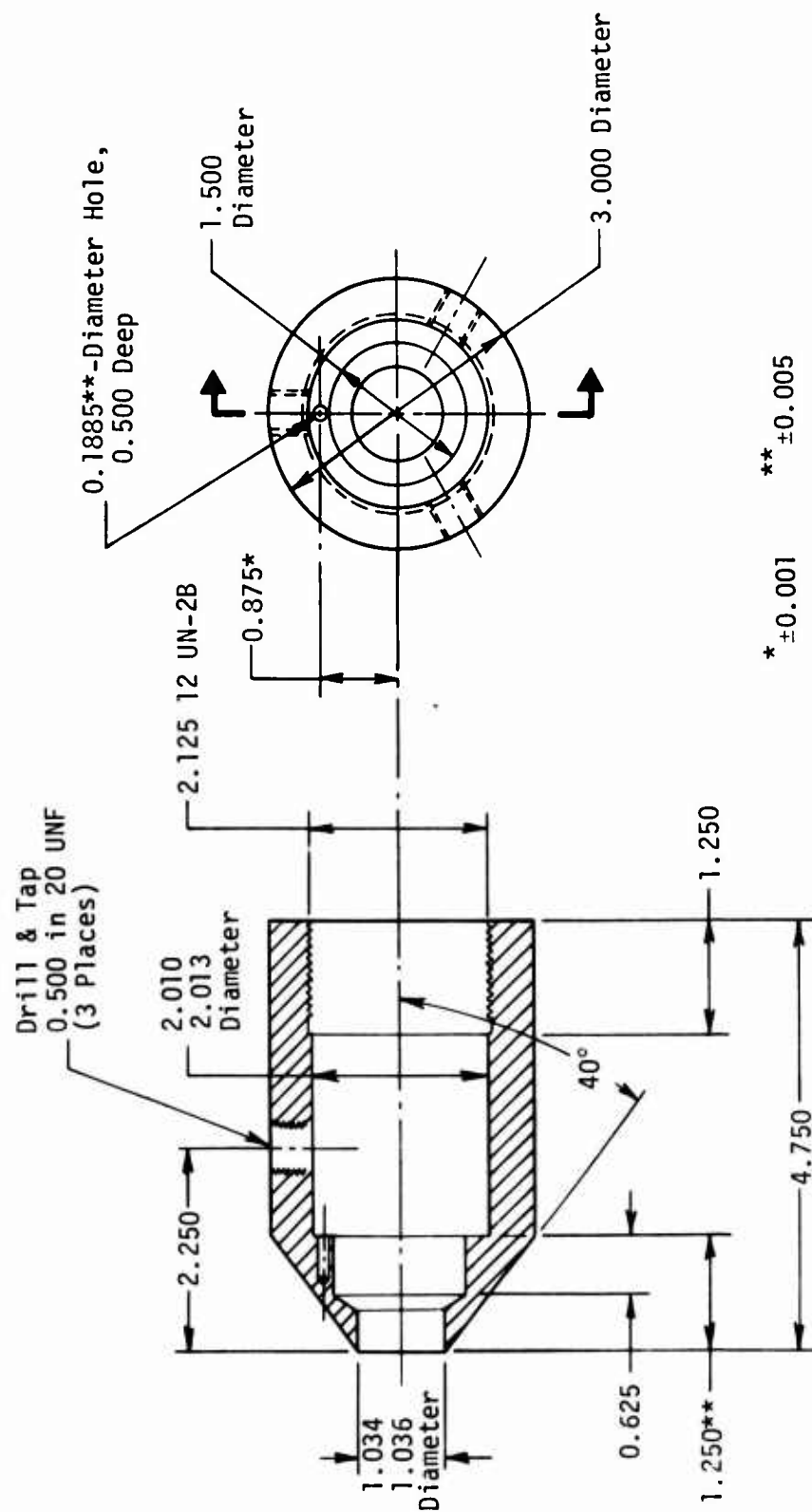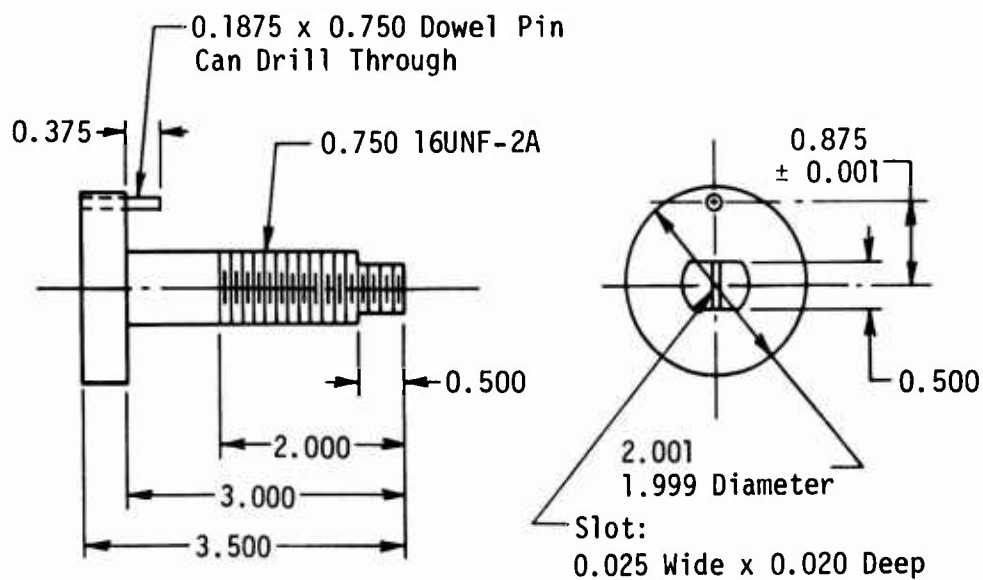
CASE INSTALLATION BOLT

Note: All dimensions are in inches.

1.500-Diameter Drill
0.875 Deep

2.175 12 UN-2A

1.250 Hex.

1.980
Diameter

0.750 Diameter
Drill Through

0.250

0.750

2.000
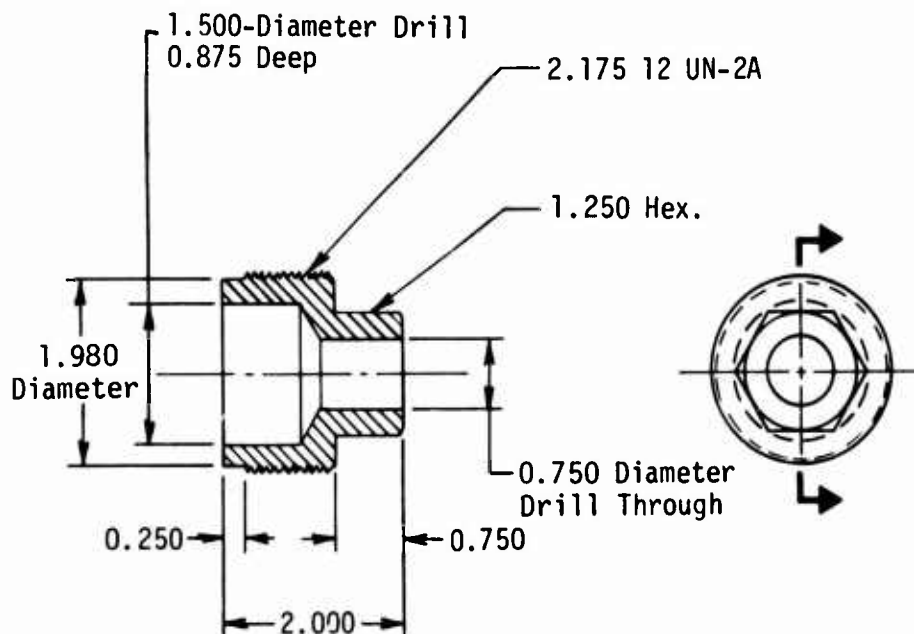
LOCK

APPENDIX B
TRANSDUCER PARTS AND ASSEMBLY PROCEDURE

REQUIRED PARTS

(1) Primary Element and Sleeve

(2) Strain Gage Locating Fixtures

(3) One M9 E-GP350-500 Strain-Gage Package (Kulite)

(4) Two PEP 350-090 Strain-Gage Package (Kulite)

(5) Glass Backing Paper

(6) No. 36 Enamel-Insulated Wire (Belden SGL)

(7) Ten No. 2 Terminal Tabs

(8) Epoxy: M-Bond 610 (Micromeasurements)

(9) Cleaning Solvents (Toluene, MEK, Alcohol) Spectral Grade

(10) Epoxy: Epocast 530 with 9816 Hardener (Furane Plastics)

(11) Embeco 630 Nonshrink Grout (Master Builders)

(12) Alpha No. 1122 Cable (24 ft)

(13) Barrier Water-Proofing GageKote No. 1: MCoatD (Micromeasurements)

(14) Four 4-40 x 1 in Flathead Screws; Eight 6-32 x 3/8 in Screws

MISCELLANEOUS MATERIALS

(1) Cotton Swabs

(2) Flux

(3) Solder: Alloy SN63 Erin Multicore

(4) Masking Tape

(5) Cellophane Tape (1/2-in. Diameter)

(6) Spotter Brushes (No. 00)

(7) Teflon Pads

(8) Soft Rubber Pads

(9) C-95 Blasting Sand

(10) Hose Clamps (1-in. Diameter)

ASSEMBLY PROCEDURE

(1) Insert eight 6-32 x 3/8 in screws into the cups on the two beams such that clearance between the top of each screw and the outer beam surface is 0.030 in.

(2) To 100 parts by weight of Epocast 530 add 15 parts by weight of 9816 hardener and mix thoroughly; to 1 part of this mix by weight add 4 parts by weight of Embeco 630 Grout and mix thoroughly. (Pot life is about 1 hr.)

(3) Carefully place the above mix in the cup on one side of the primary element and allow 4 hr to set.

(4) Repeat step 2.

(5) Repeat step 3 for the other side of the primary element and cure for 24 hr at room temperature.

(6) Thoroughly degrease all parts with solvent (MEK, Toluene, or freon TF).

(7) Apply masking tape around center of primary element (reference mass) and sand blast both element beams only, using C-95 sand.

(8) Using the locating fixture (fig. B1), accurately mark one normal-stress strain-gage pair location on the active beam radially 45° between the two shear axes and 0.650 in. from the free end of the beam. Locate the second mark 180° radially from the first and also 0.650 in. from the free end of the beam.

(9) Locate the shear-stress strain-gage locations accurately as follows: The center of the locating pin is to be considered zero degrees radially from the center of both beam surfaces. The shear-stress strain-gage locations are located exactly 1 in. from the free end of the beams and radially at exactly 0°, 90°, 180°, and 270°. Use both locating fixtures (fig. B1 and B2).

(10) Clean the 10 specimen areas thoroughly with toluene and then with alcohol and cotton swabs.

(11) Place the normal-axis gages (M9 E-GP350-500) as follows: Using clear cellophane tape, place tape over one gage pair and center gage at one normal-stress specimen point. Secure tape; release one end and remove gage pair from

44
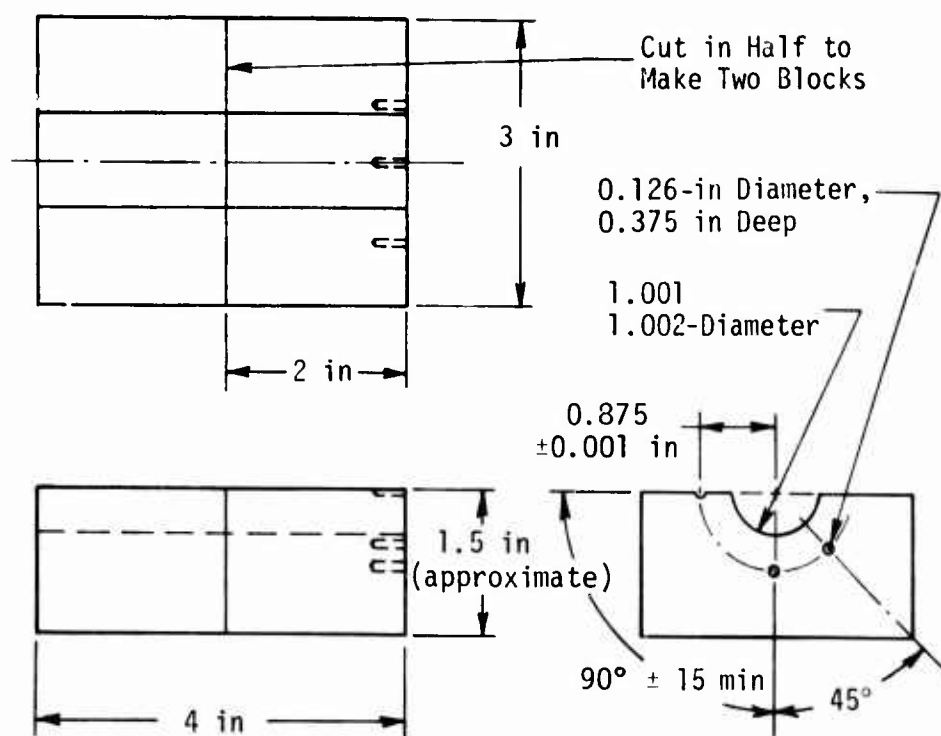
Figure B1.   Locating Fixture for Normal-Strain Gage
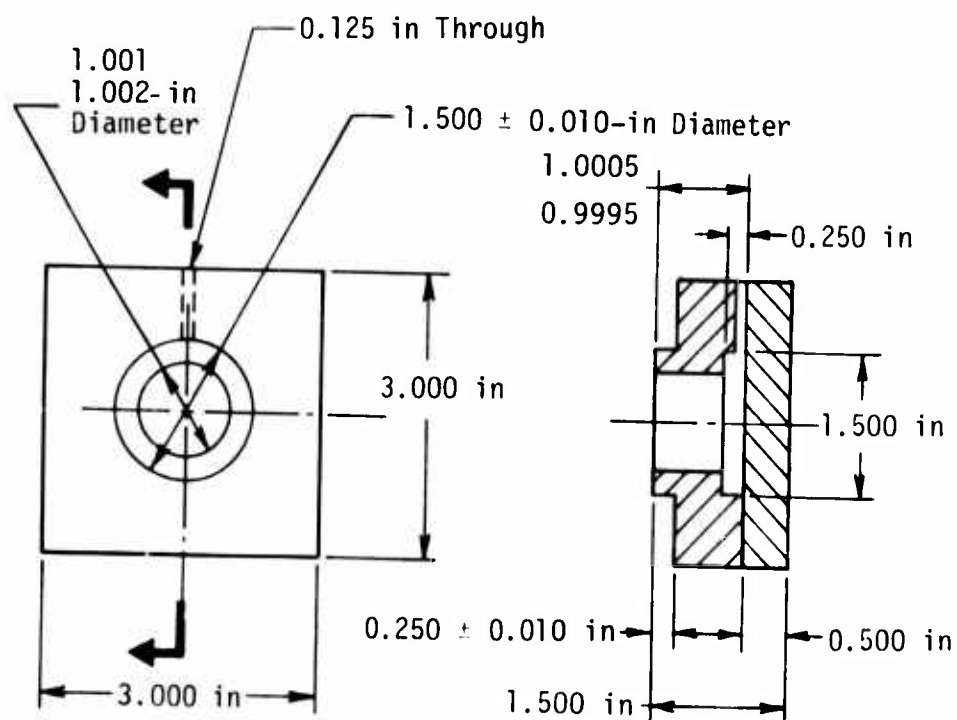
Figure B2.   Locating Fixture for Shear-Strain Gage

primary element. Repeat for the second normal-stress
specimen point.

(12) Place M-Bond 610 Epoxy on primary element at specimen
points and air dry for 20 min.

(13) Using a hose clamp with Teflon and soft rubber pads,
clamp gages firmly in place.

(14) Oven cure at 250°F for 4 hr.

(15) Remove pads, clamp, and tape.

(16) Place the shear-stress gages in each of the eight locations
as follows: Cut glass paper into three 0.125- by 0.075-in.
rectangles. Bend leads up on each strain gage with tweezers.
Individually place glass paper segments over specimen areas
and apply M-Bond 610 Epoxy to glass papers on two gage loca-
tions on the upper working surface. Place gages individually
over each paper centering the gages exactly on the specimen
points and carefully aligning gage axis with beam axis. Hold
leads up until cement dries (10 to 15 min).

(17) After all gages are placed, oven cure at 250°F for 4 hr.

(18) Install 10 gage tabs on the exterior extension of the sleeve
using the same epoxy and curing procedure as above.

(19) Examine all strain-gage installations for proper location
and bonding.

(20) Wire vertical shear axis (fig. B3). Use No. 36 SGL Belden
wire on all wiring in the main body of elements; tape
the wire down to the body; then use Gagekote No. 1 over
wire and gages; use routing holes in the primary element
for interconnections between active beam elements and
dummy beam elements.

(21) Wire horizontal shear axis (same as vertical axis wiring).

(22) Wire normal axis (fig. B4). Use No. 36 SGL Belden wire on
all wiring in the main body of elements. Tape the wire down
to the body; then use Gagekote No. 1 over wire and gages; use
routing holes in the primary element for routing leads to the
dummy side of the transducer.
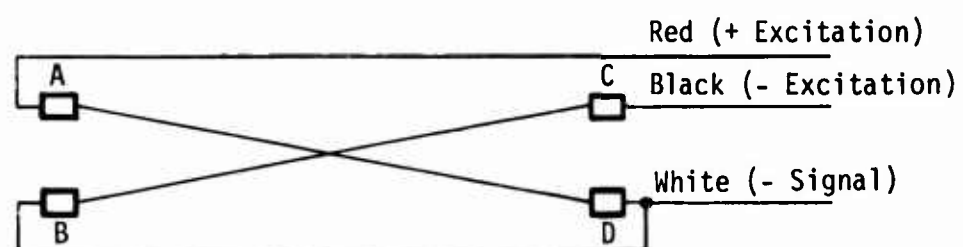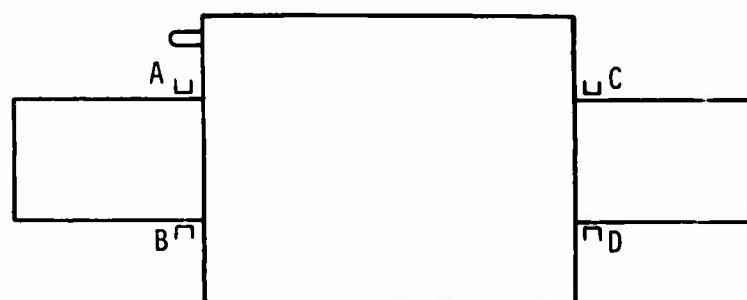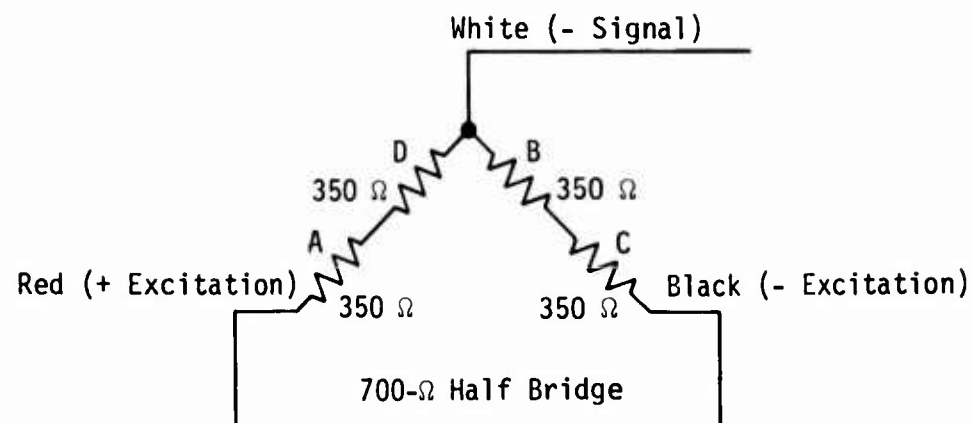
Figure B3.   Wiring Diagram for Vertical and Horizontal Shear Axes
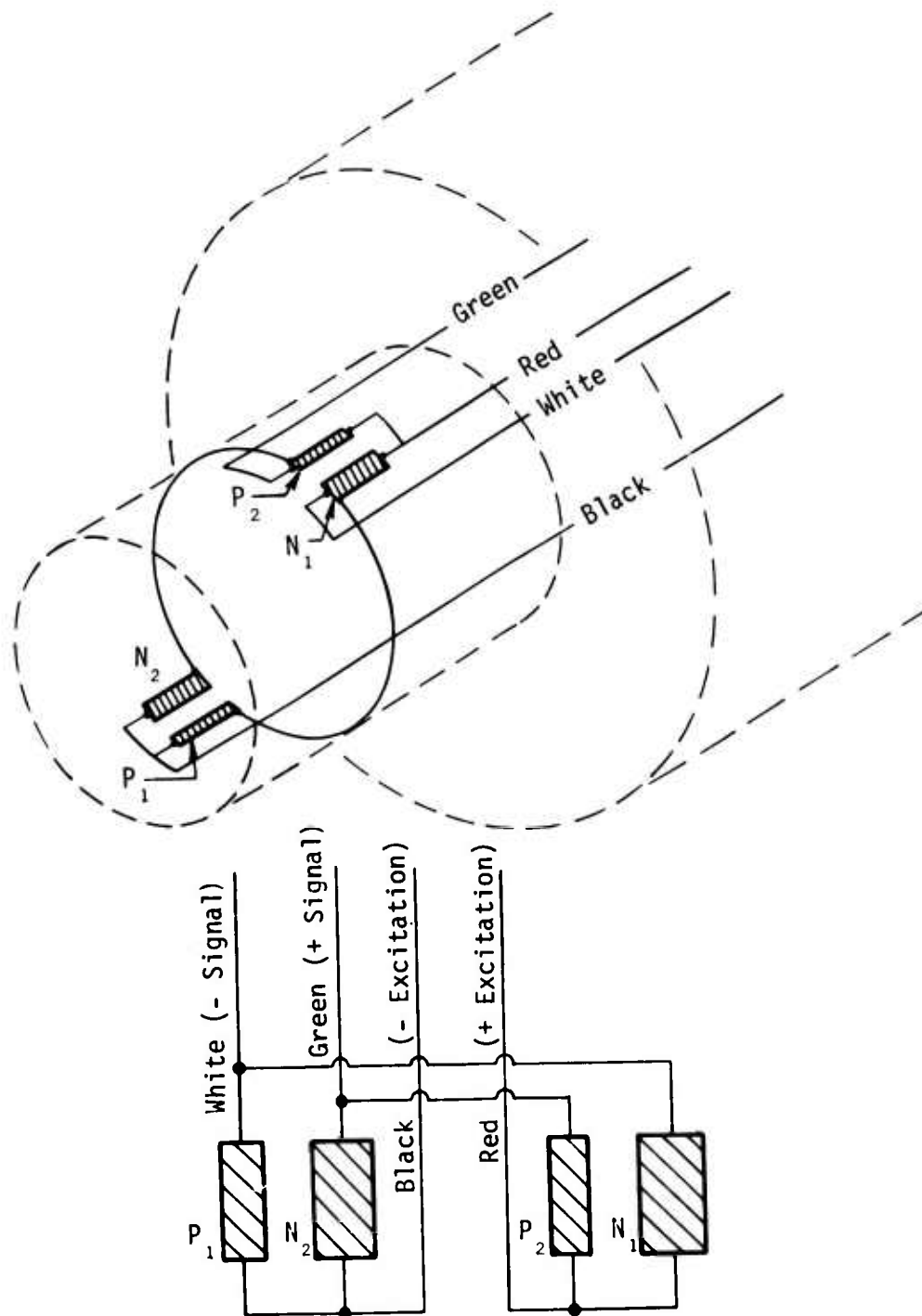
Note: The narrow gage elements are P-type gages;
      the wide gage elements are N-type gages.

Figure B4. Wiring Diagram for Normal Axis

48

(23) Route and tape all lead wires between gages on the dummy beam to the end of the dummy beam; apply Gagekote No. 1 over wire leaving about 4 in. of wire extending past the end of the dummy beam.

(24) Pass wires through the wire exit holes in the sleeve and attach sleeve with 4-40 x 1 in flathead screws.

(25) Trim wires and solder to the 10 terminal tabs.

(26) Using three 8-ft lengths of Alpha No. 1122 cable, prepare leads and trim shields, stretching insulation well over shield to prevent shield contact with any part of the transducer.

(27) Insert cables through rear cable exit hole in shield and bring leads through the two side holes near the tabs.

(28) Solder cable leads to the appropriate tabs (figs. B3 and B4); apply RTV to solder tabs and fill cable exit holes and allow adequate time for curing.

(29) Check all circuits on external cable leads for ohmic leakage (readings should be greater than $10^{10}\Omega$). Transducer is now ready for calibration.

APPENDIX C
TRANSDUCER CASE INSTALLATION PROCEDURE

(1) On the outside surface of the form, mark the direction of the sensitive shear axis with a line; also mark the location of the hole for the transducer.

(2) Drill a 13/16-in. diameter hole in the form at the location marked.

(3) Remove the nut, washer, and rubber shipping block from the case assembly; discard the rubber shipping block and retain the nut and washer for installing the case to the form.

CAUTION

Be careful in handling the case so that lip is not dented.
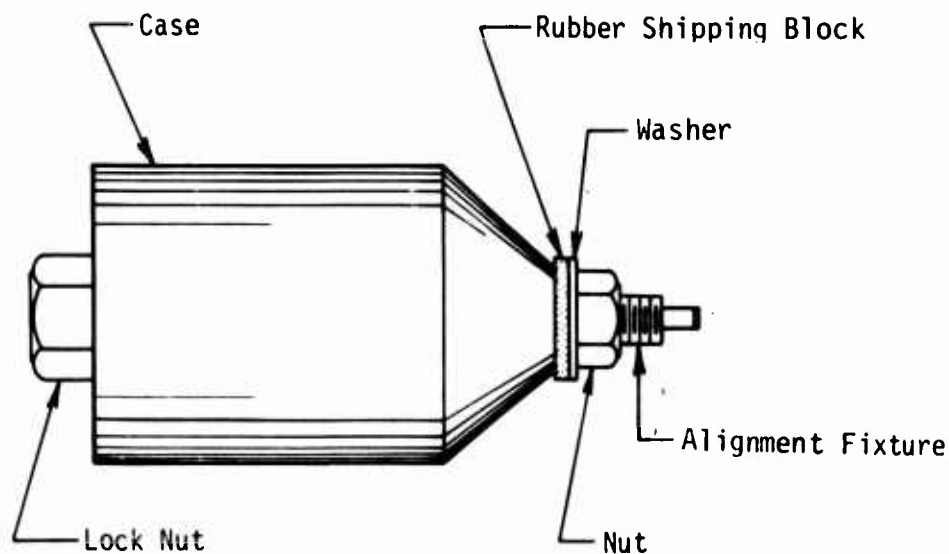
(4) Insert the bolt through the hole in the form so that the case will be
     cast into the concrete with the tapered portion toward the outside of
     the form; attach the nut loosely to the bolt.

Outside Form
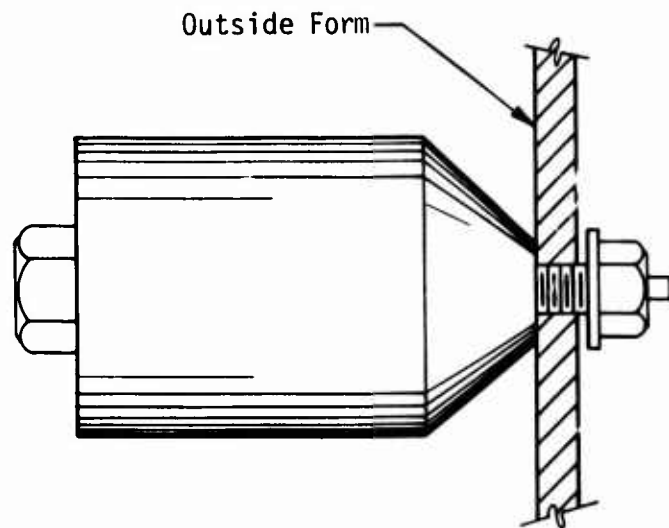
(5) Align the slot in the positioning fixture with the line drawn in step 1
     to mark the sensitive shear axis; point the arrowhead on the positioning
     fixture in the direction chosen for positive shear.

Line Drawn on Form
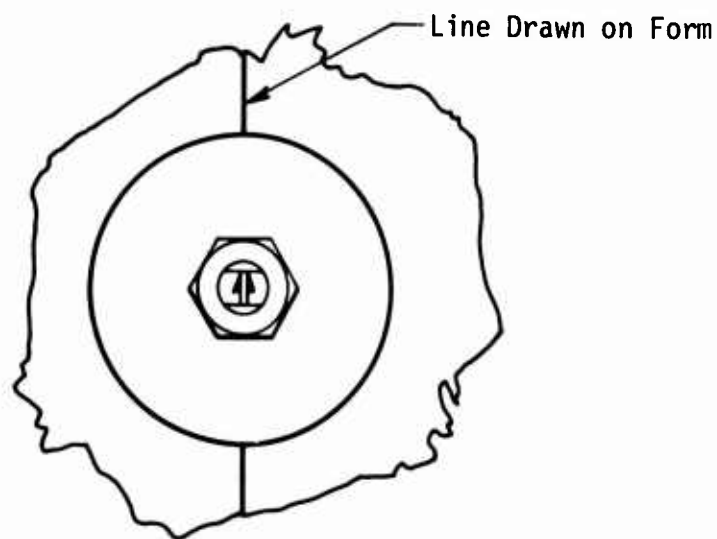
(6) Hold the positioning fixture in place with a 1/2-in. open-end wrench and tighten the nut until the case is held snuggly against the form.

CAUTION

Do not overtighten.

(7) Insert three 1/2-in. diameter 20 UNF bolts of a convenient length (6-in. long bolts are furnished) into the three tapped holes in the case and hand tighten.

CAUTION

Be careful not to disturb the alignment of the case.

(8) Tie or weld the three bolts installed in step 7 to reinforcing steel.

CAUTION

Do not weld on the case and do not attempt to bend the bolts once they have been installed in the case. Even slight deformation of the case will make it unfit for its intended use.

(9) Cut a 3-in. diameter cardboard tube long enough to extend from 1/2 in. behind the three bolts in the case to the inner form, and place the tube over the case; before pouring the concrete, be sure that the cardboard tube fits snuggly against the inner form; caulk between the tube and the inner form if needed to prevent concrete from entering the tube.

(10) Check to see that the slot and arrow on the positioning fixture are still in proper alignment.

(11) While pouring the concrete, be especially conscientious to insure that the concrete completely fills the region between the case and the outside form.

(12) Before removing the forms, remove the nut and positioning fixture from the case; replace the large lock nut in the case after the positioning fixture is removed.

APPENDIX D

STATIC-SHEAR TEST DATA
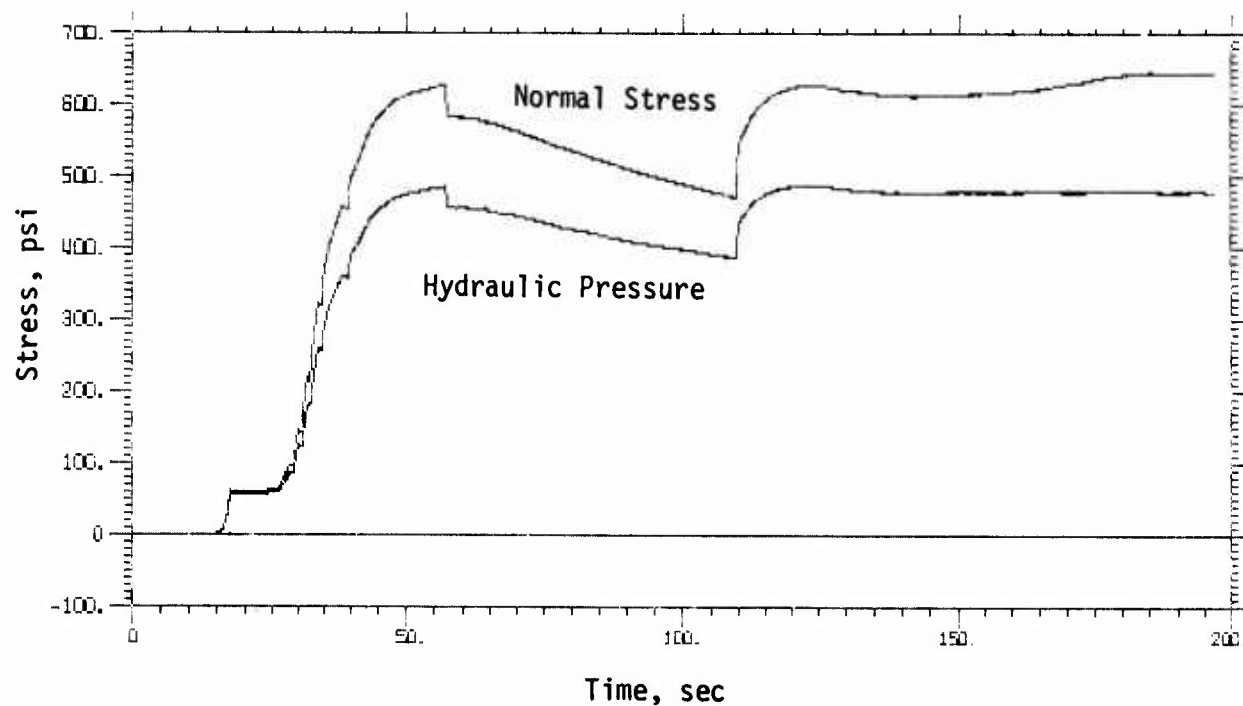
Hydraulic Pressure and Normal Stress
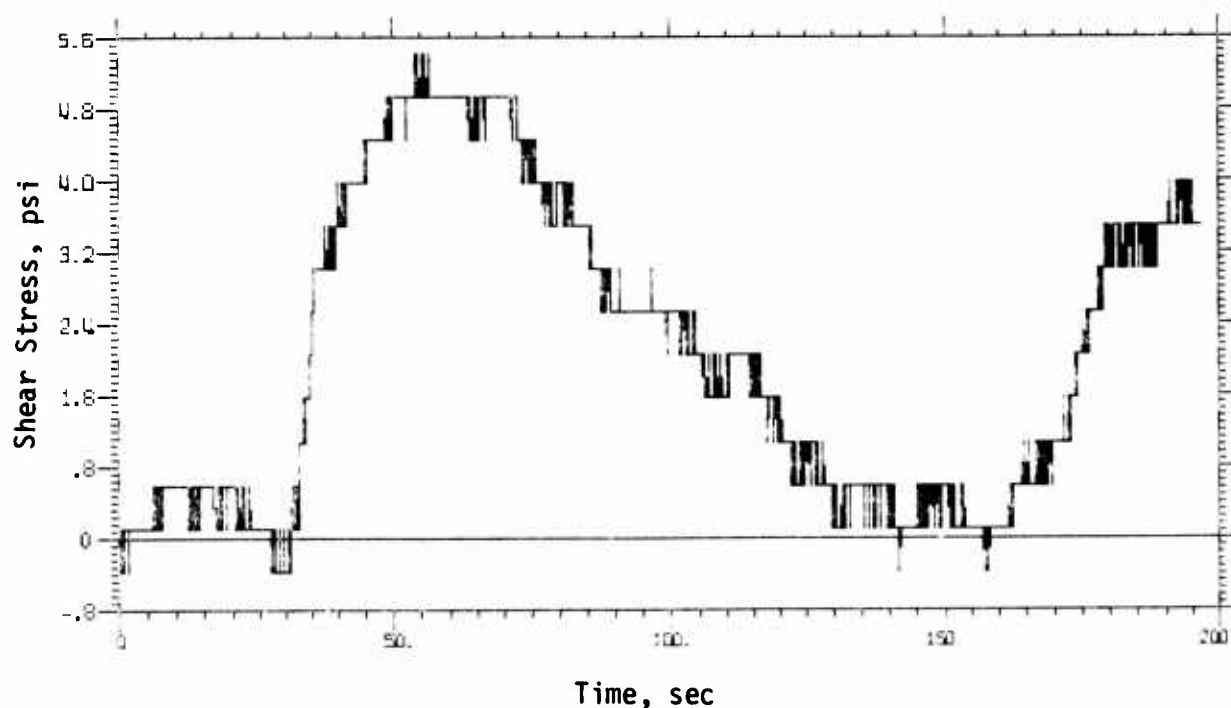
Horizontal Shear Stress

TEST 3 (1 of 2)
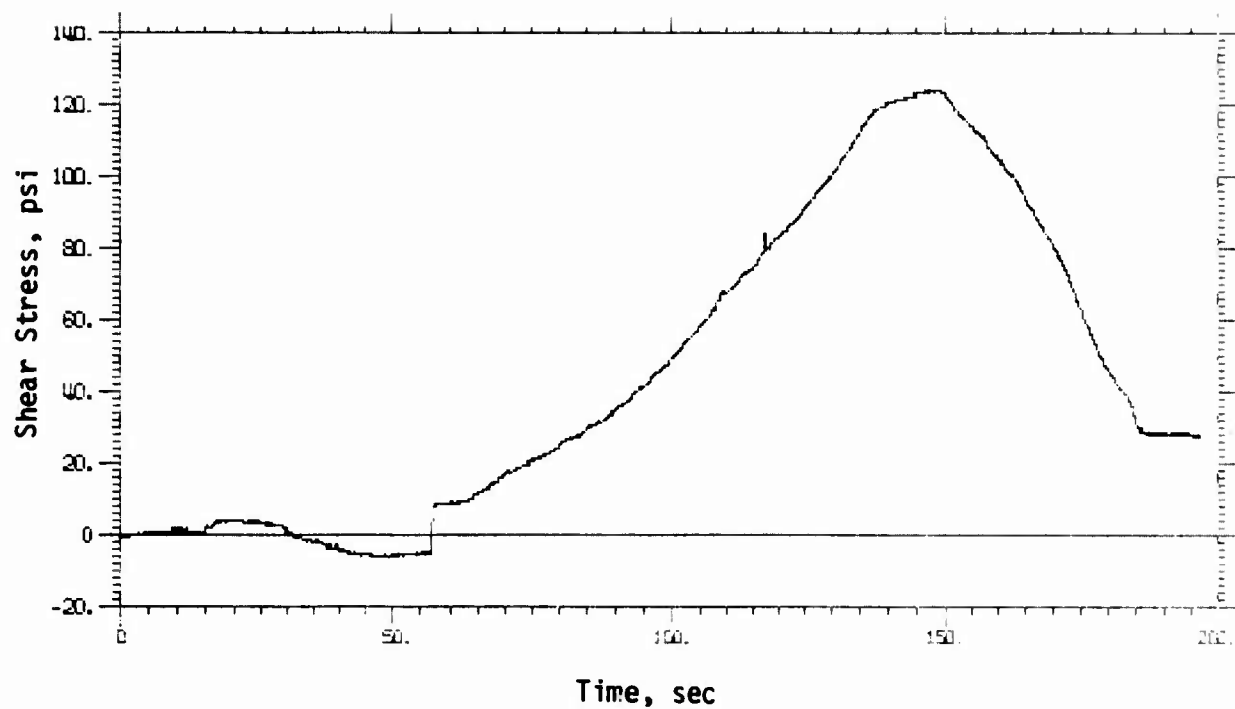
Vertical Shear Stress
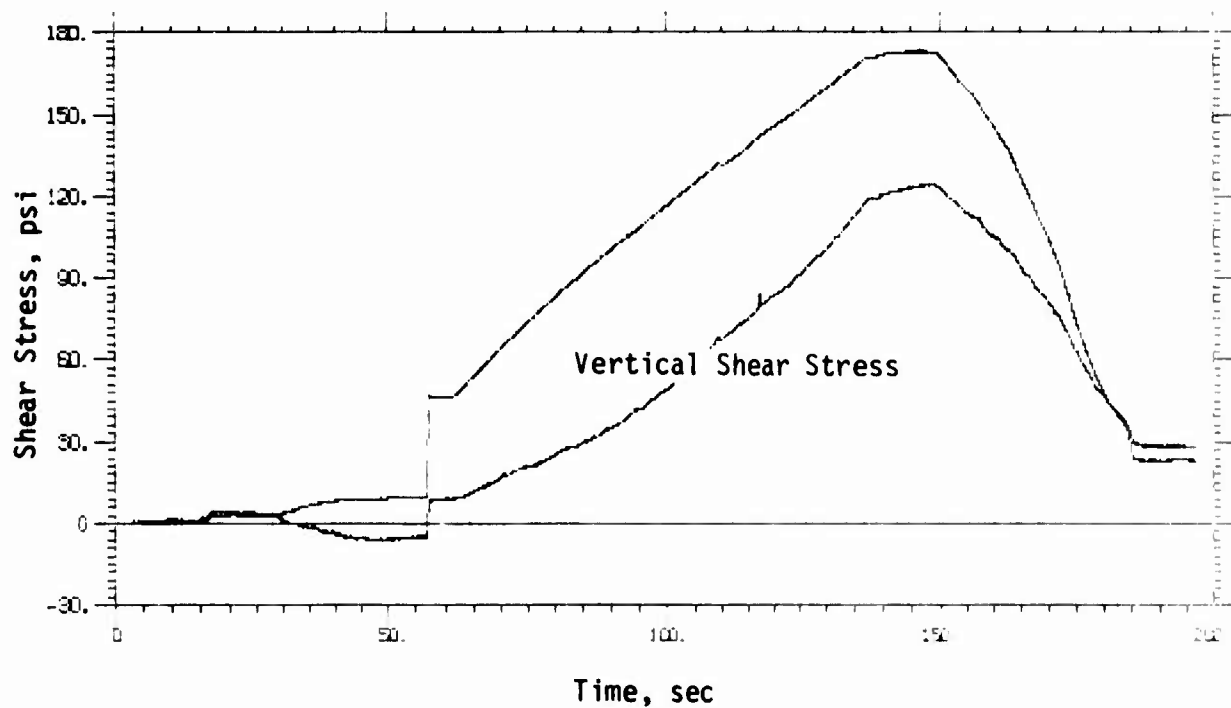
Inferred Vertical Shear Stress

TEST 3 (2 of 2)
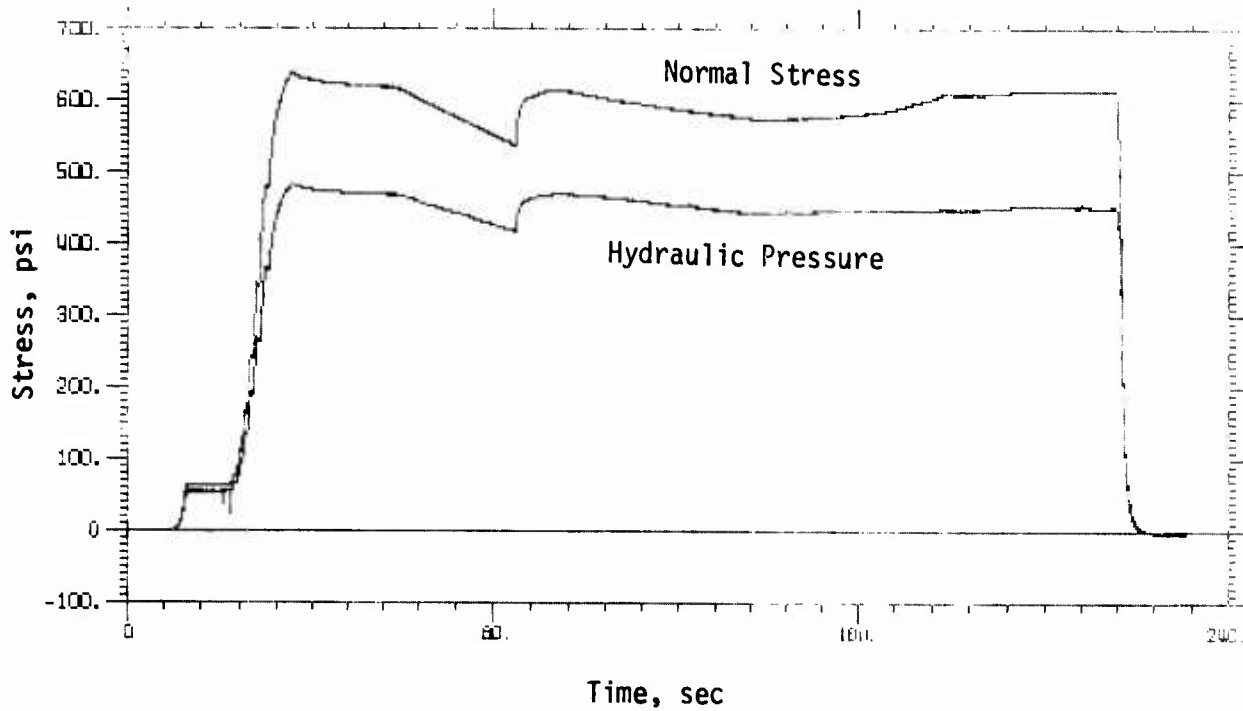
Time, sec

Hydraulic Pressure and Normal Stress
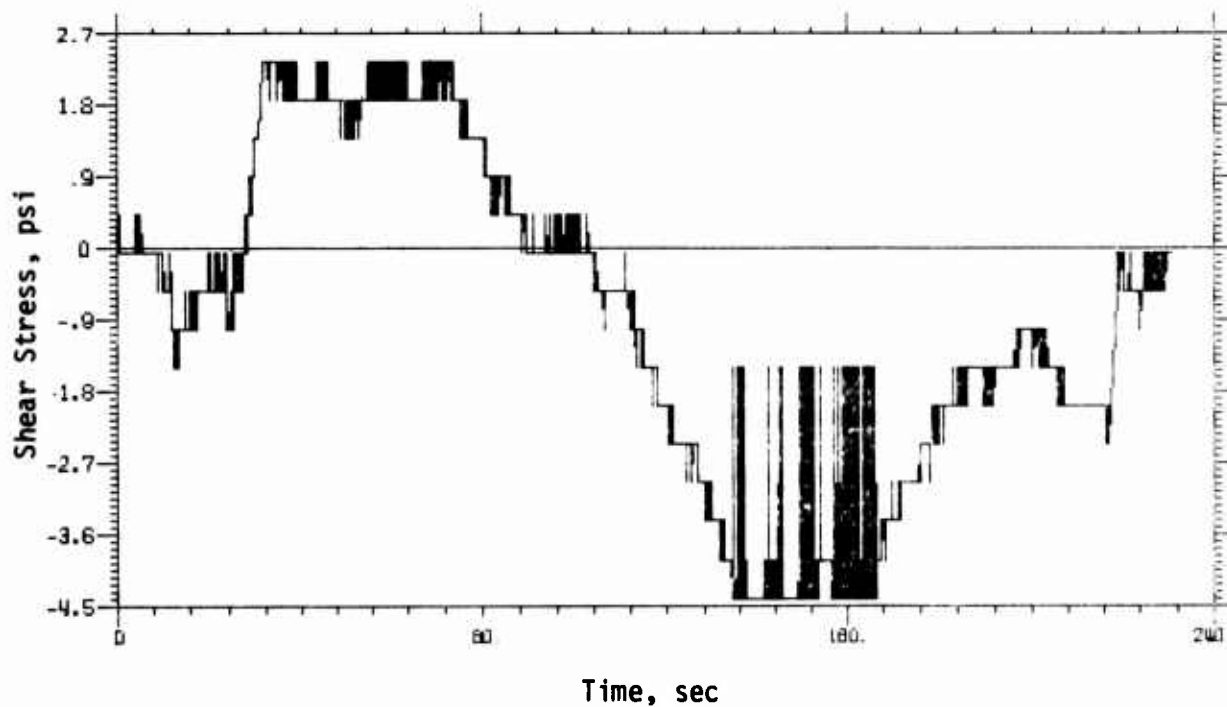
Time, sec

Horizontal Shear Stress

TEST 4 (1 of 2)

Time, sec
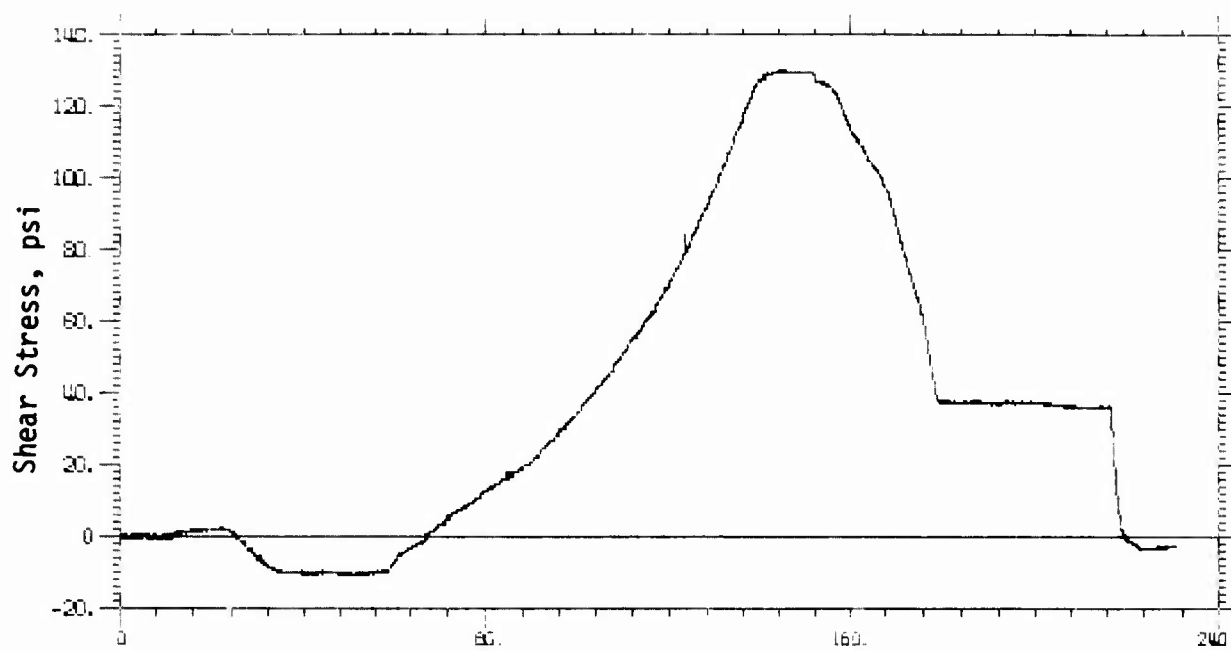
Vertical Shear Stress

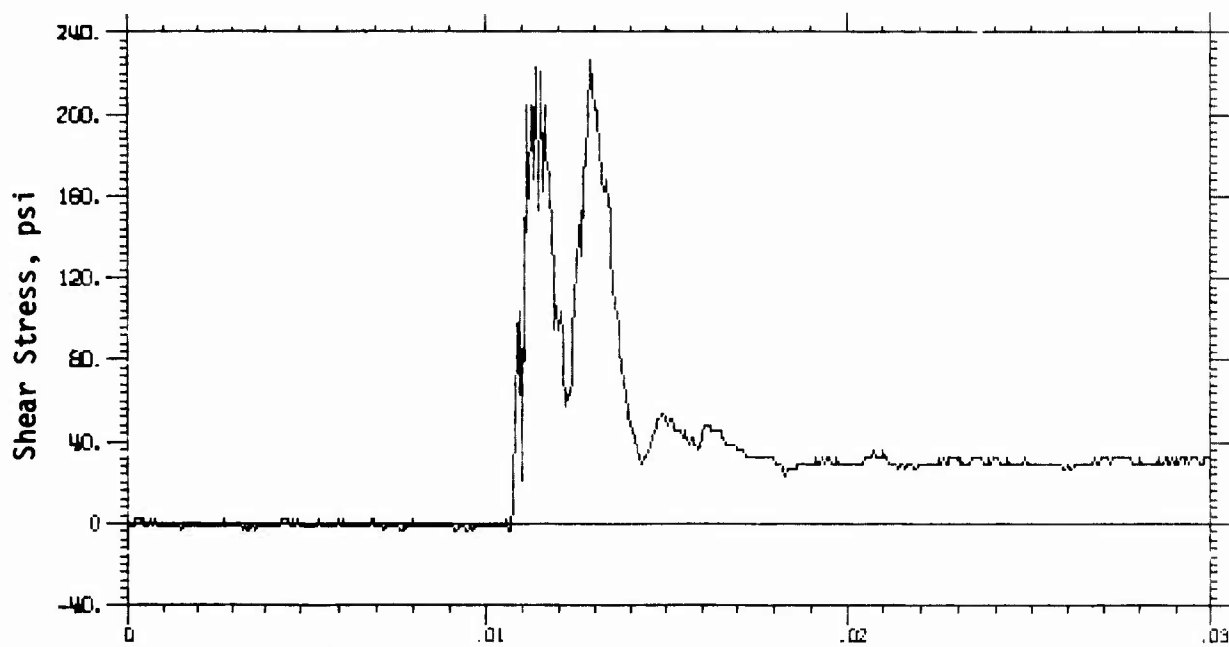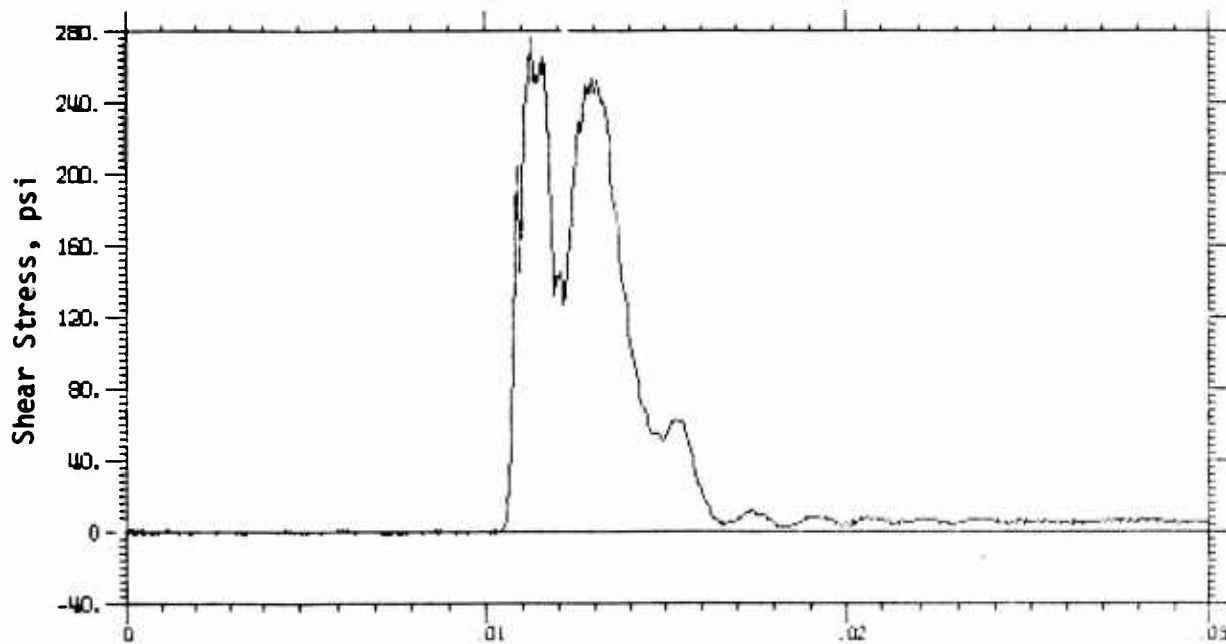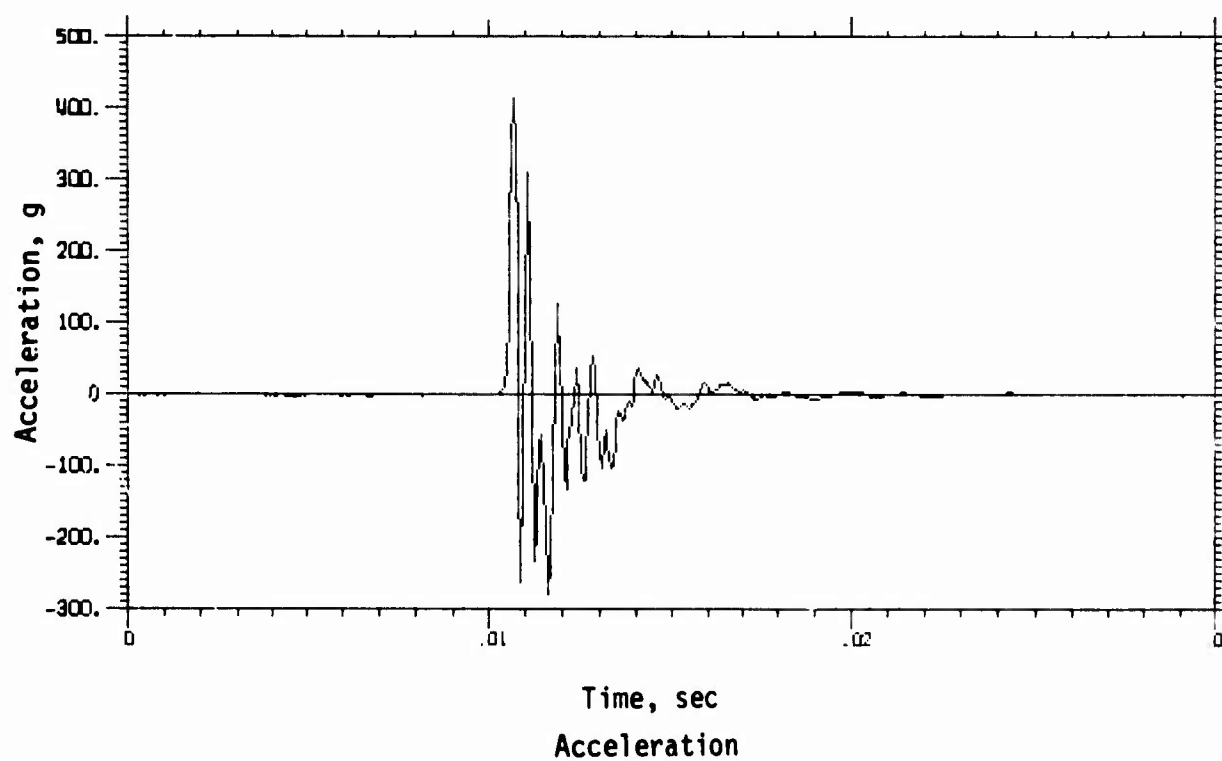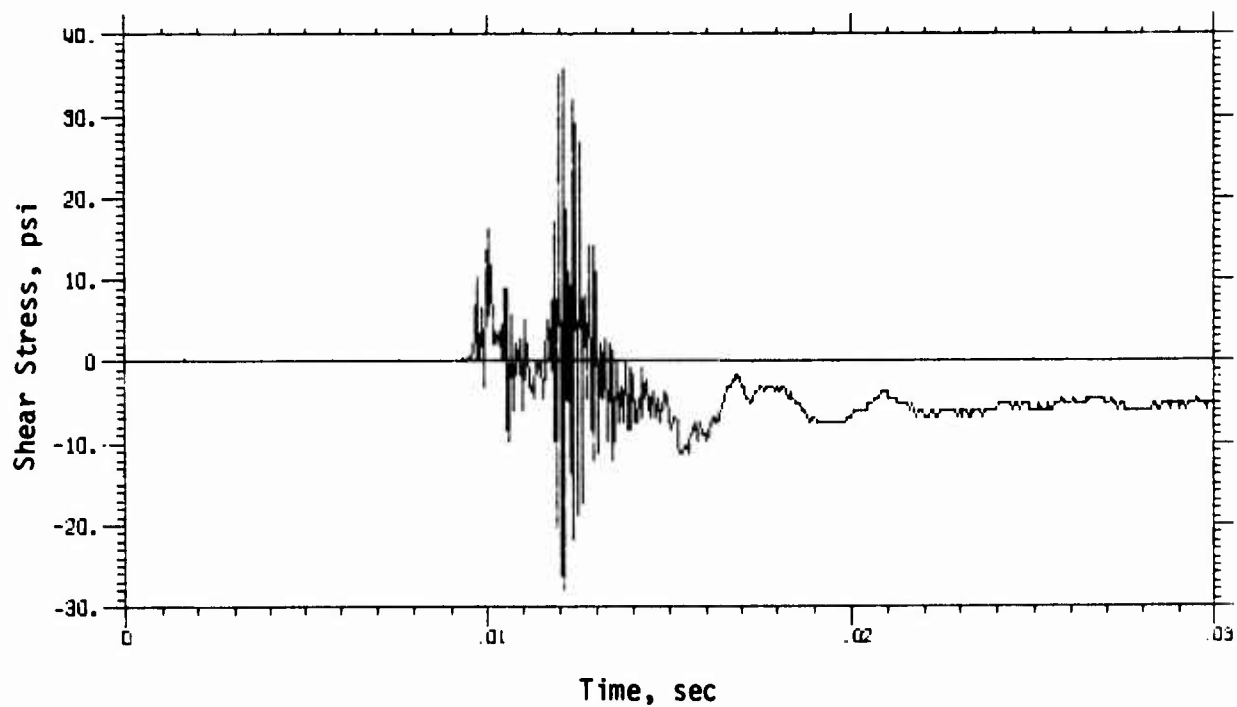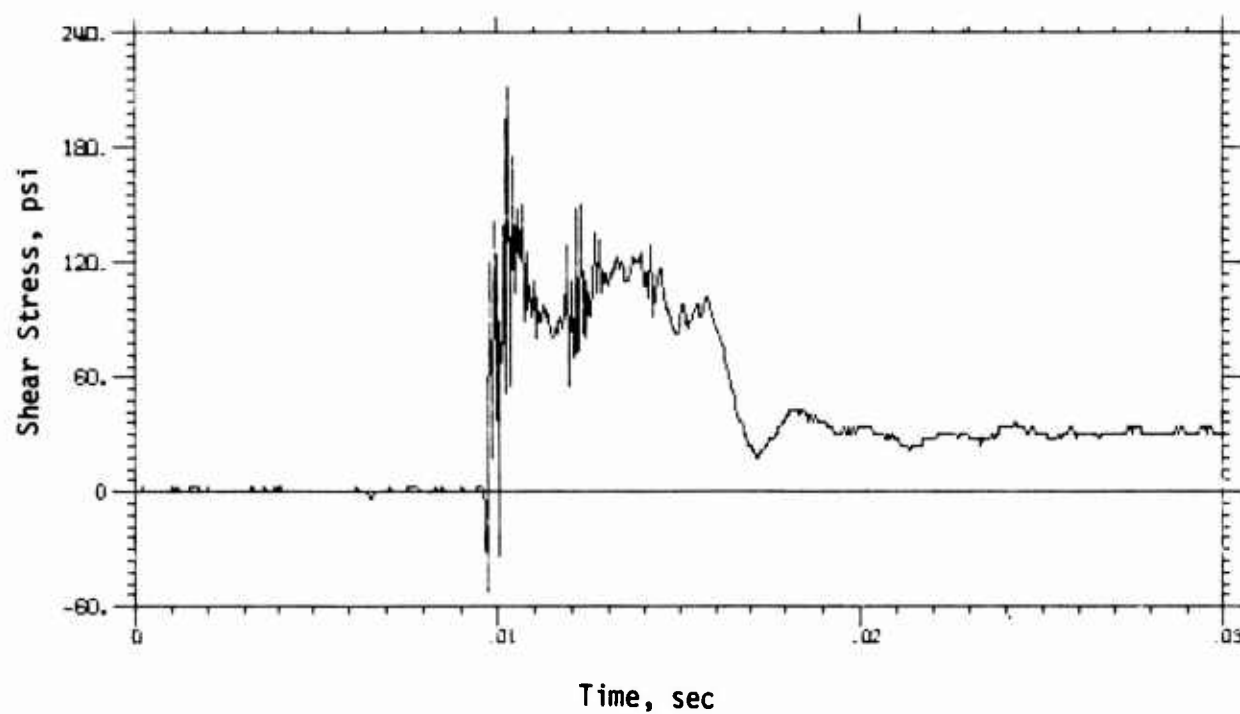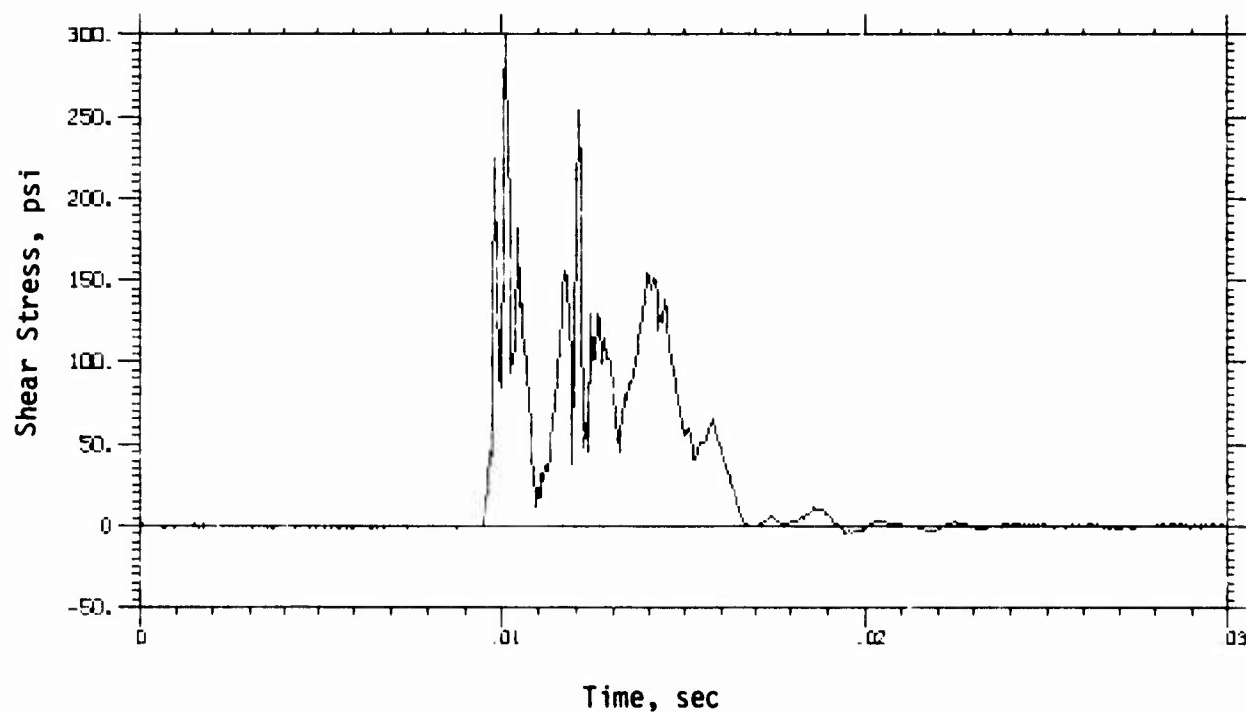Vertical Shear Stress
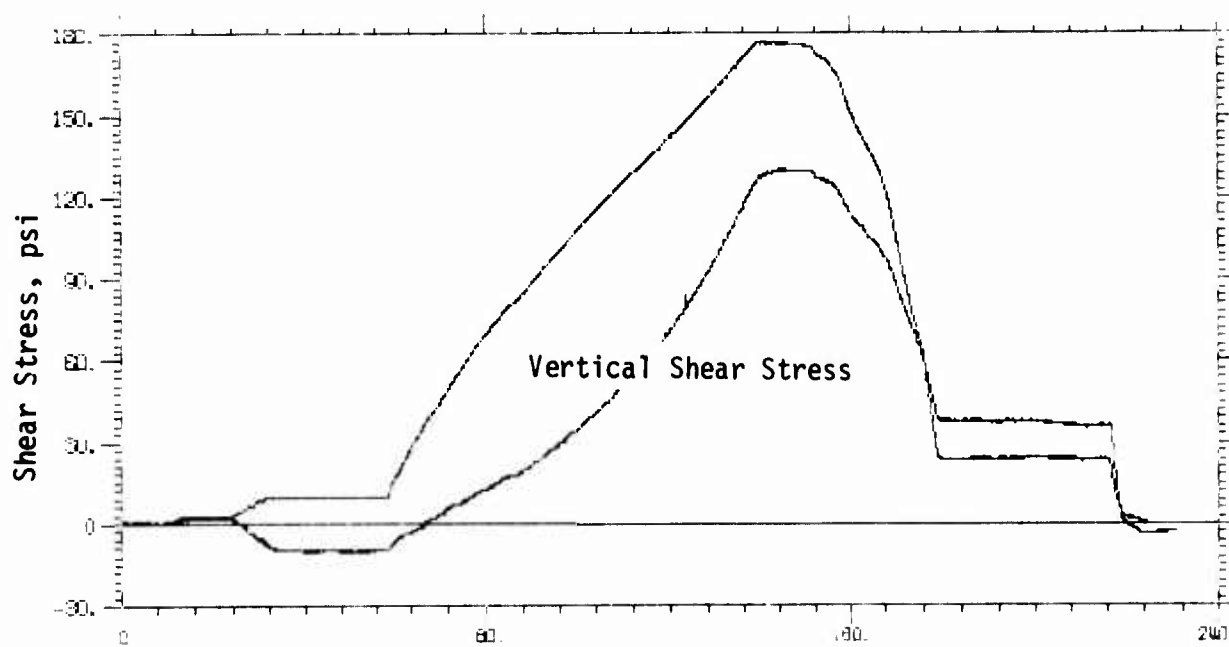
Time, sec

Inferred Vertical Shear Stress

TEST 4 (2 of 2)

57

Time, sec

Hydraulic Pressure and Normal Stress

Time, sec
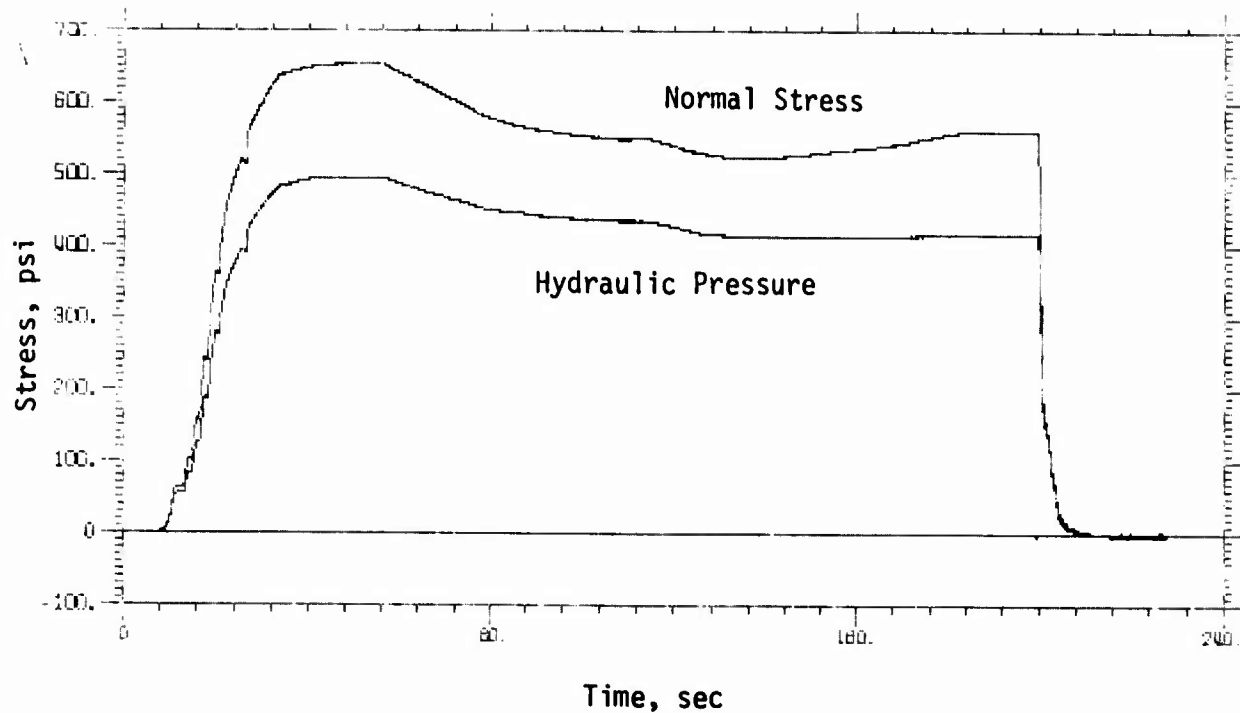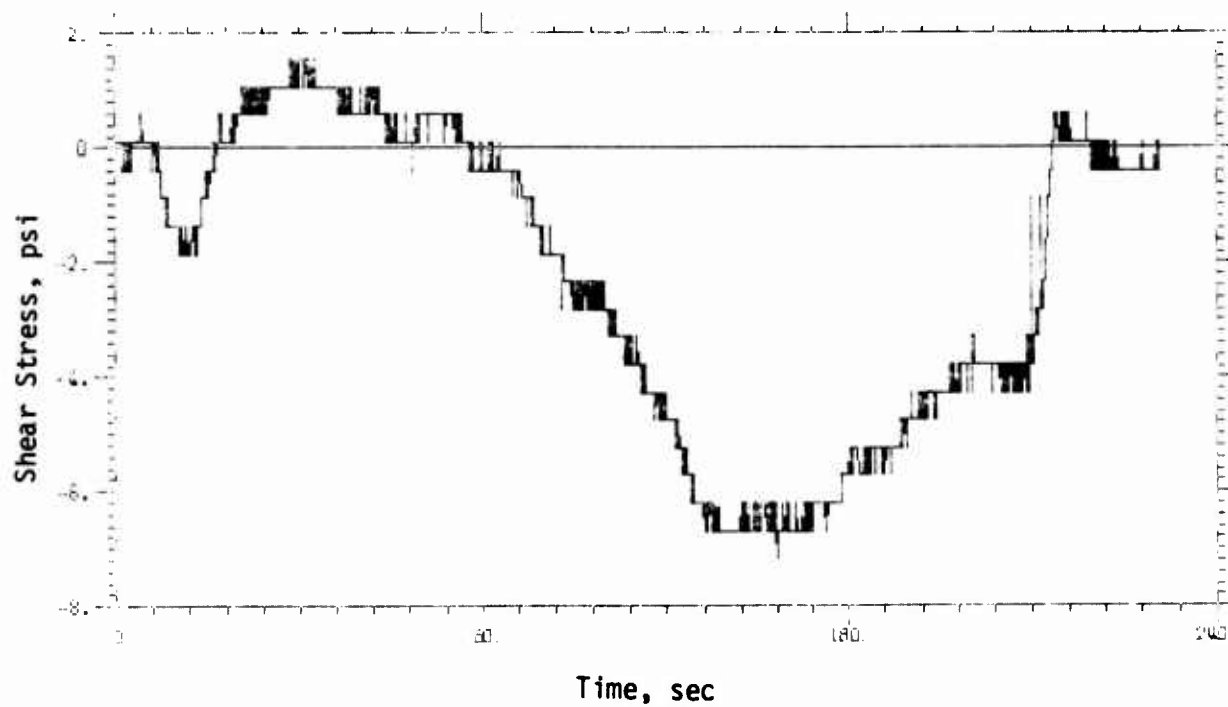
Horizontal Shear Stress

TEST 5 (1 of 2)

Time, sec

Vertical Shear Stress

Time, sec
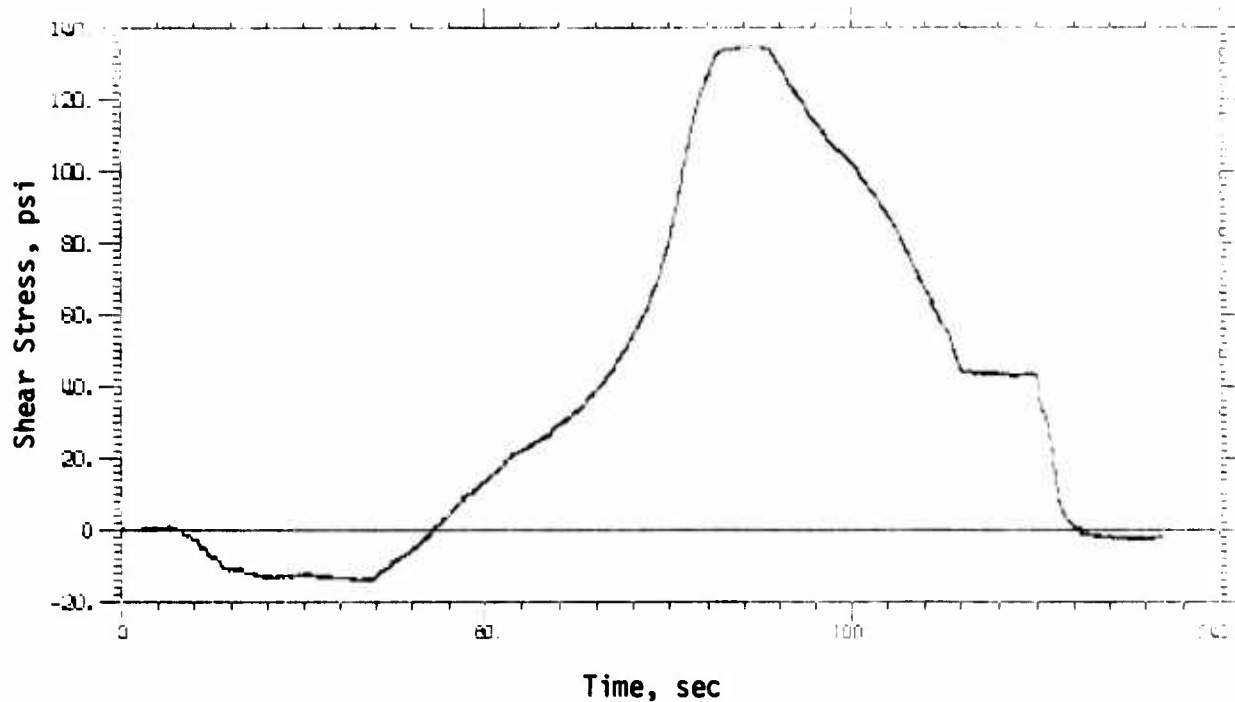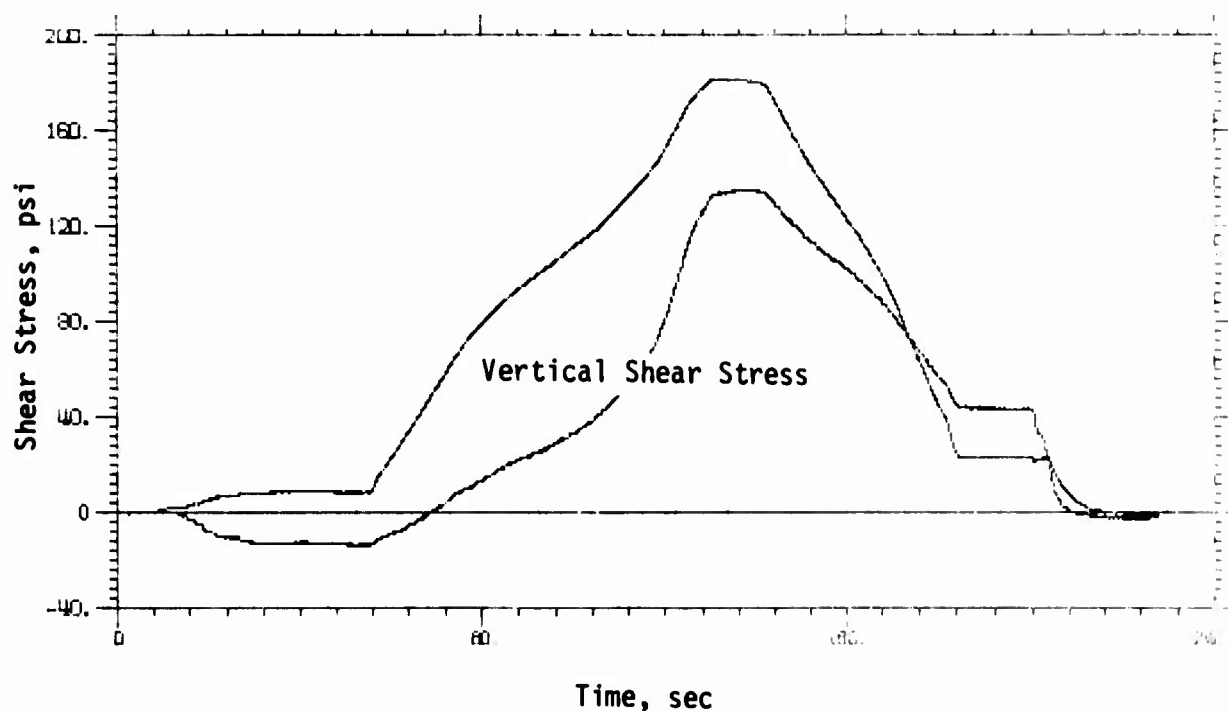
Inferred Vertical Shear Stress

TEST 5 (2 of 2)

59
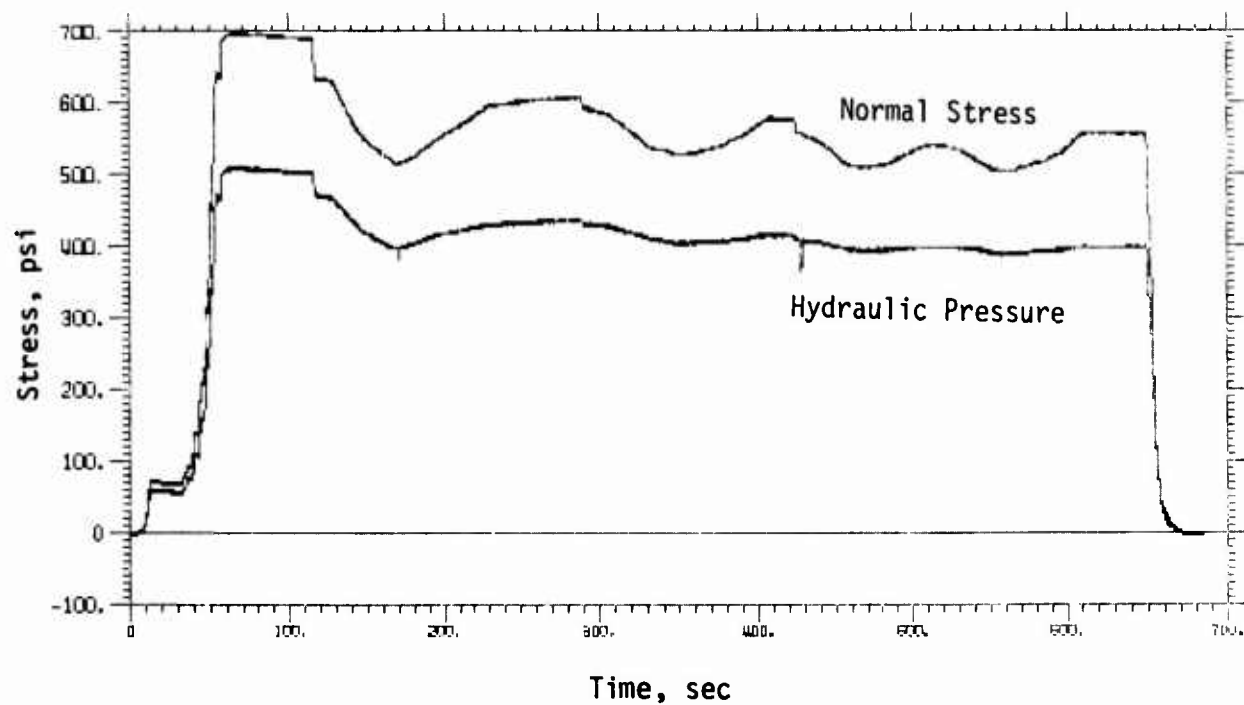
Hydraulic Pressure and Normal Stress
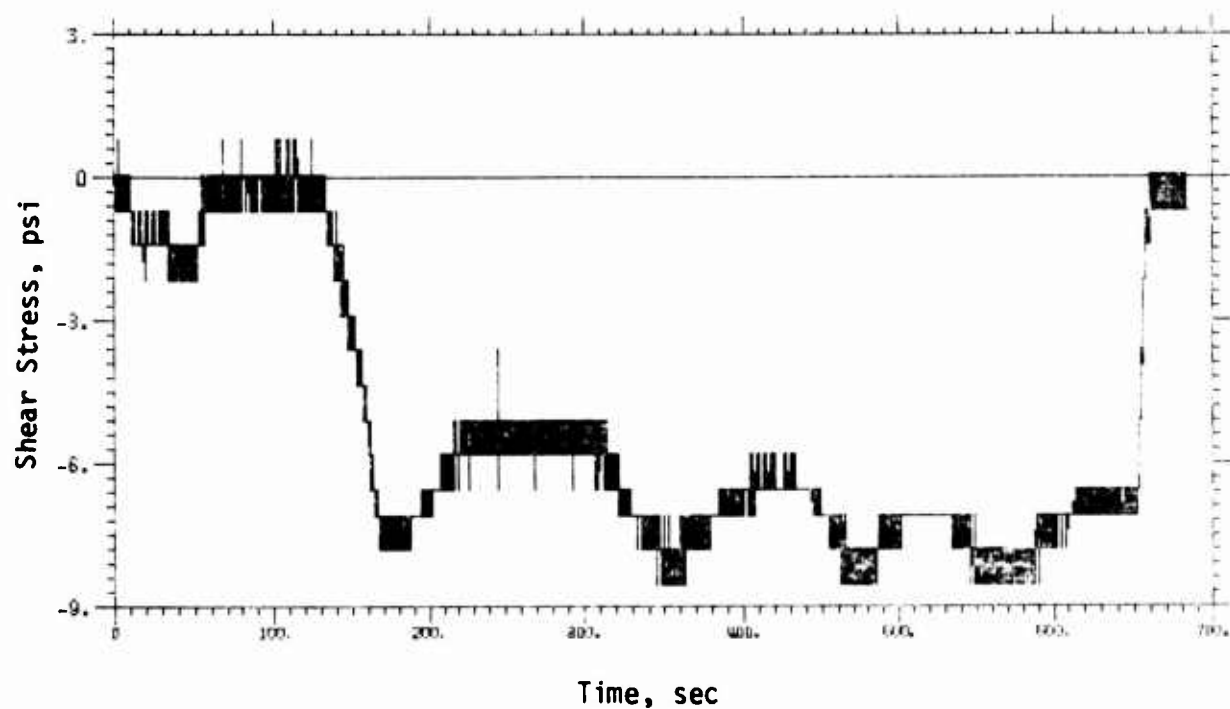
Horizontal Shear Stress

TEST 6 (1 of 2)
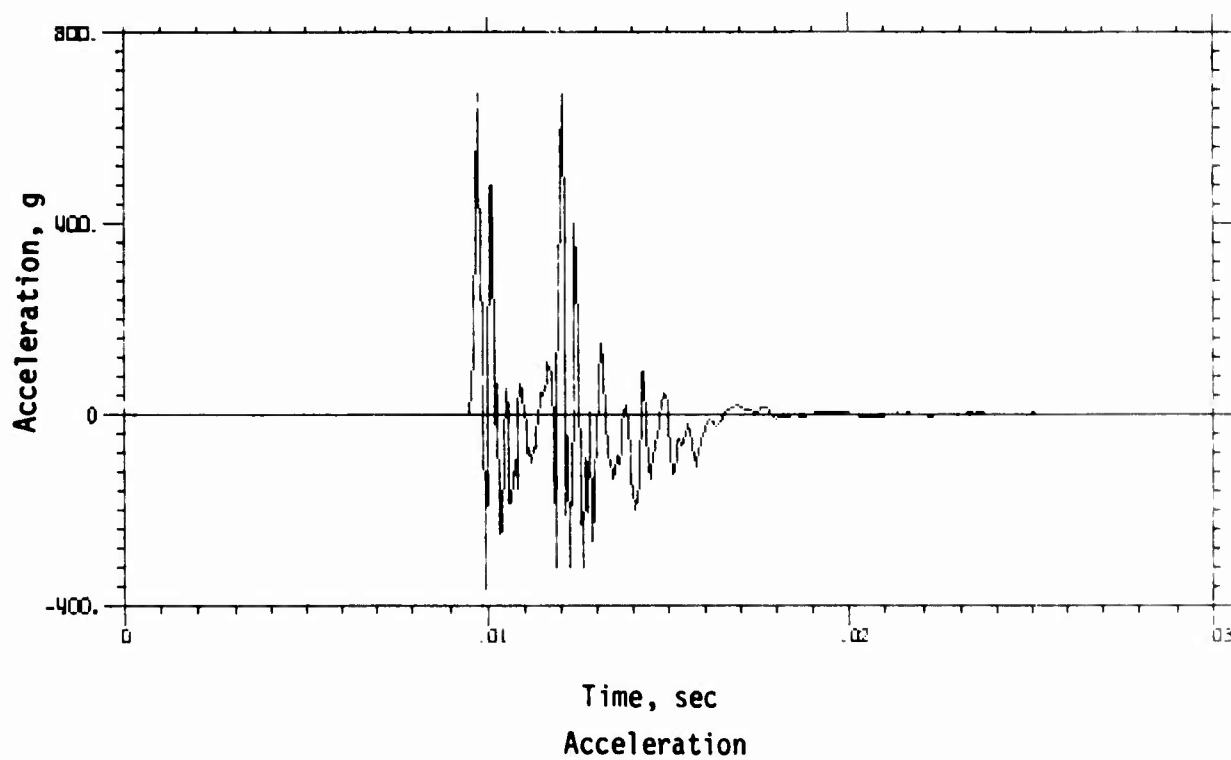
60
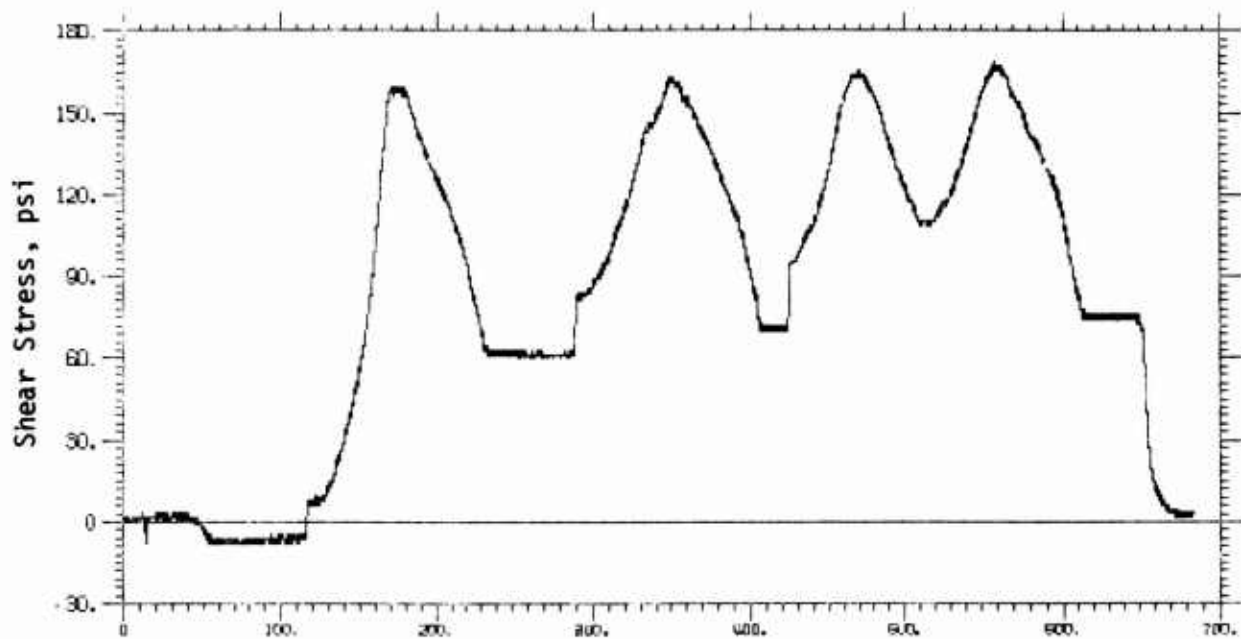
Time, sec

Vertical Shear Stress
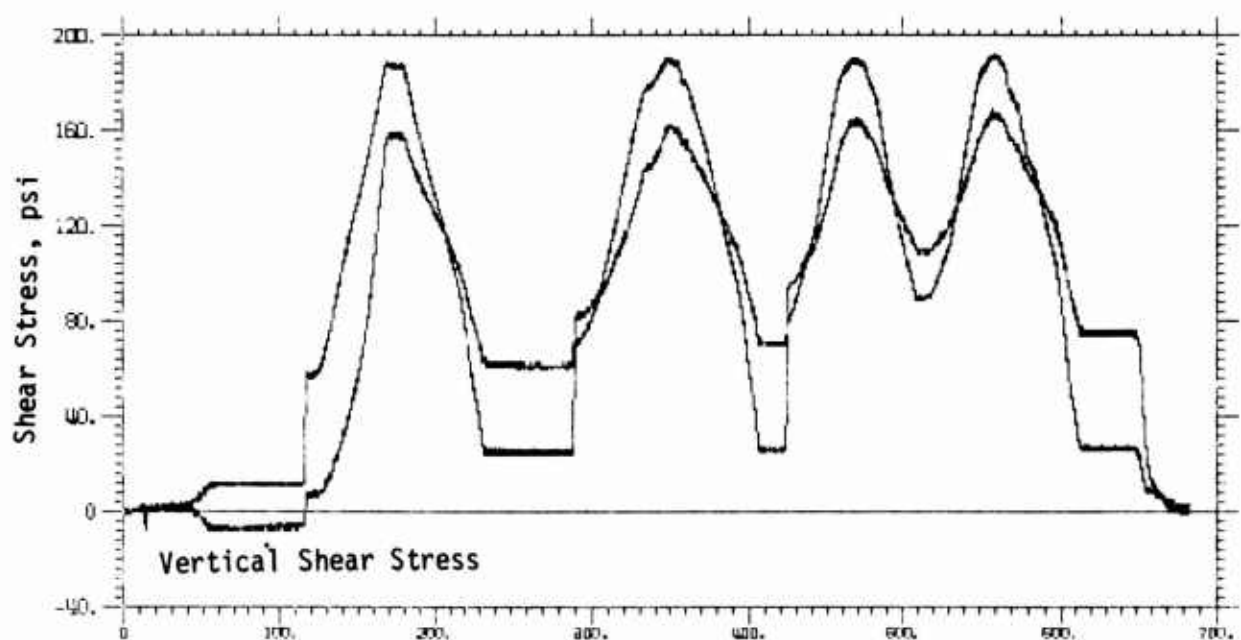
Time, sec

Inferred Vertical Shear Stress

TEST 6 (2 of 2)
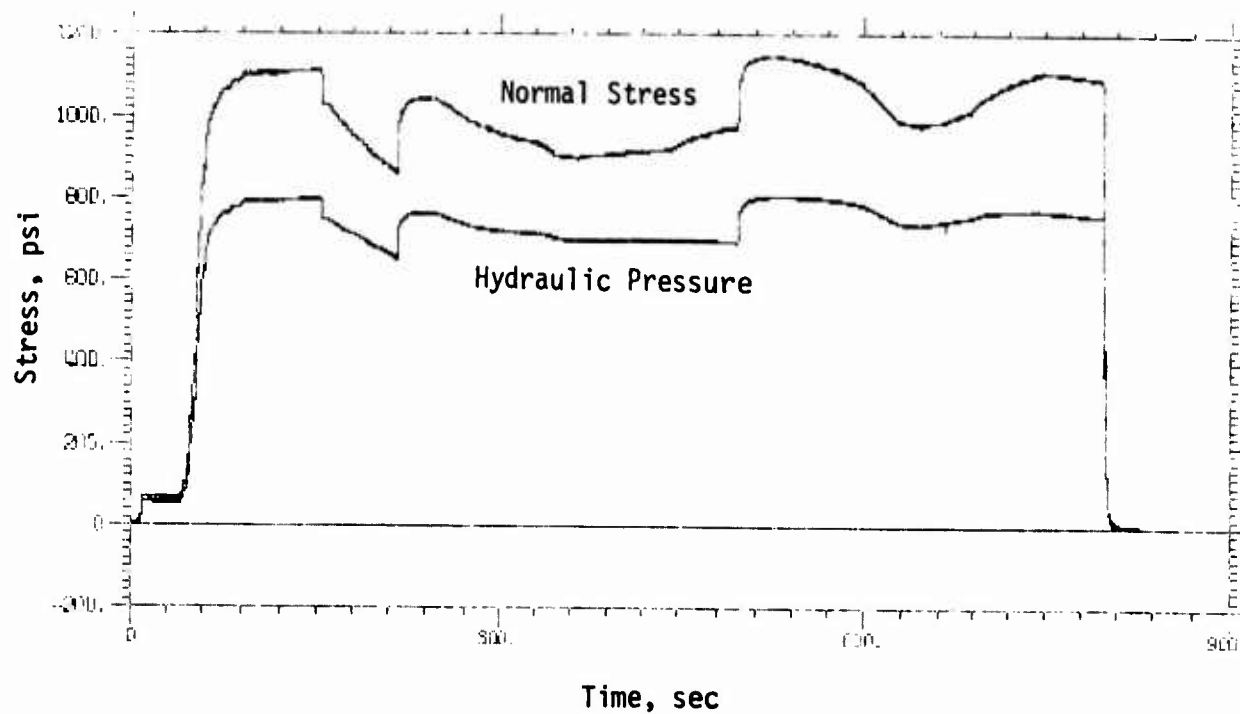
Hydraulic Pressure and Normal Stress
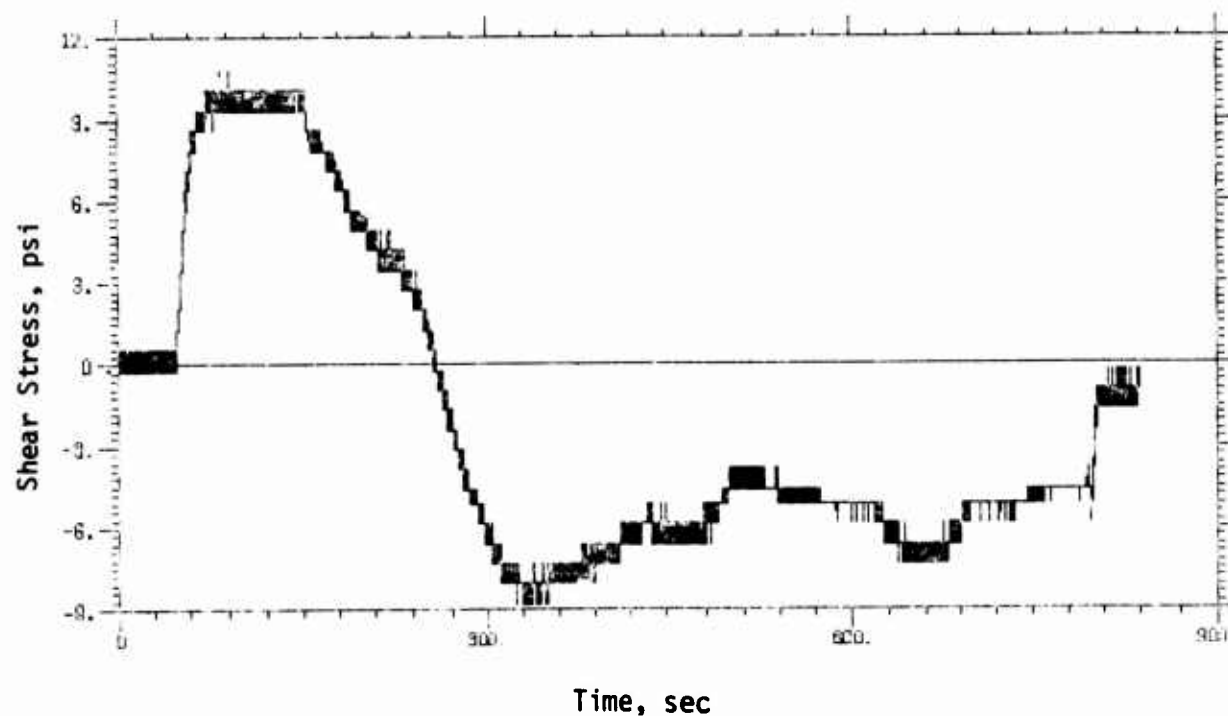
Horizontal Shear Stress

TEST 8 (1 of 2)

62
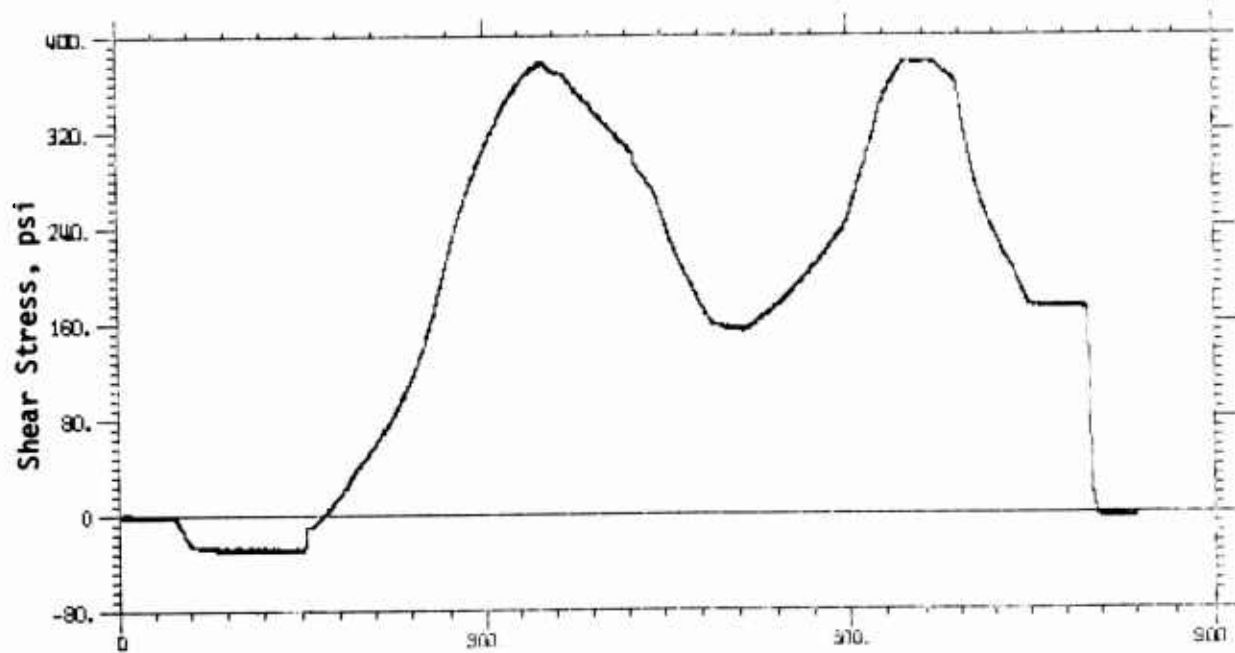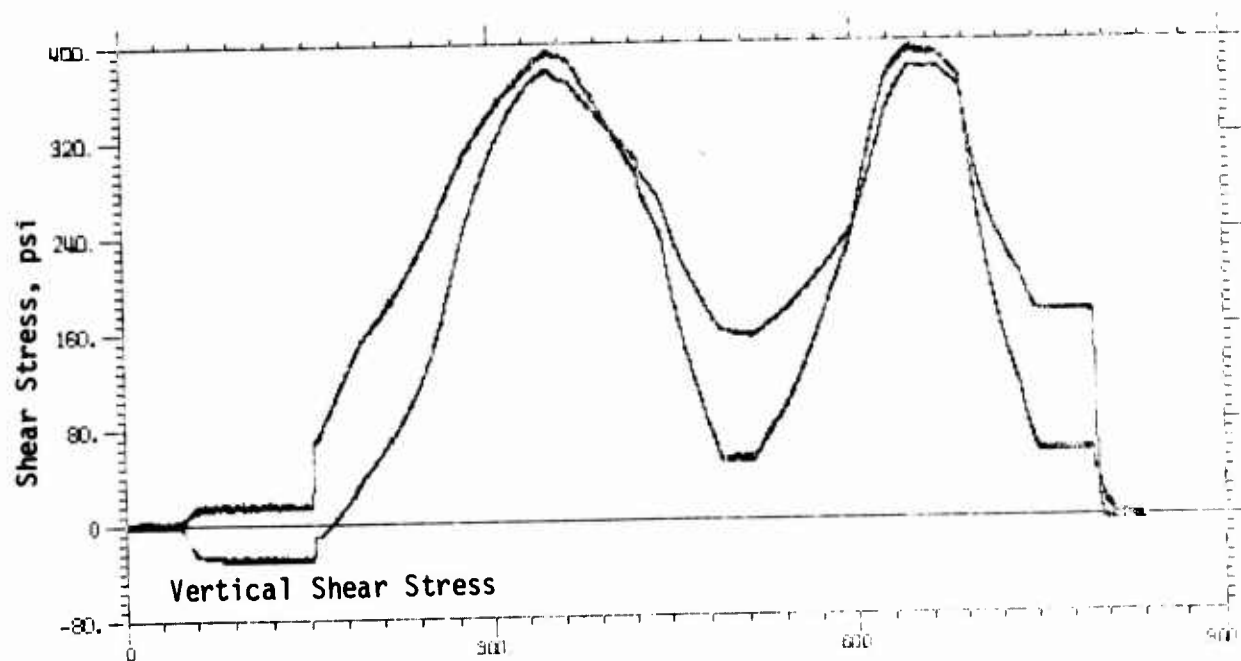
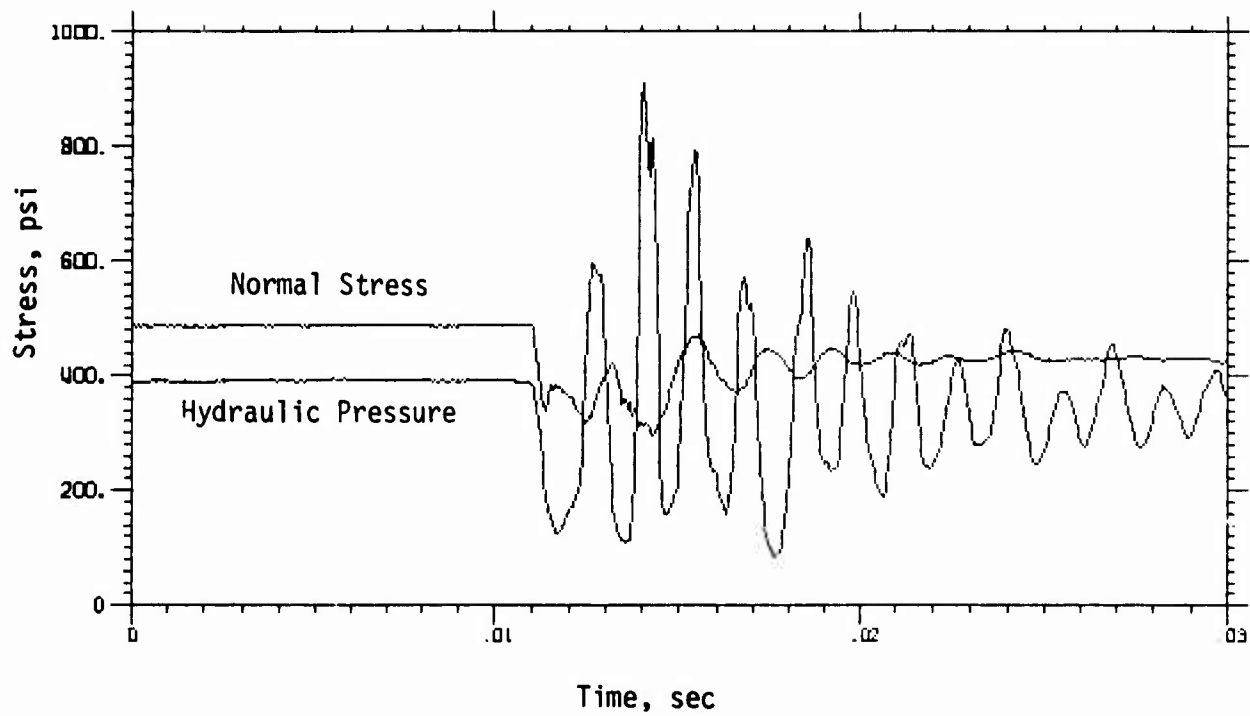Vertical Shear Stress

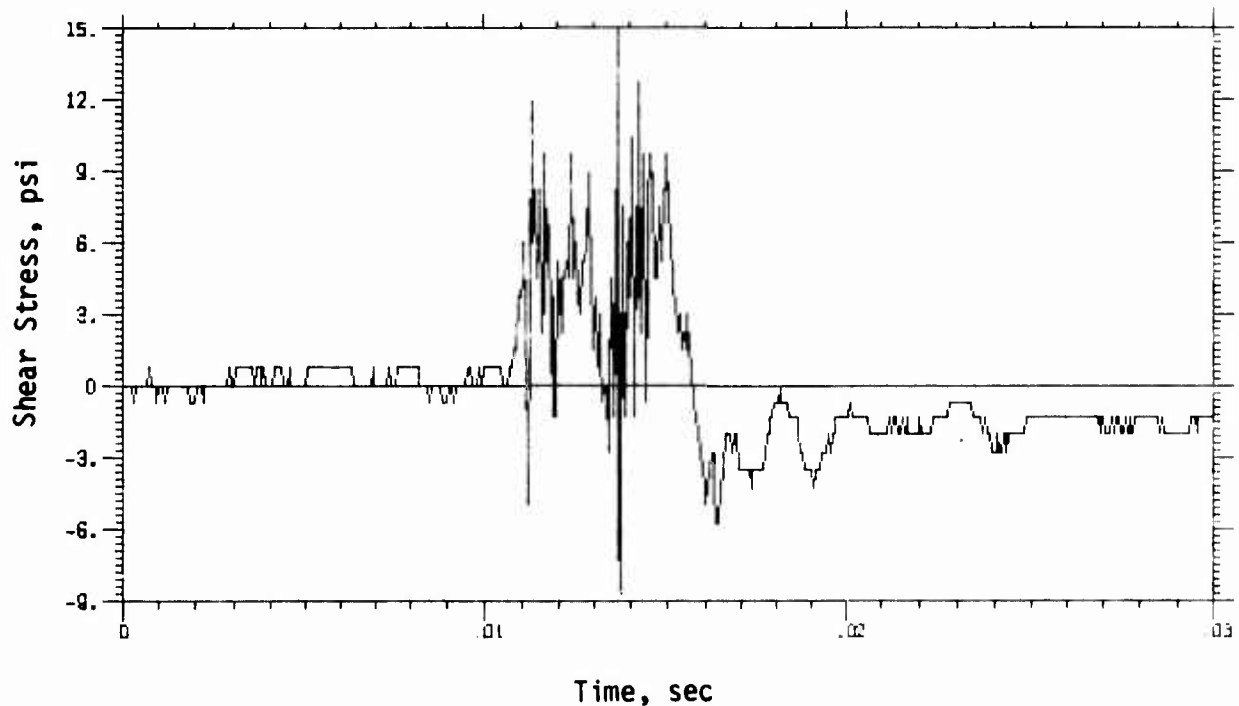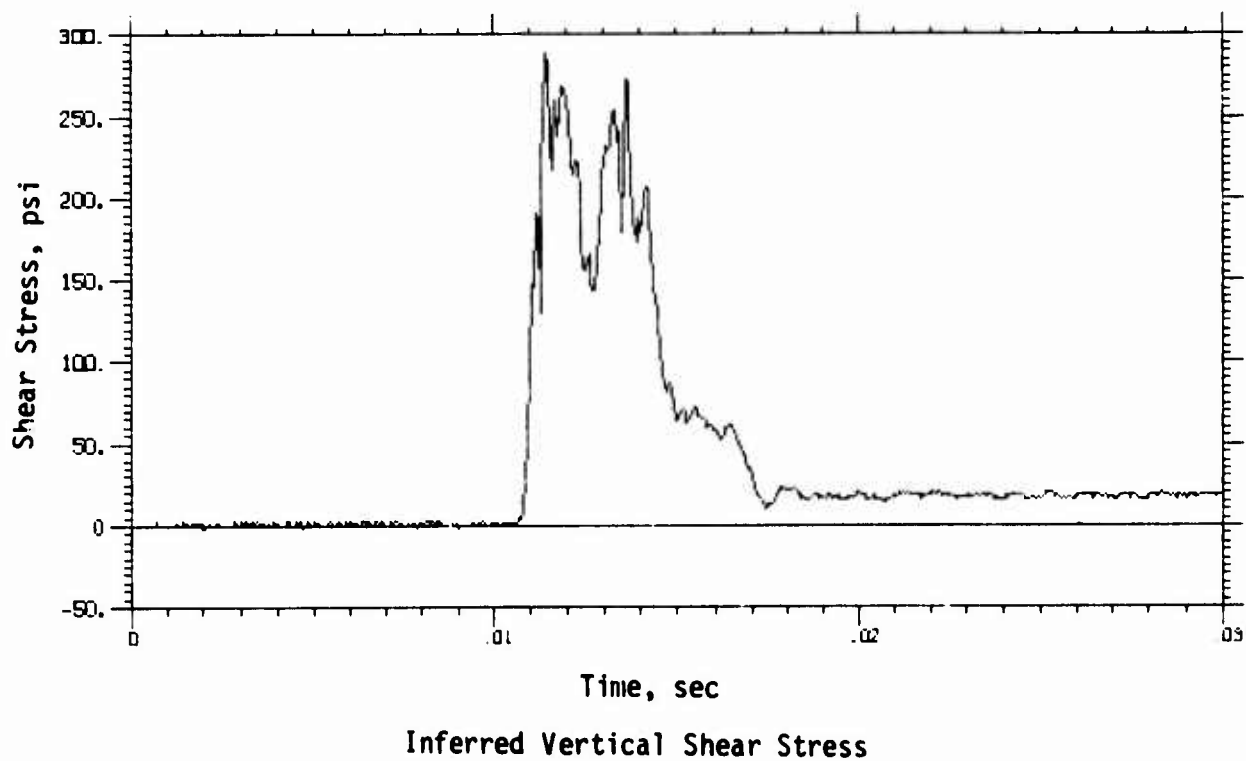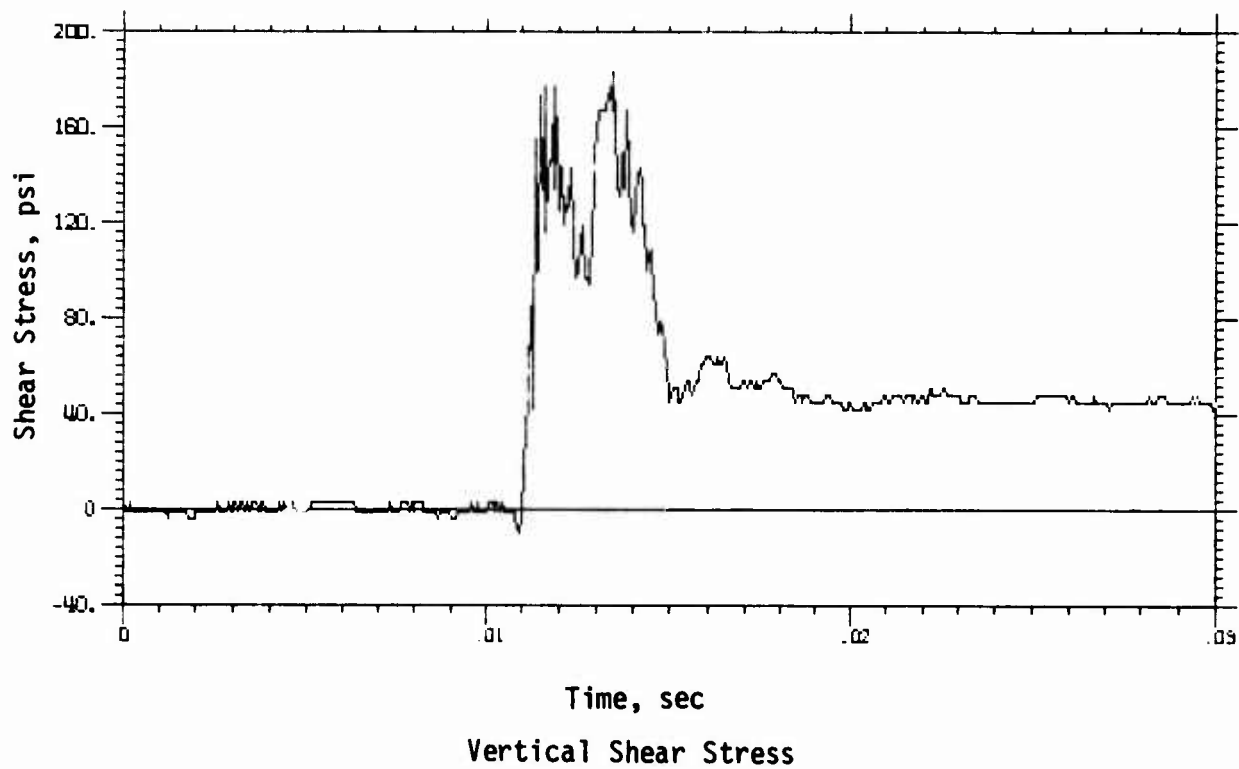Inferred Vertical Shear Stress

TEST 8 (2 of 2)
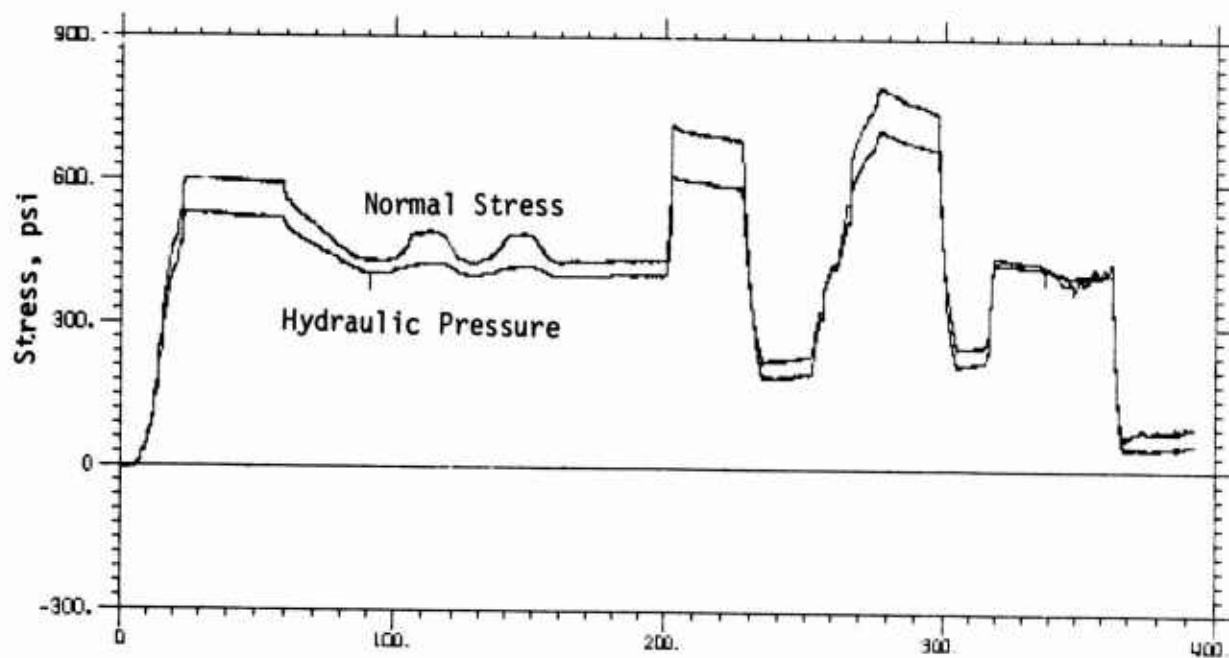
Hydraulic Pressure and Normal Stress
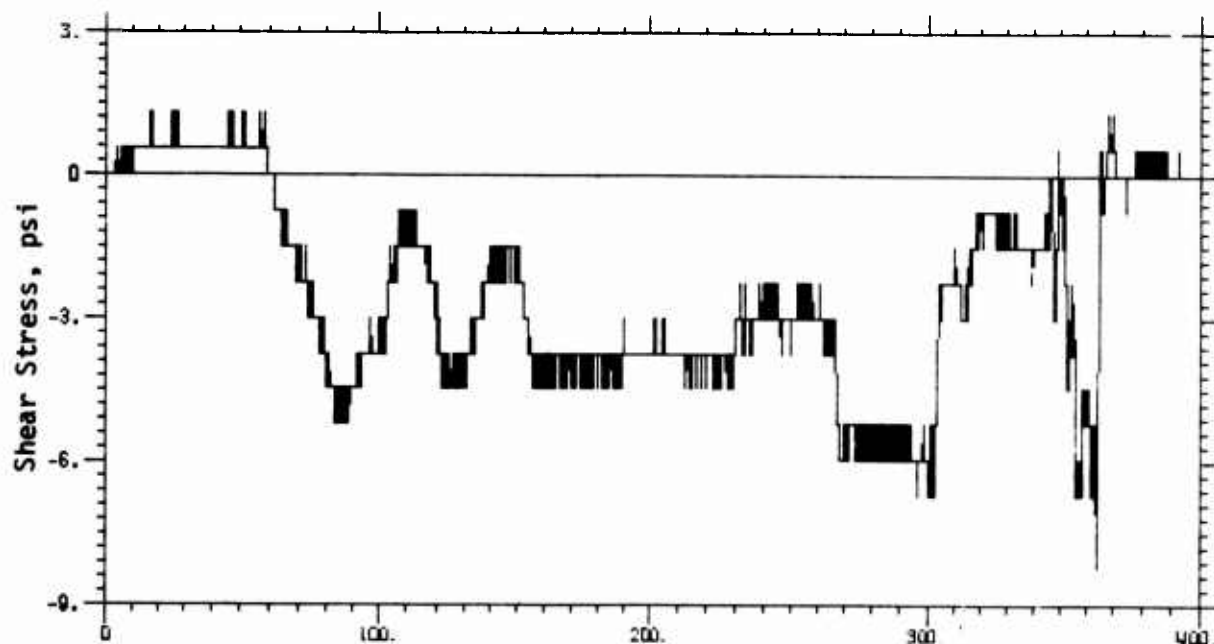
Horizontal Shear Stress

TEST 11 (1 of 2)
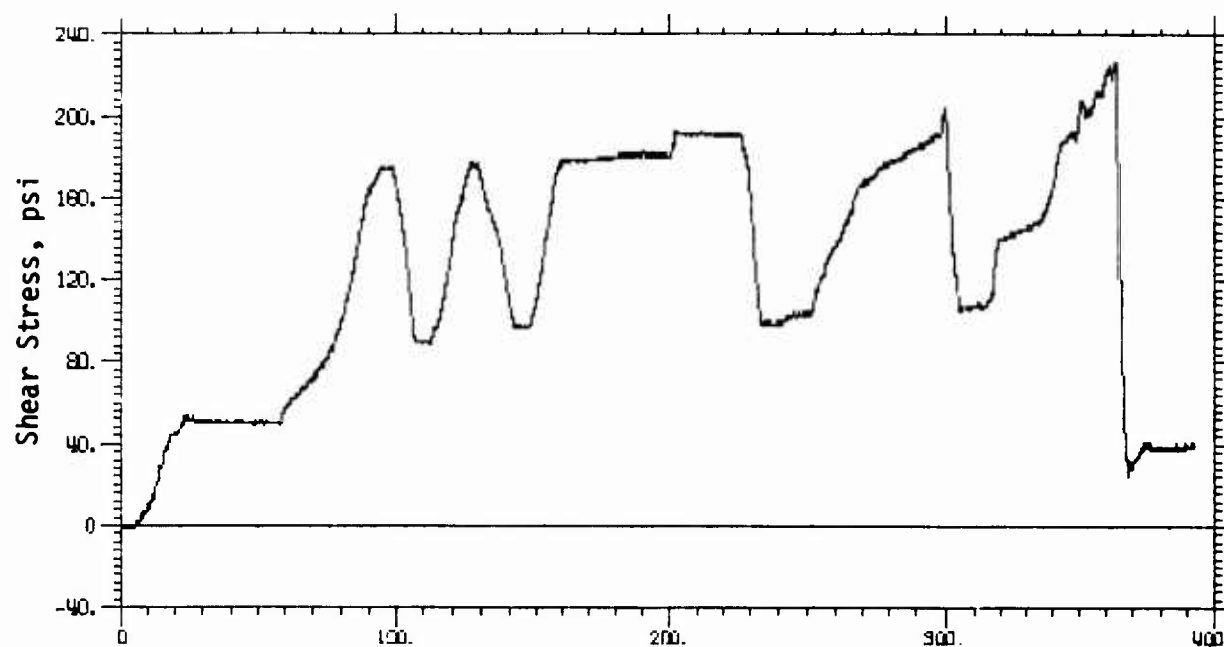
Time, sec

Vertical Shear Stress
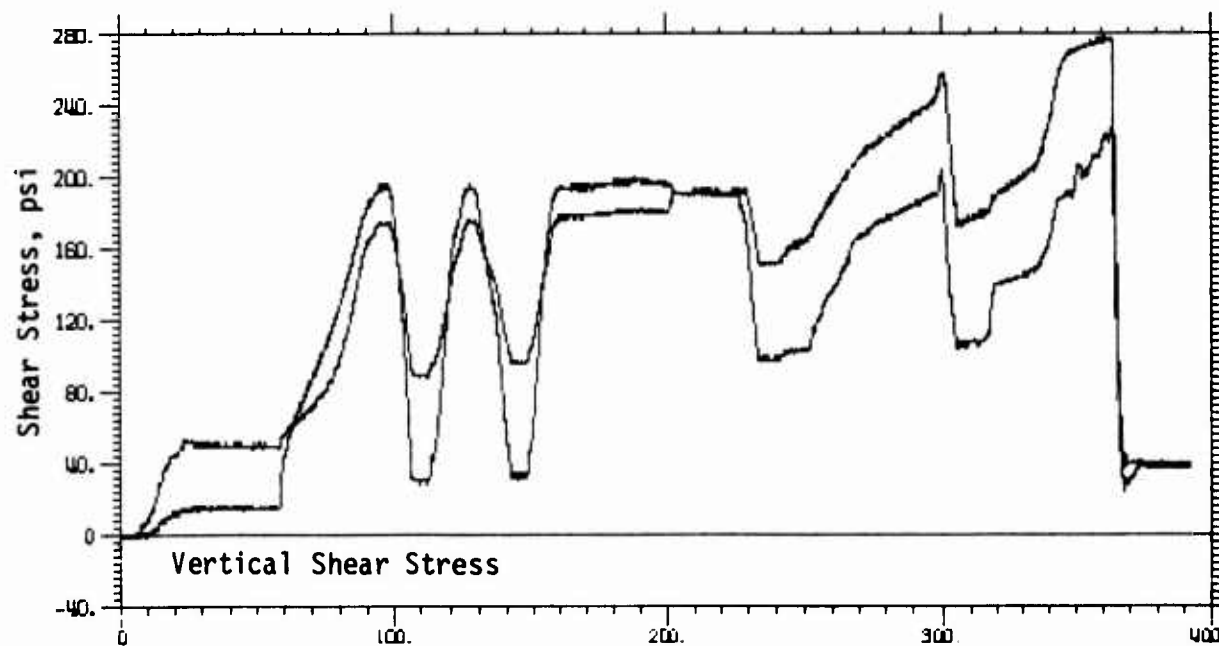
Time, sec

Inferred Vertical Shear Stress

TEST 11 (2 of 2)
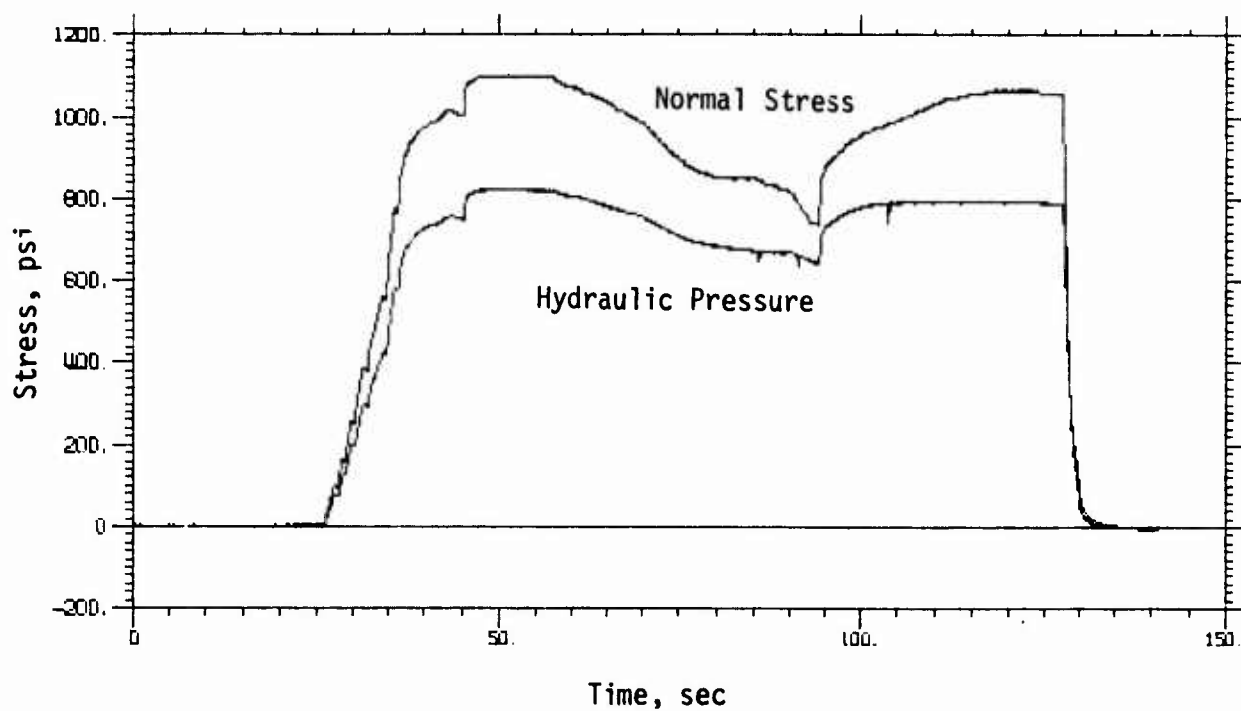
Hydraulic Pressure and Normal Stress
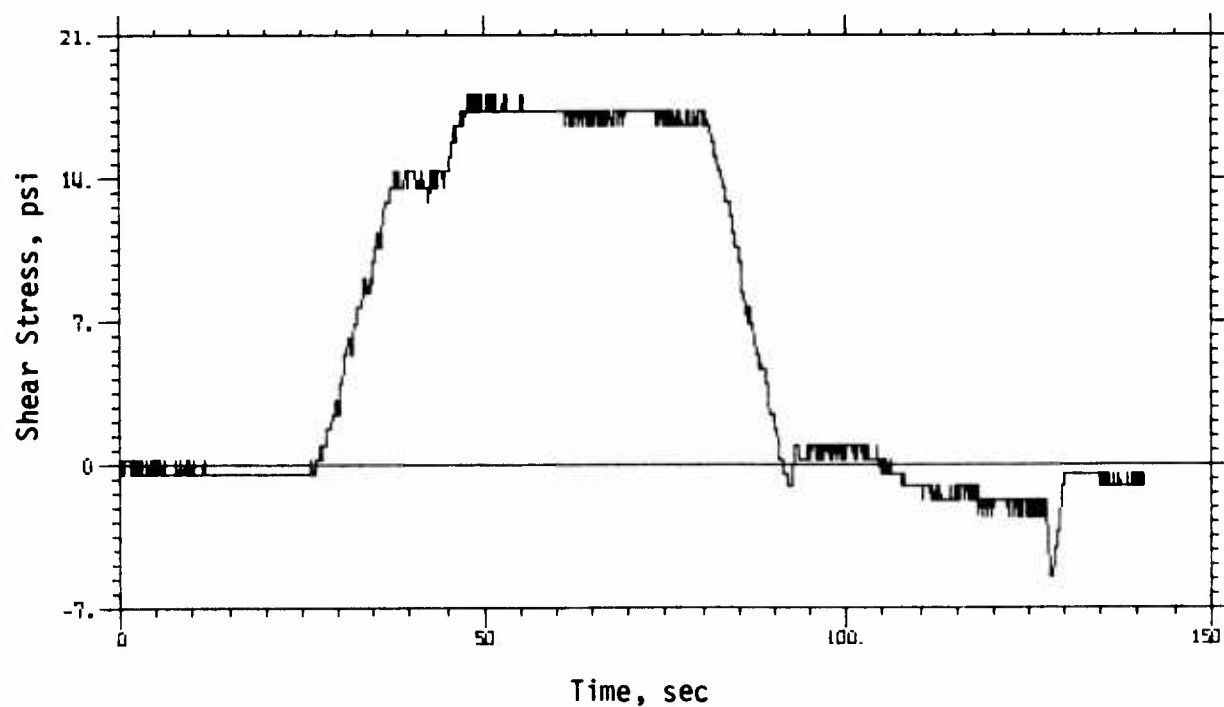
Horizontal Shear Stress

TEST 16 (1 of 2)
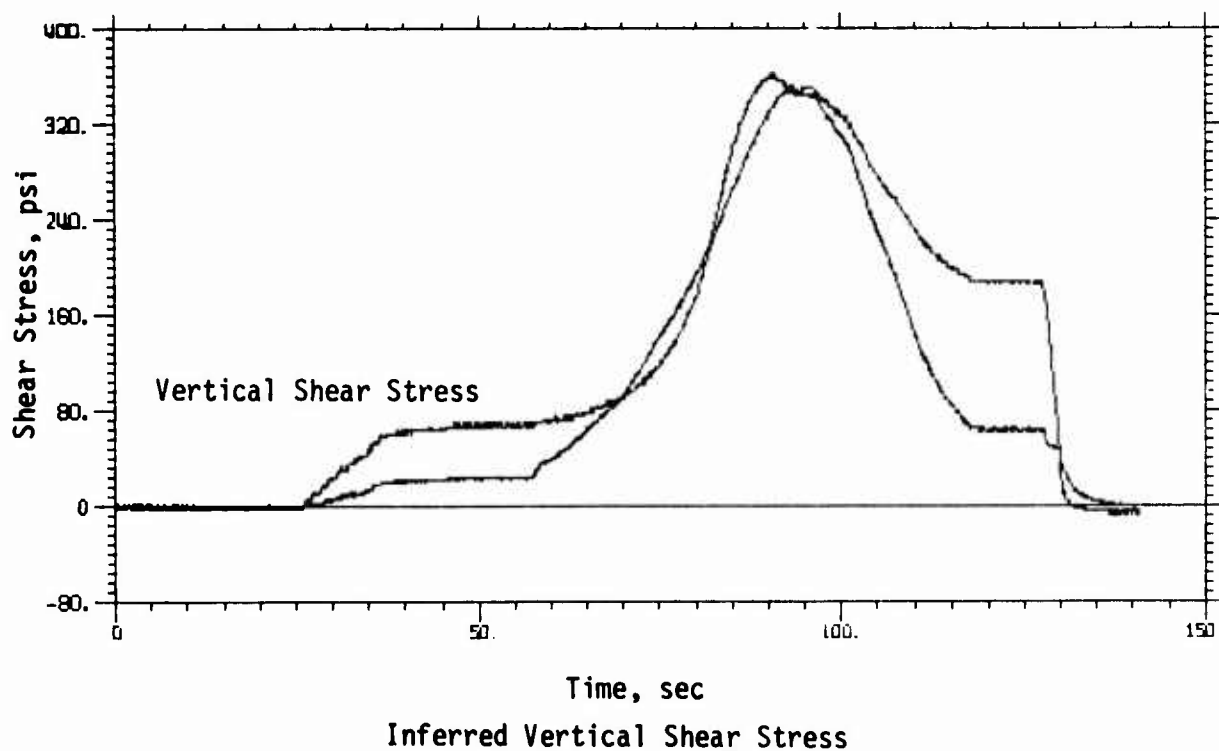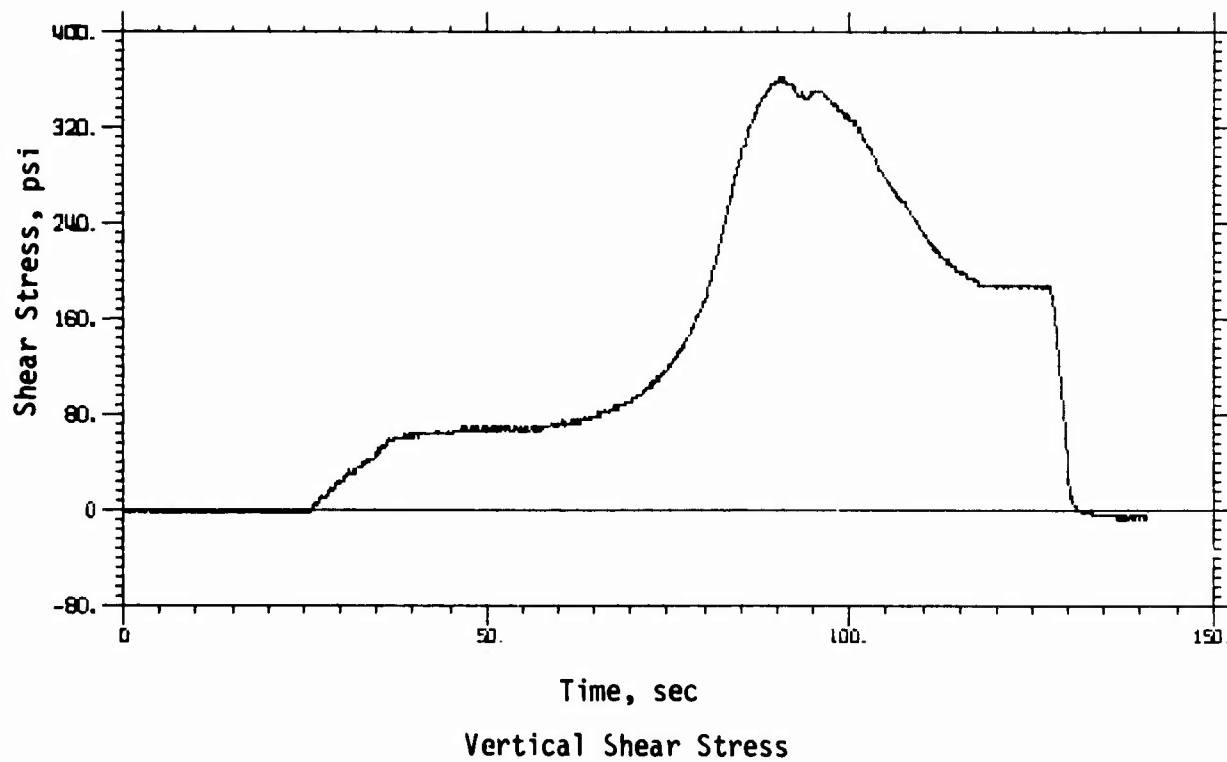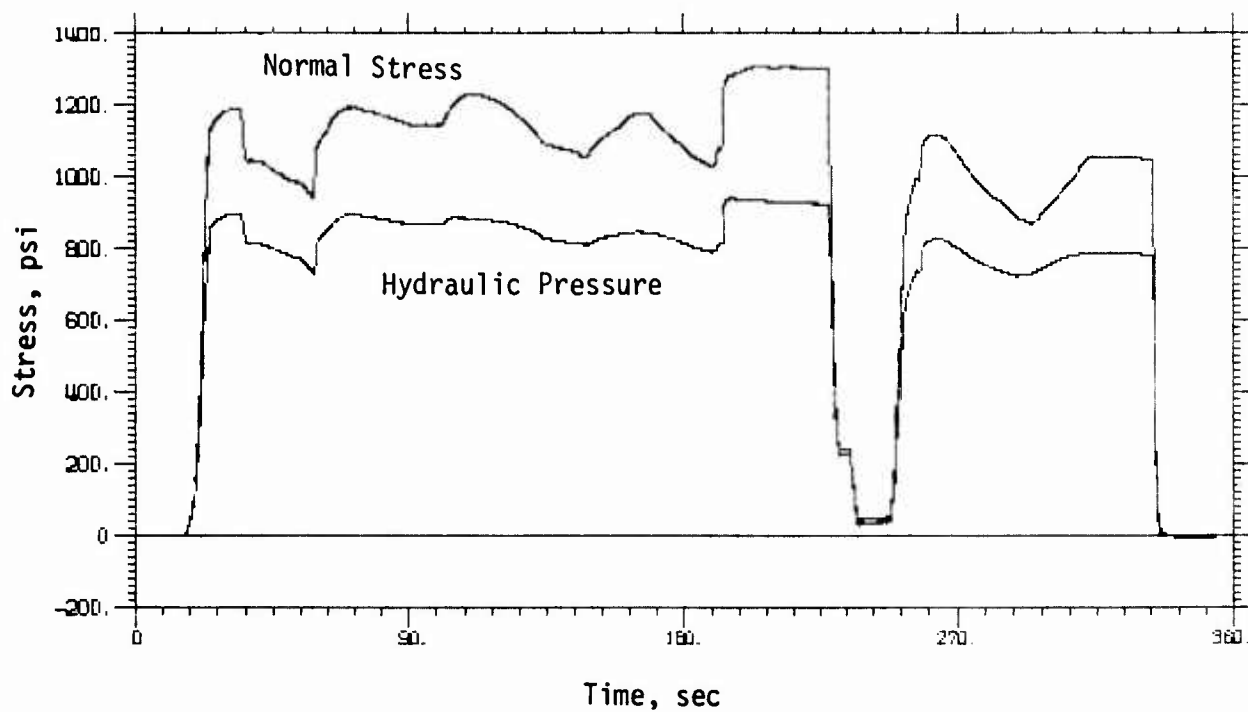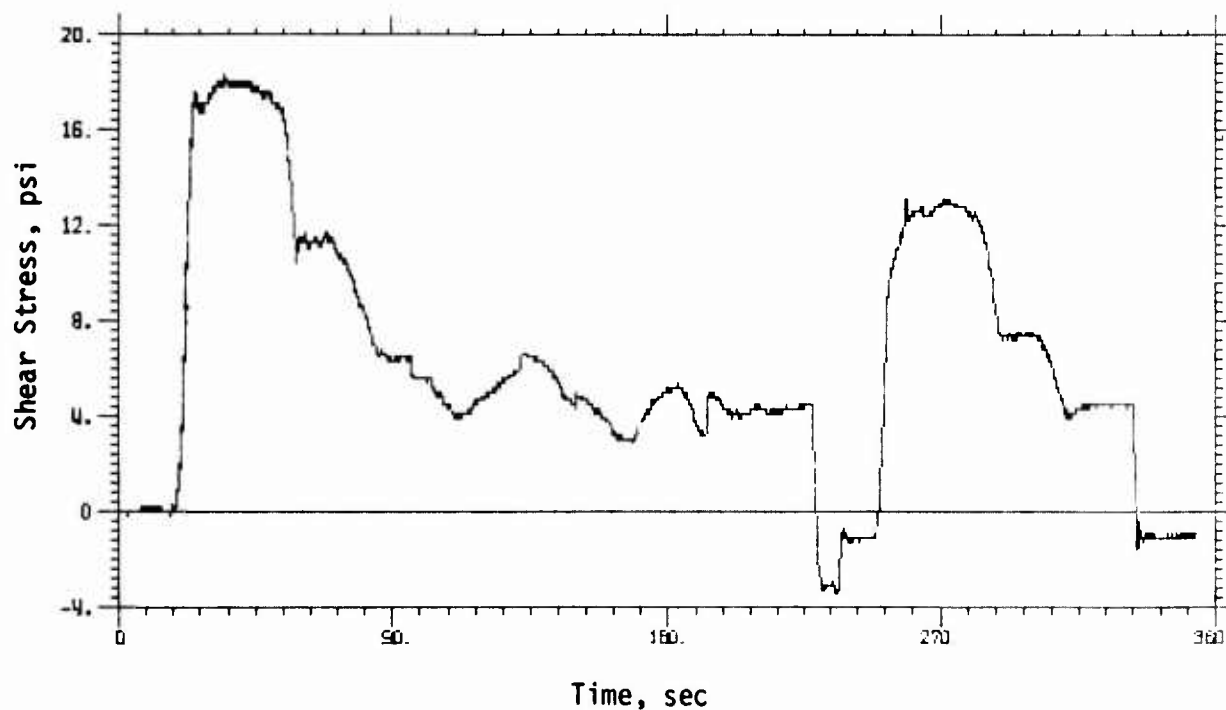
66

Vertical Shear Stress

Inferred Vertical Shear Stress

TEST 16 (2 of 2)

67

Hydraulic Pressure and Normal Stress

Horizontal Shear Stress

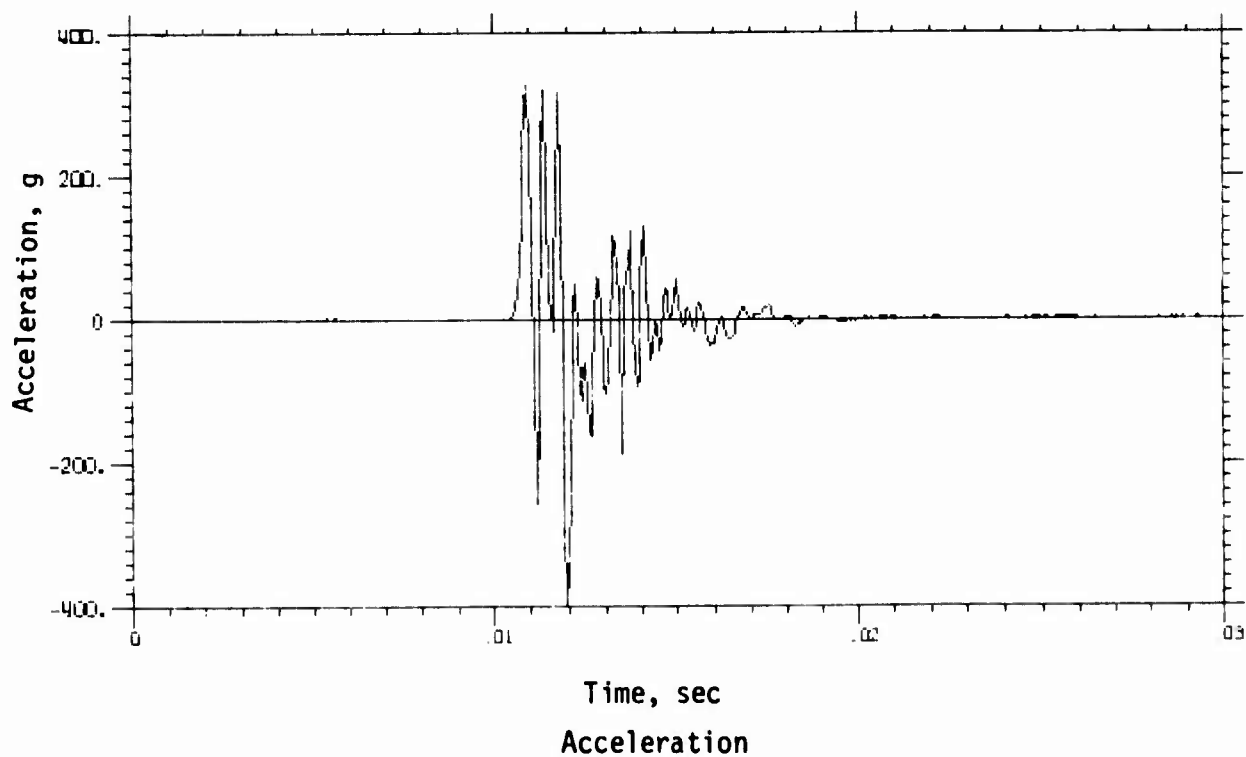TEST 17 (1 of 2)

68

Vertical Shear Stress

Inferred Vertical Shear Stress

TEST 17 (2 of 2)

69

Hydraulic Pressure and Normal Stress

Horizontal Shear Stress

TEST 18 (1 of 2)
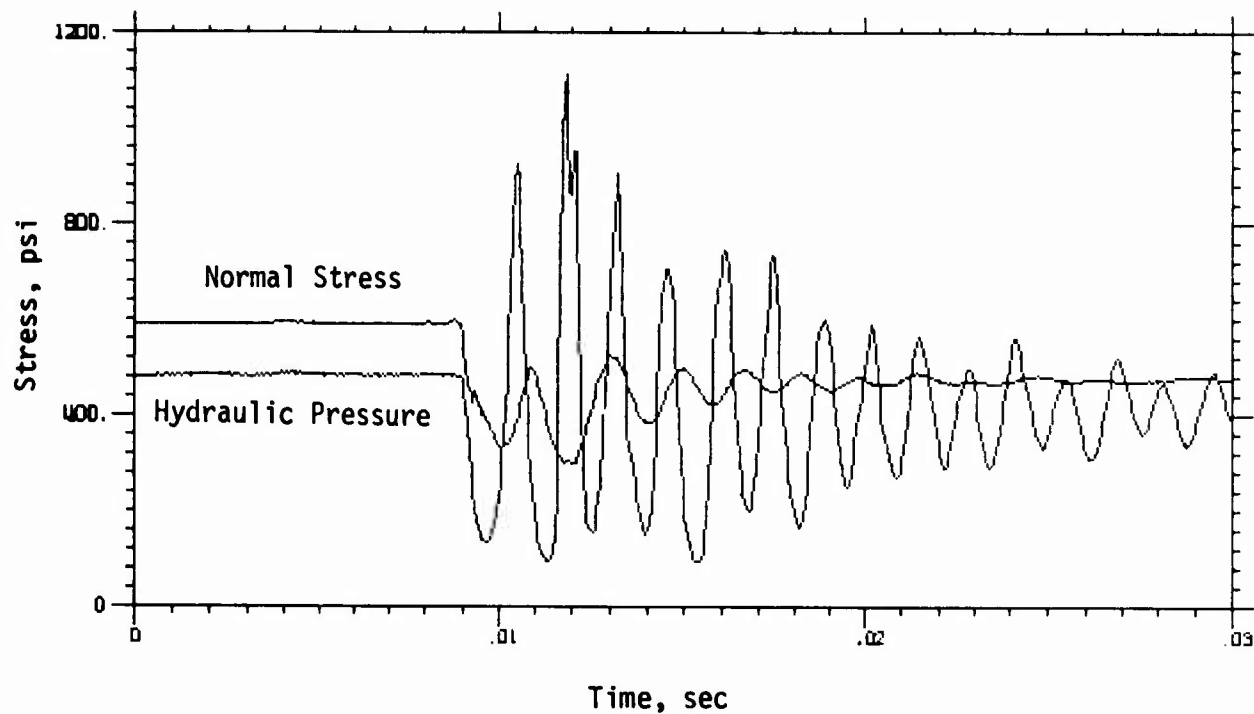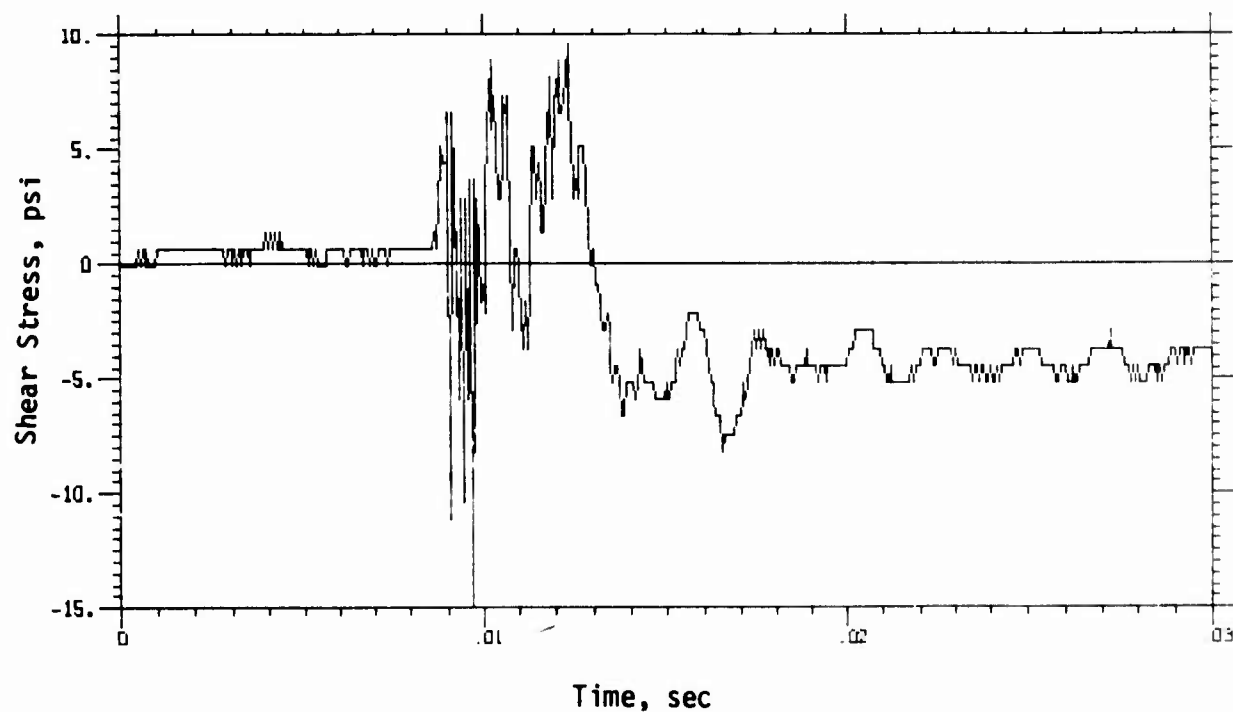
Vertical Shear Stress

Inferred Vertical Shear Stress
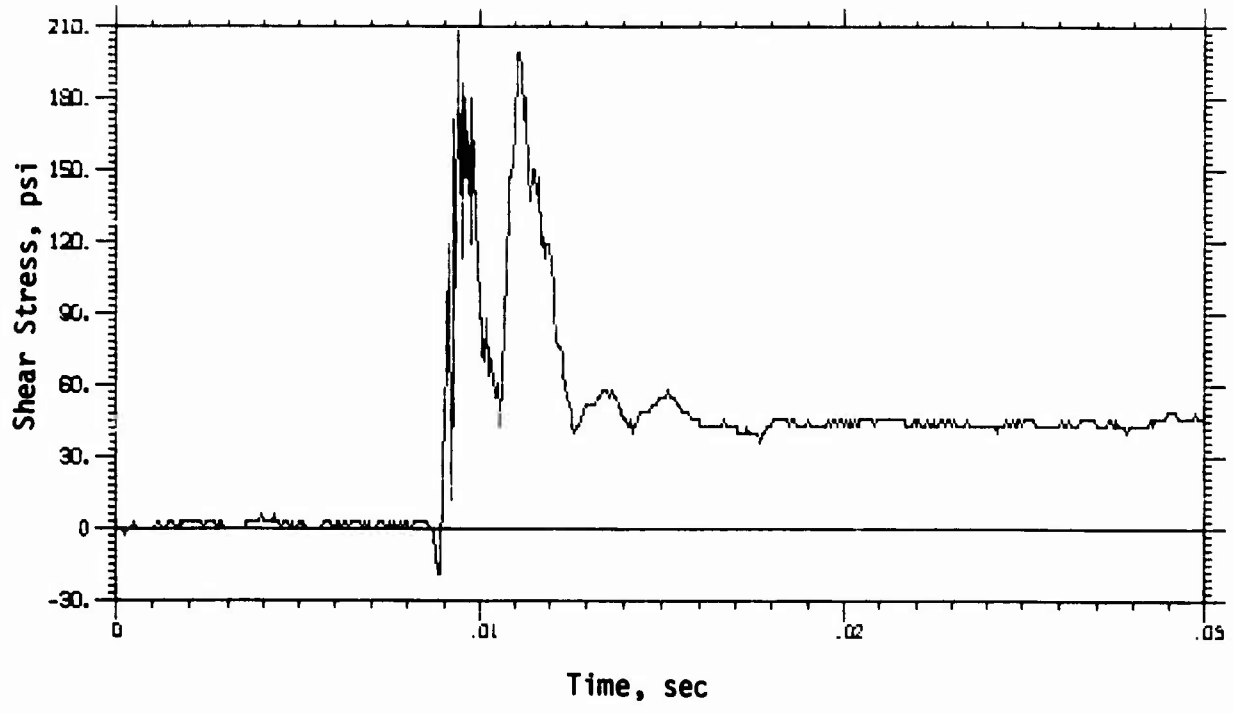
TEST 18 (2 of 2)

71
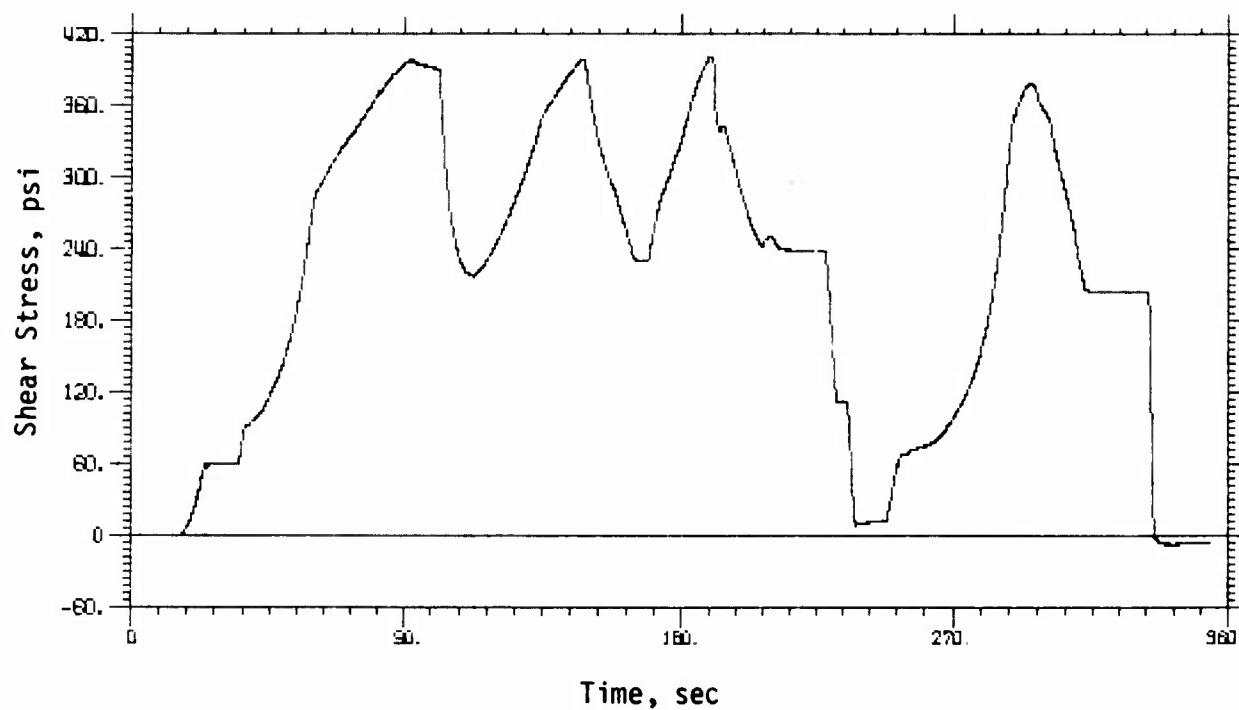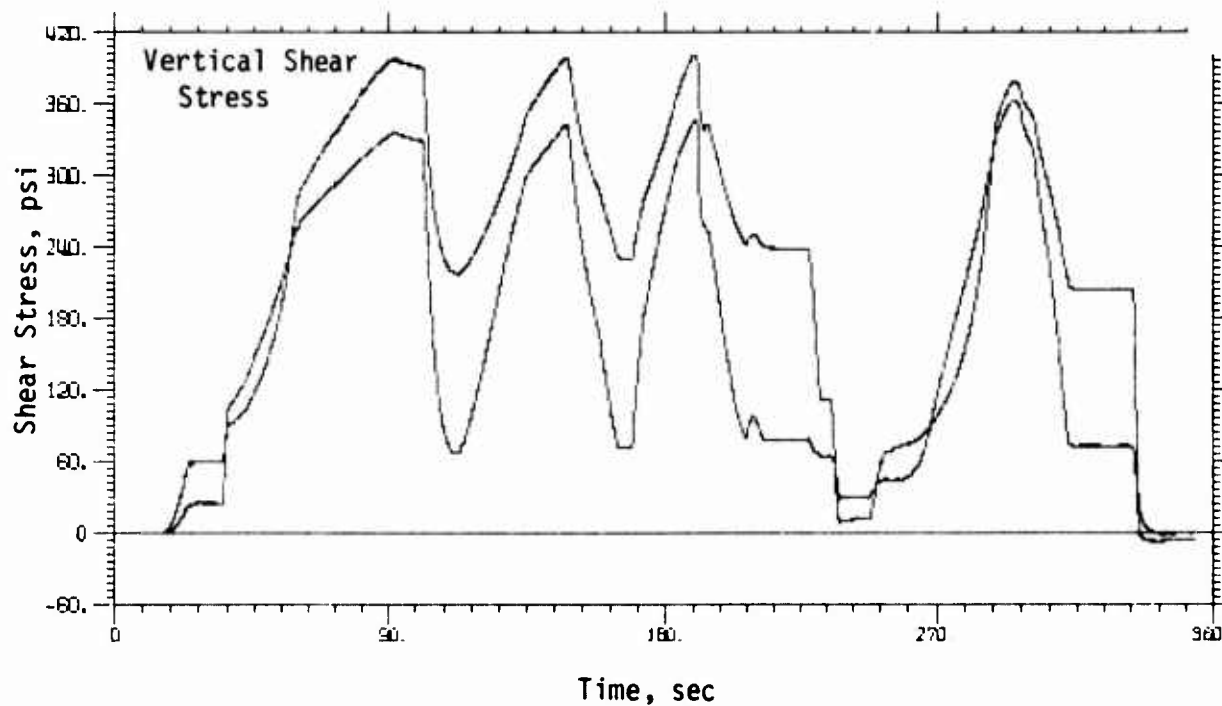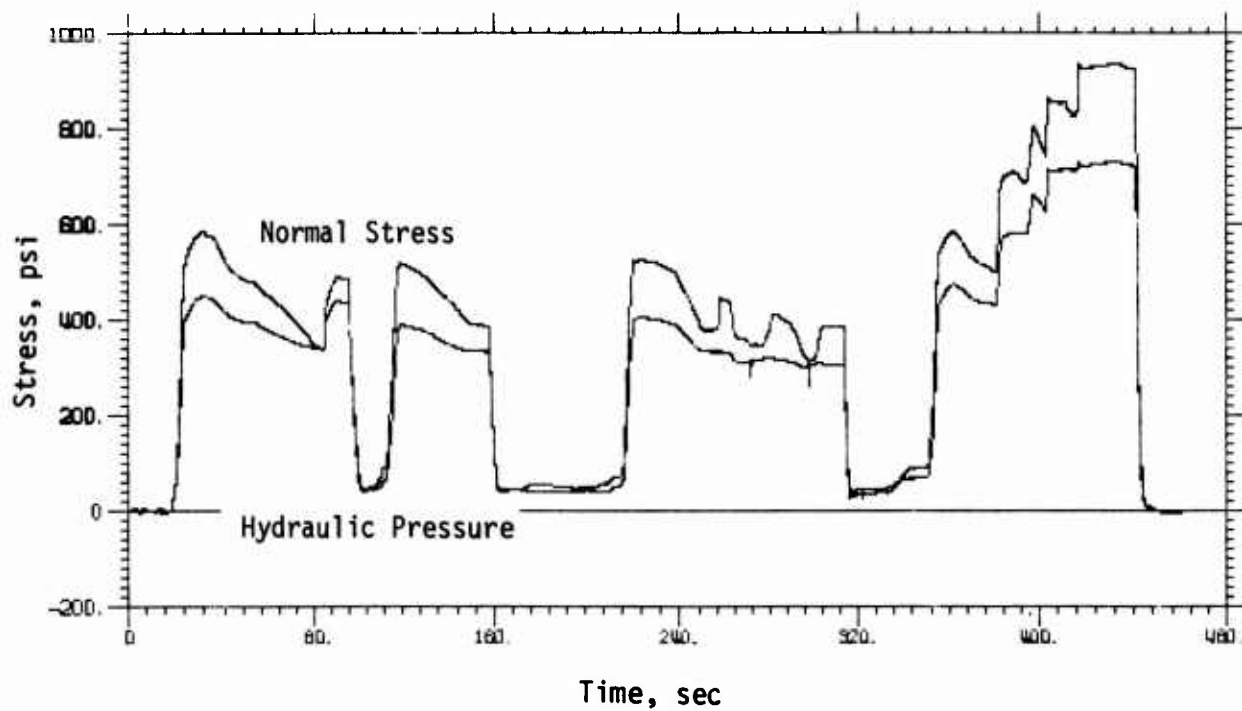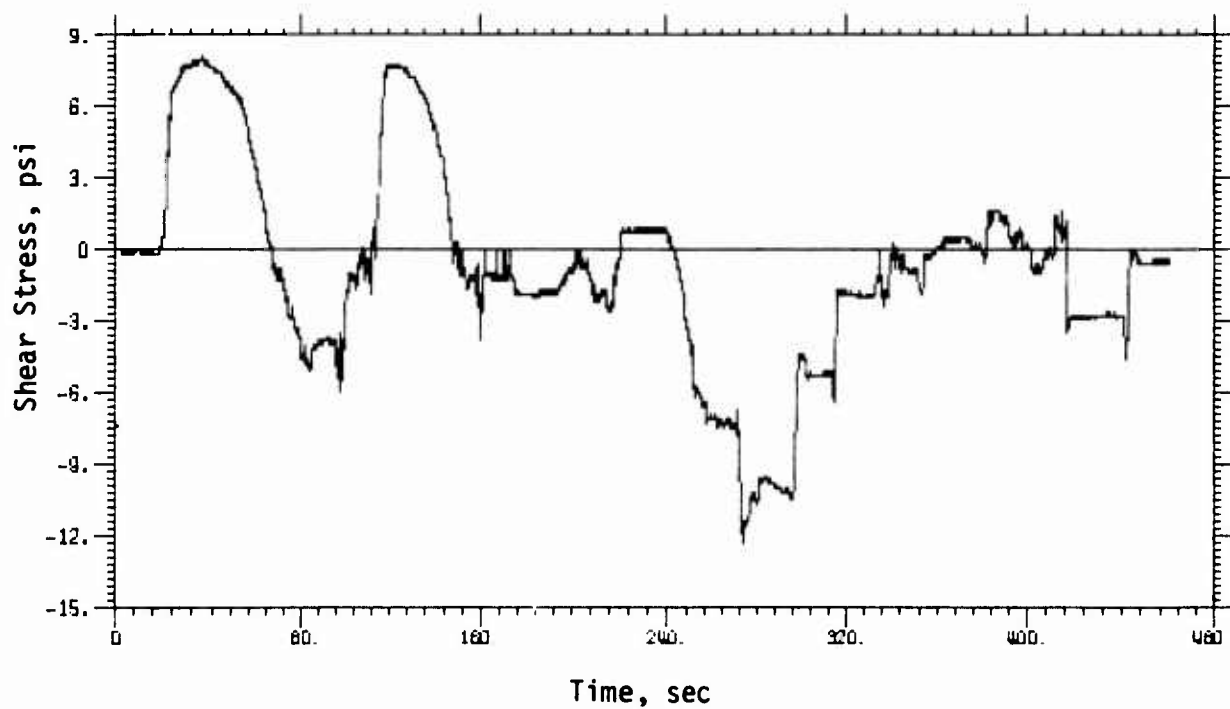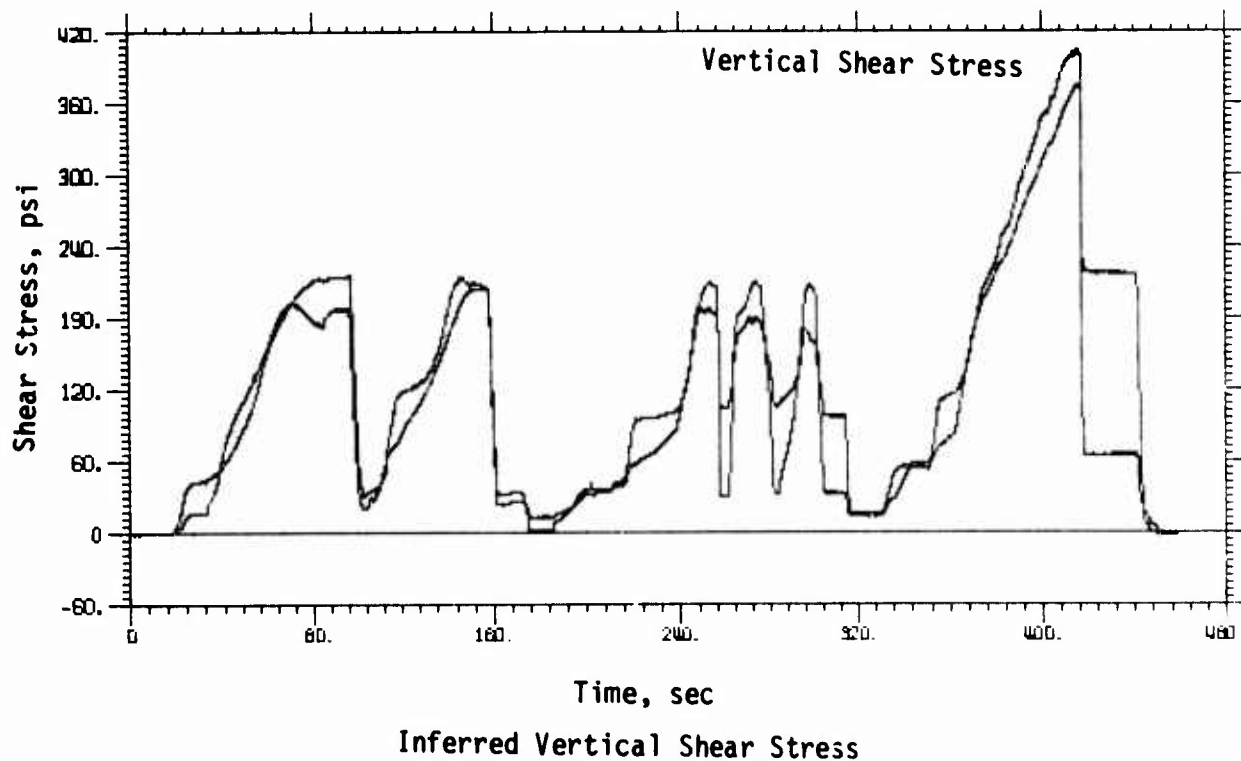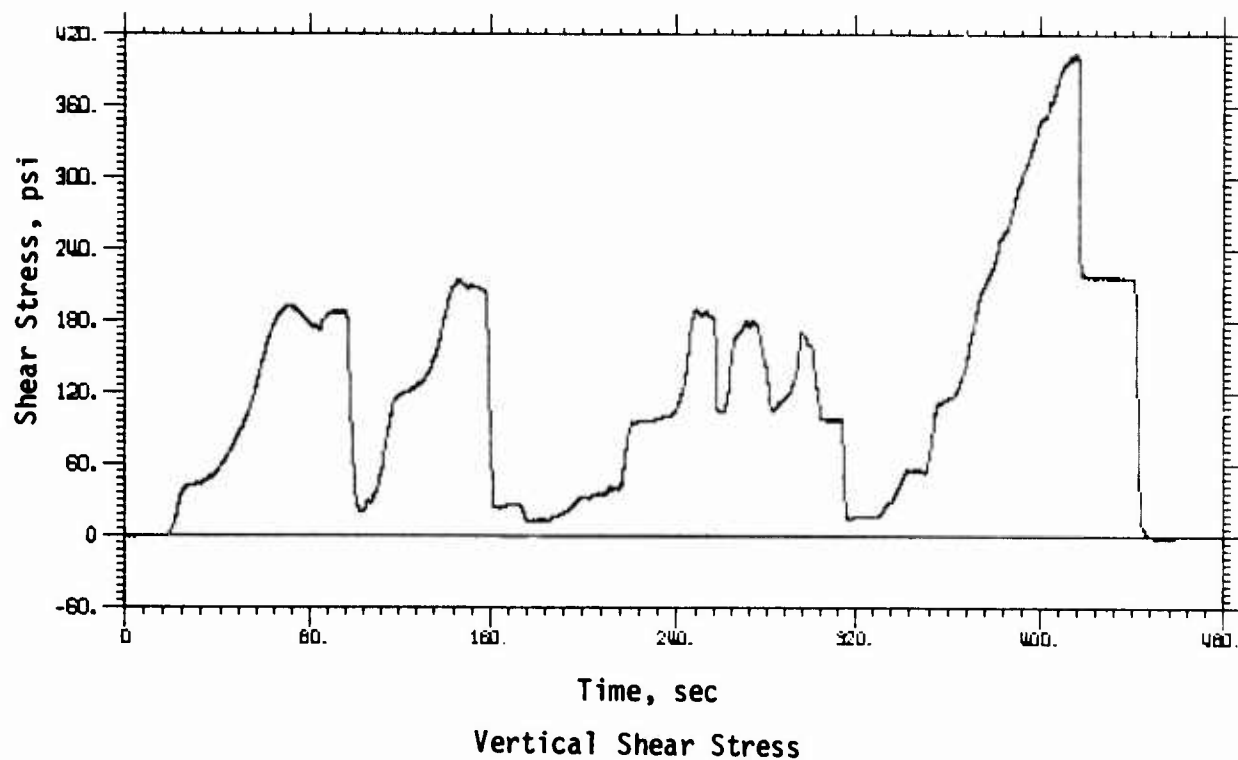
APPENDIX E

DYNAMIC-SHEAR TEST DATA
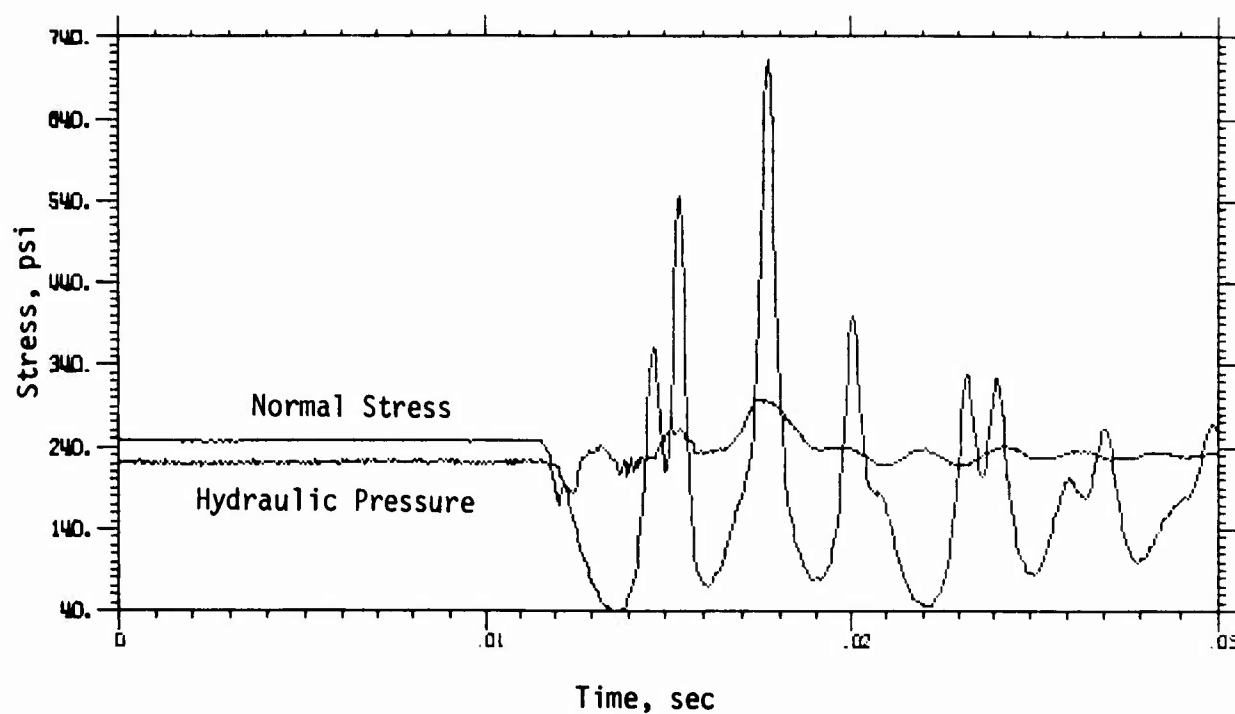
Hydraulic Pressure and Normal Stress
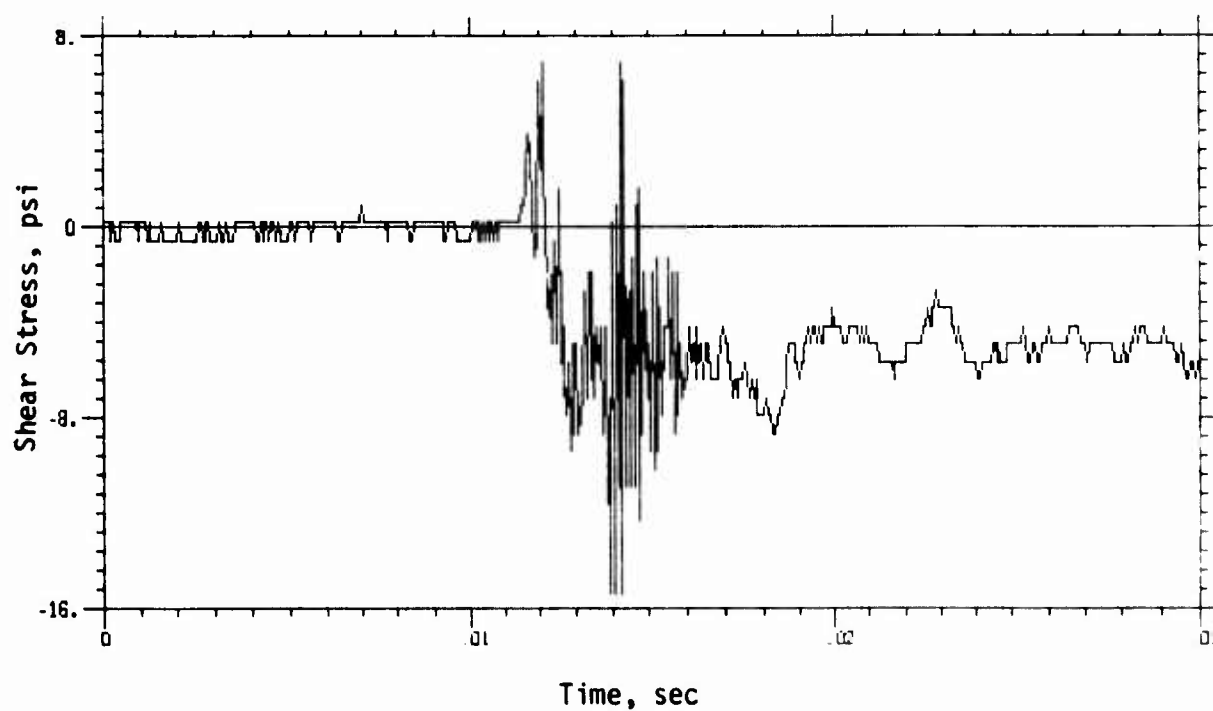
Horizontal Shear Stress

TEST 10 (1 of 3)
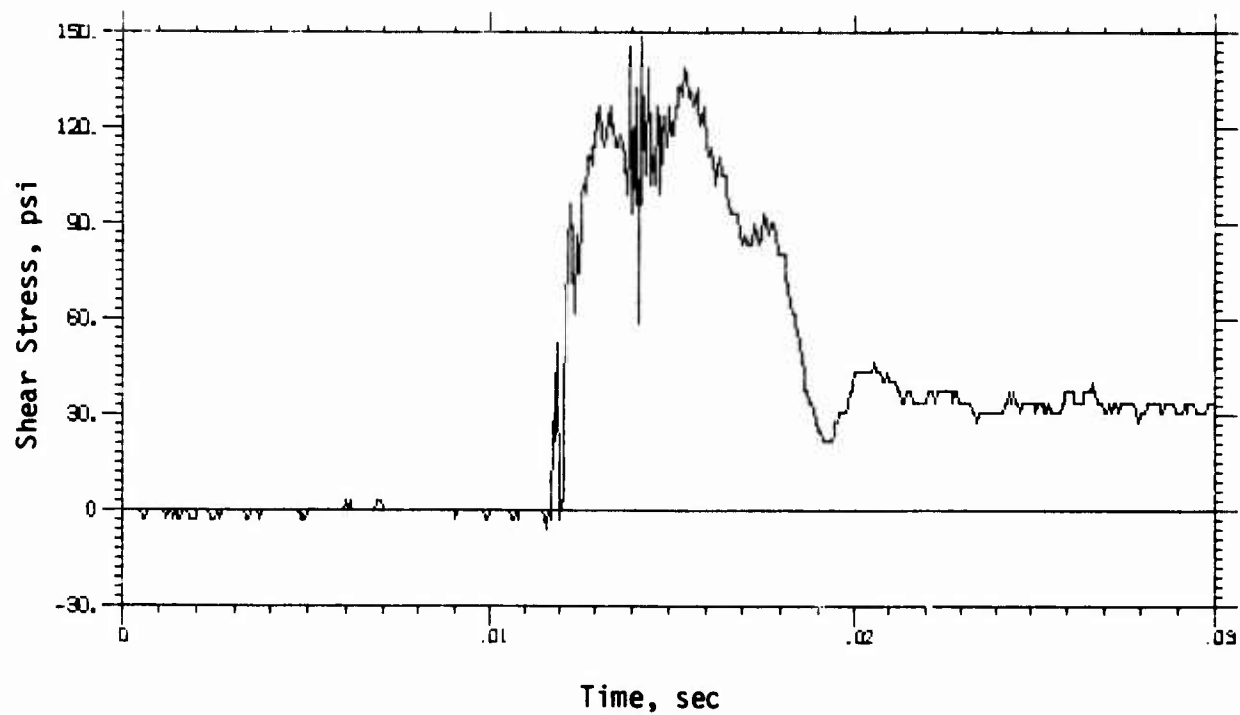
Vertical Shear Stress
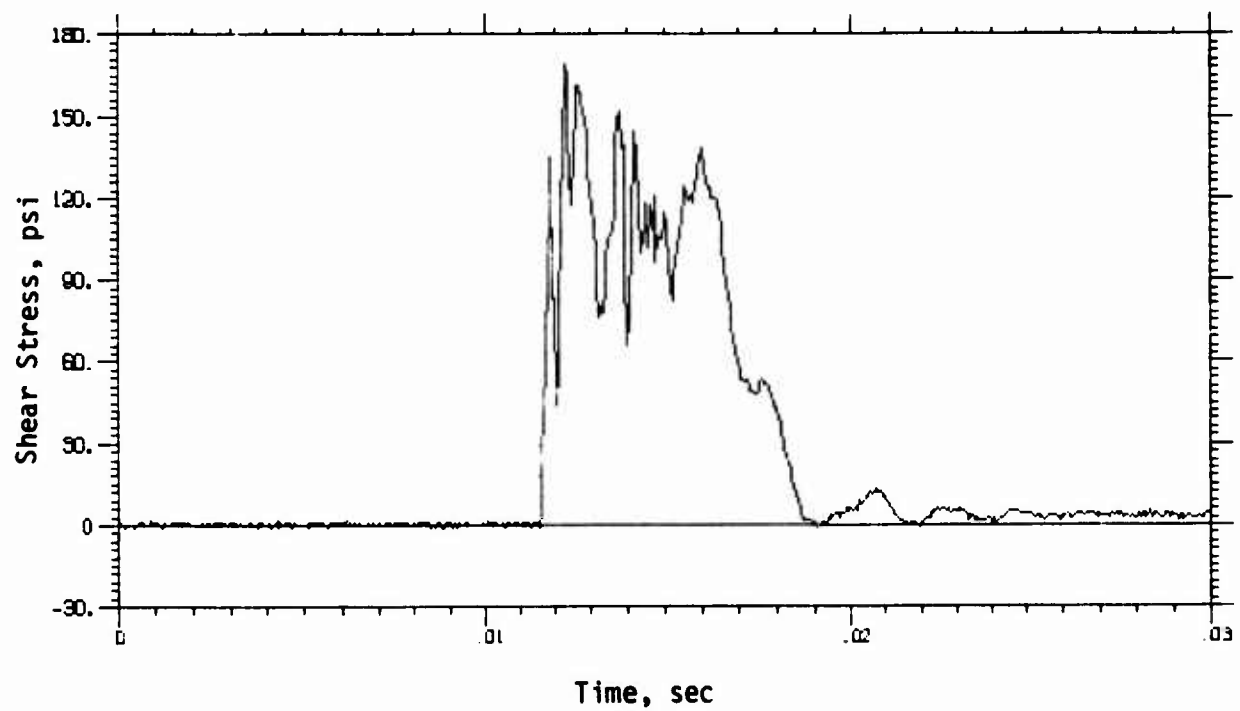
Inferred Vertical Shear Stress

TEST 10 (2 of 3)
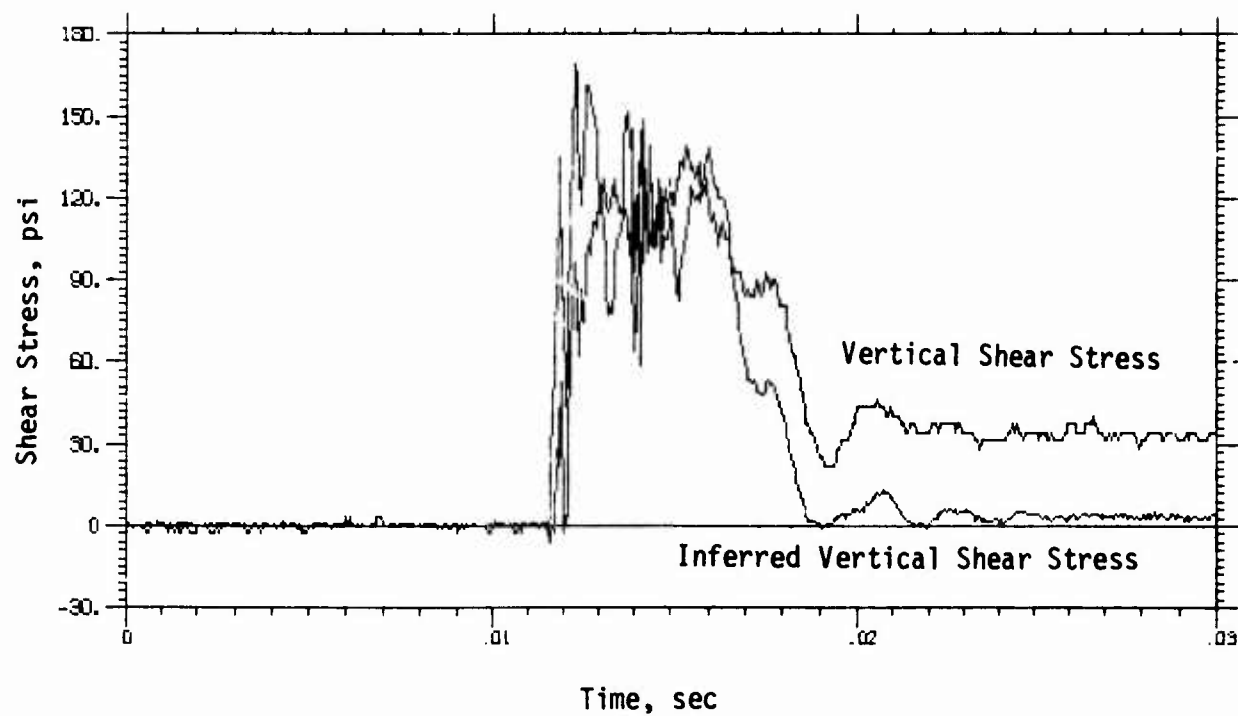
74

Vertical Shear Stresses (Comparison)

Acceleration

TEST 10 (3 of 3)

75
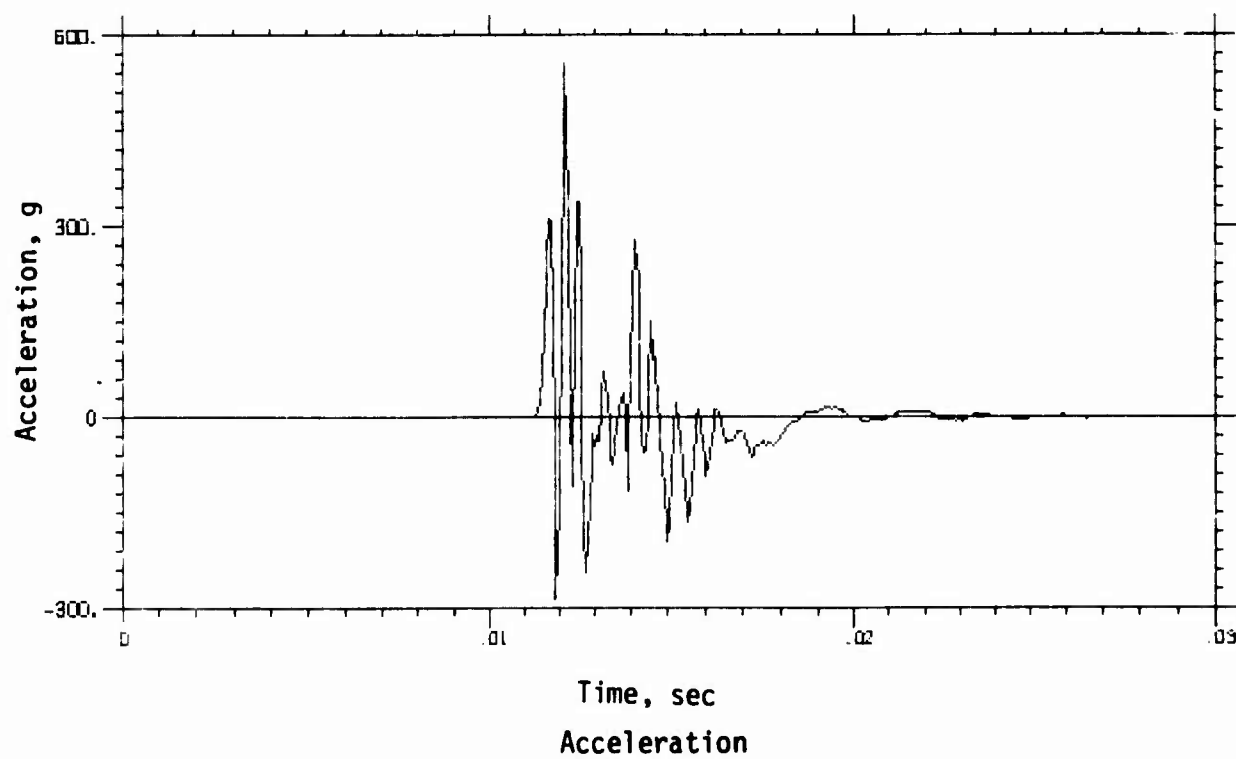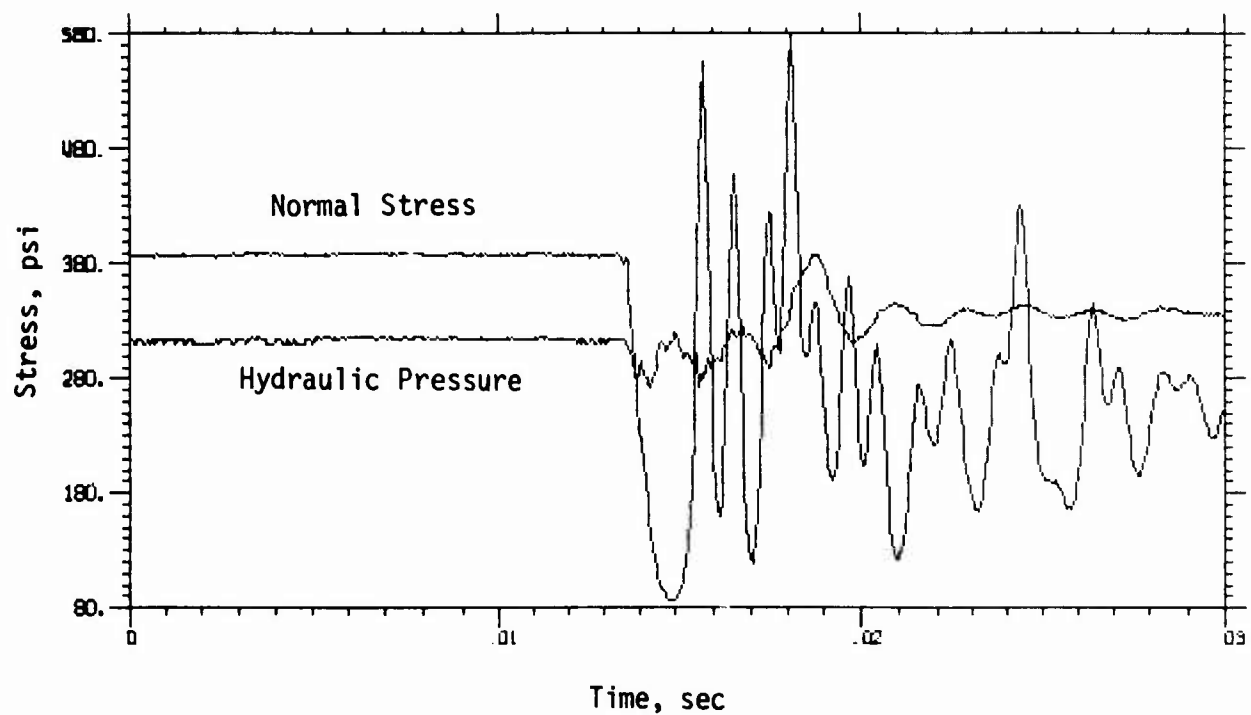
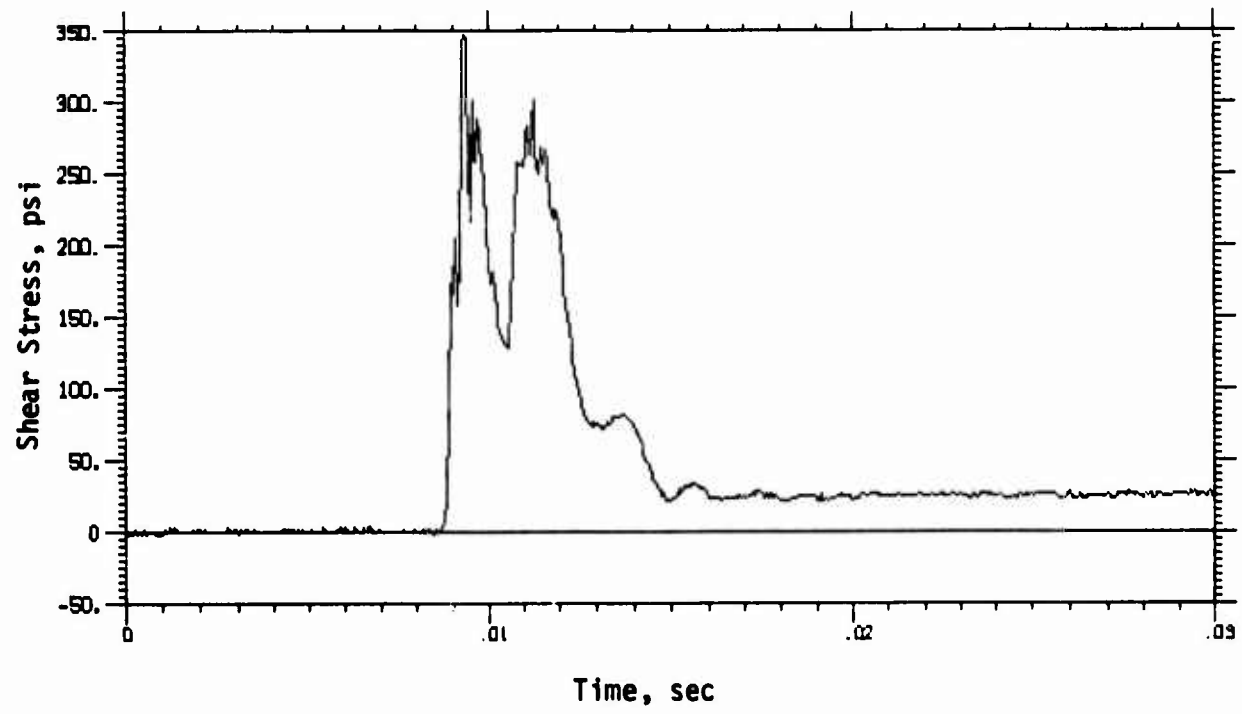Hydraulic Pressure and Normal Stress
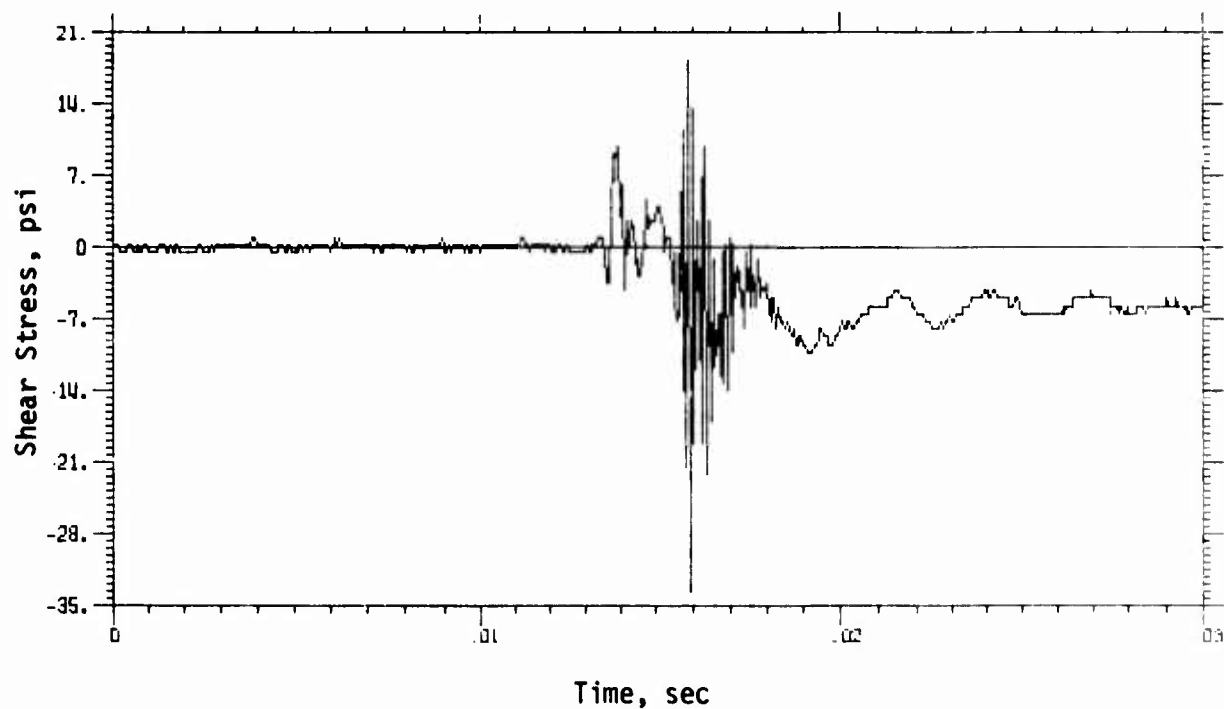
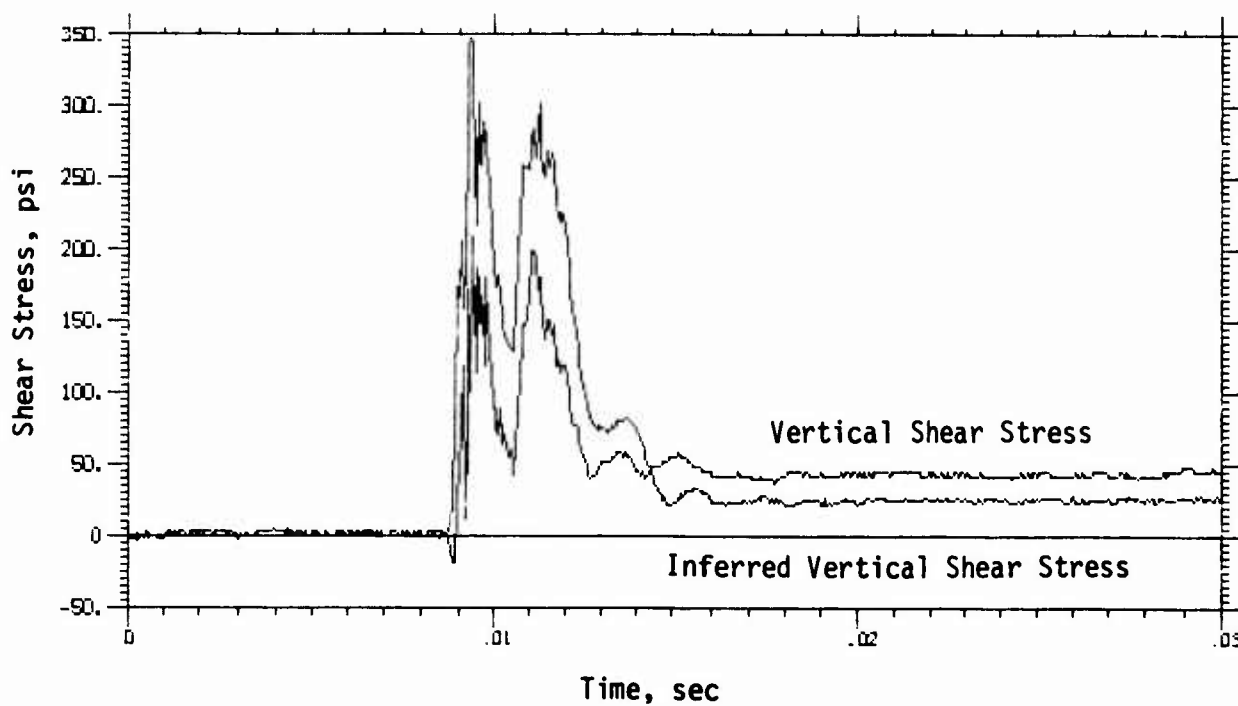Horizontal Shear Stress

TEST 11 (1 of 3)
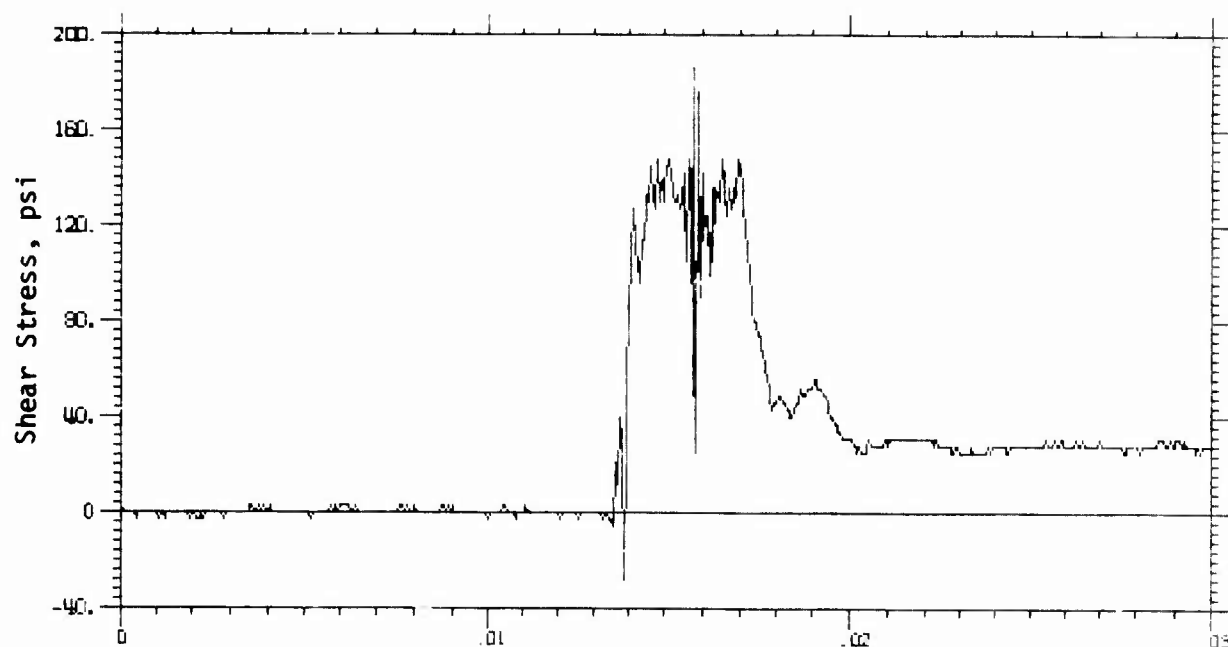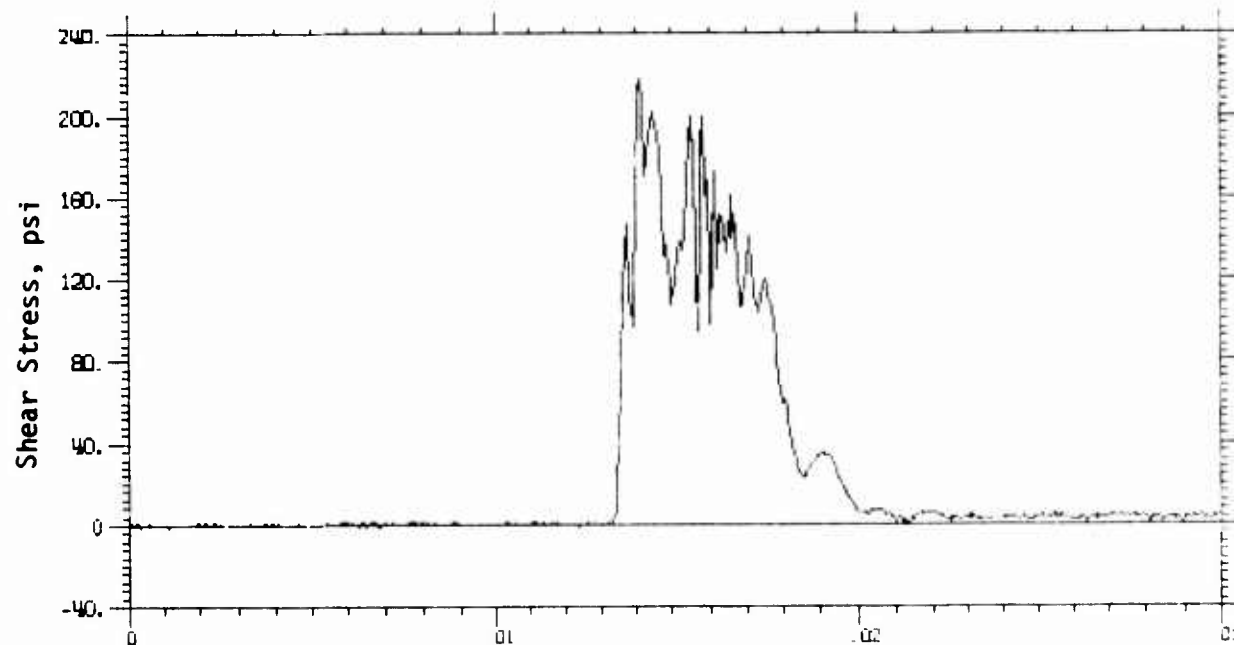
Vertical Shear Stress

Inferred Vertical Shear Stress

TEST 11 (2 of 3)
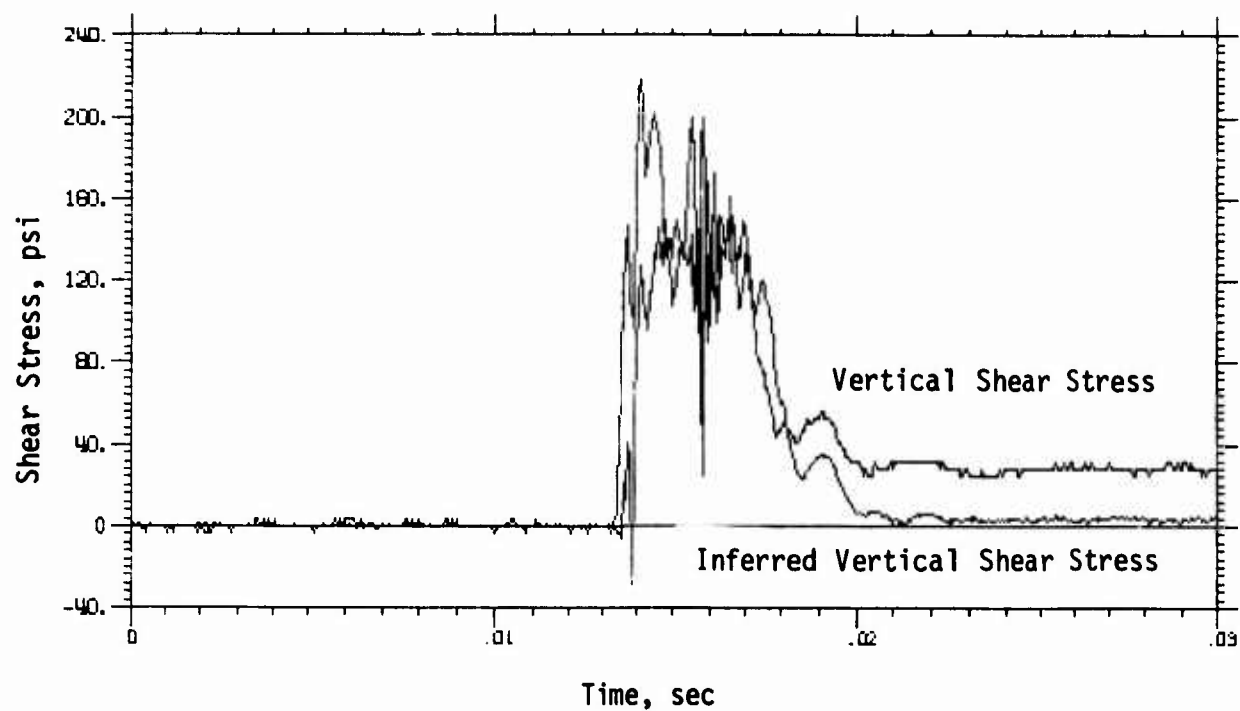
Vertical Shear Stresses (Comparison)

Acceleration
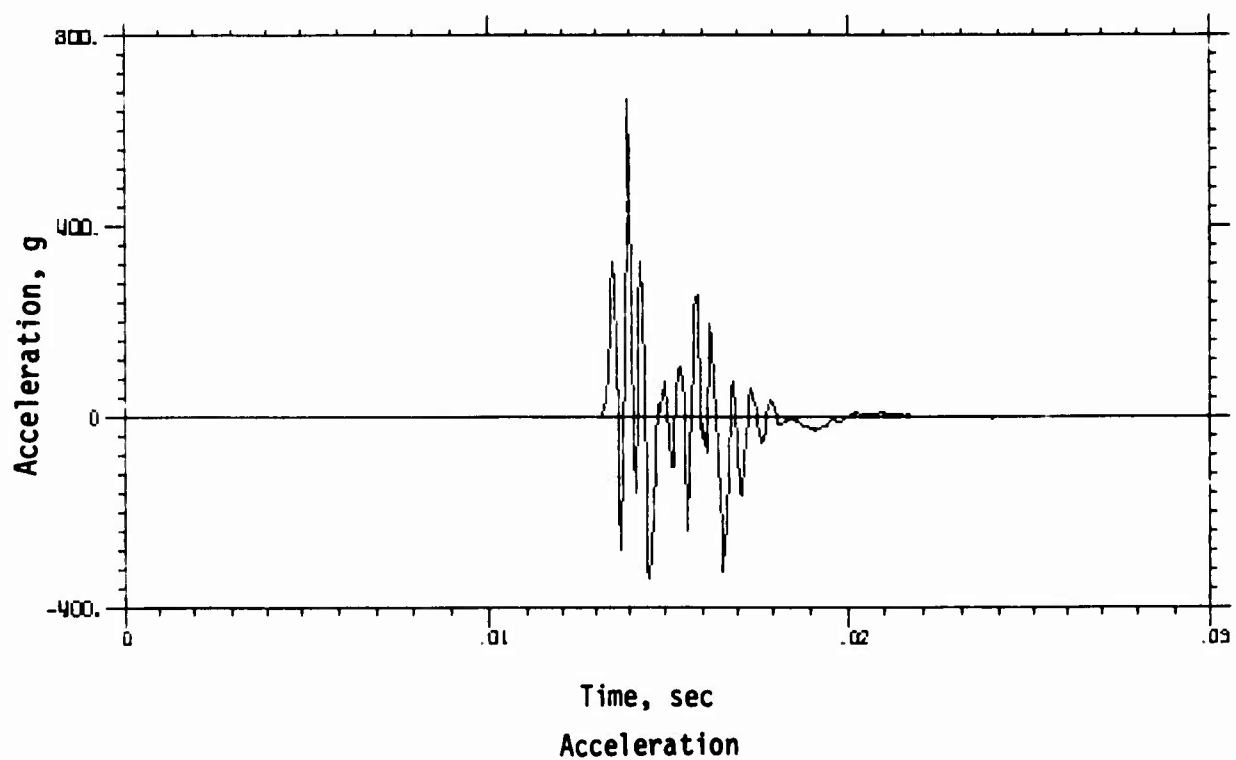
TEST 11 (3 of 3)
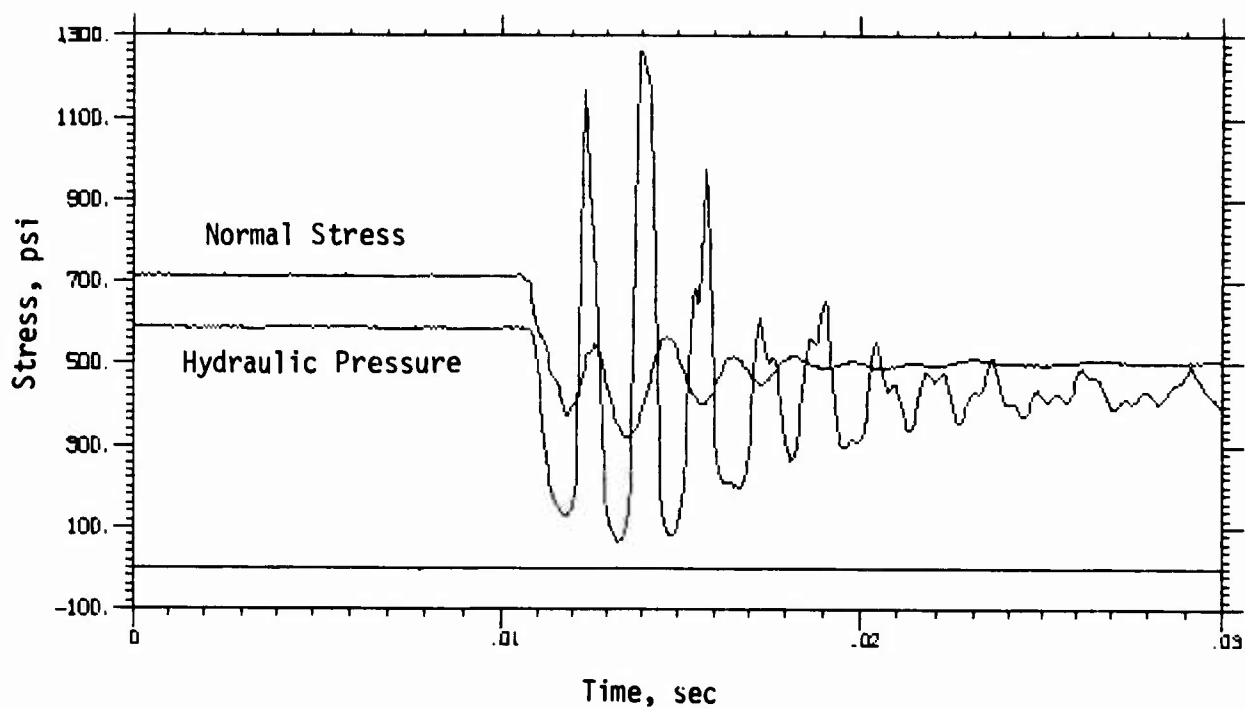
Hydraulic Pressure and Normal Stress
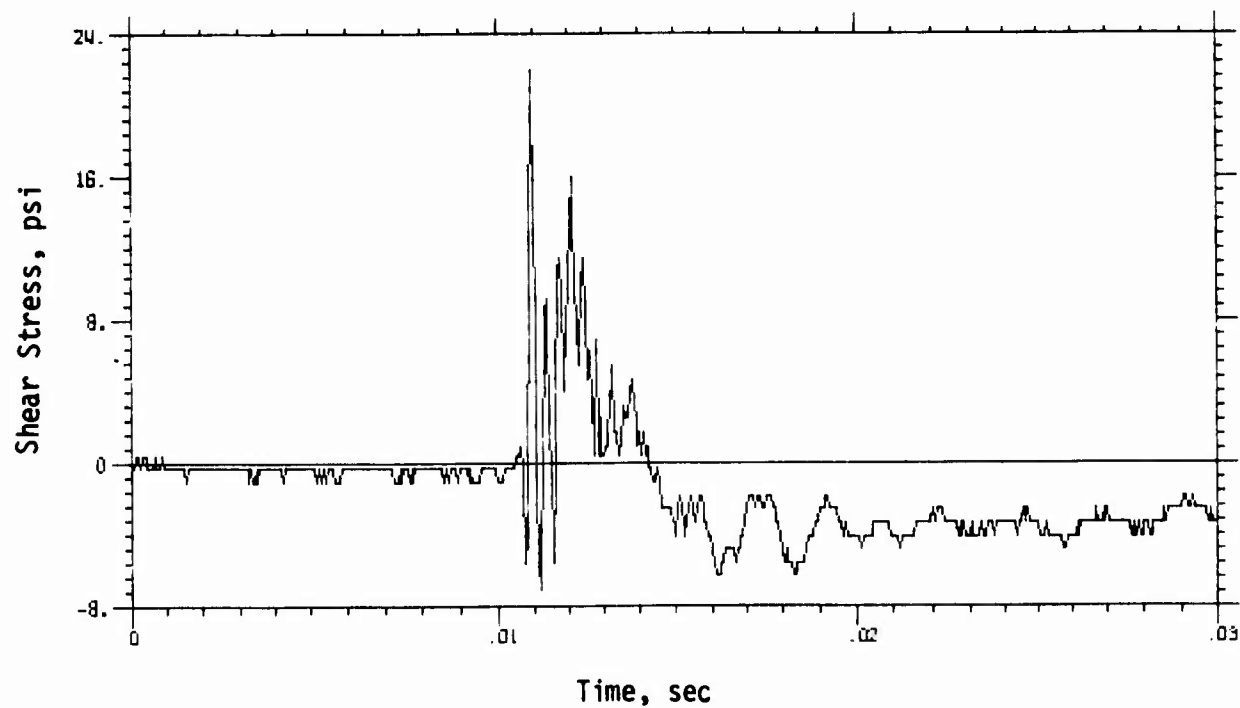
Horizontal Shear Stress
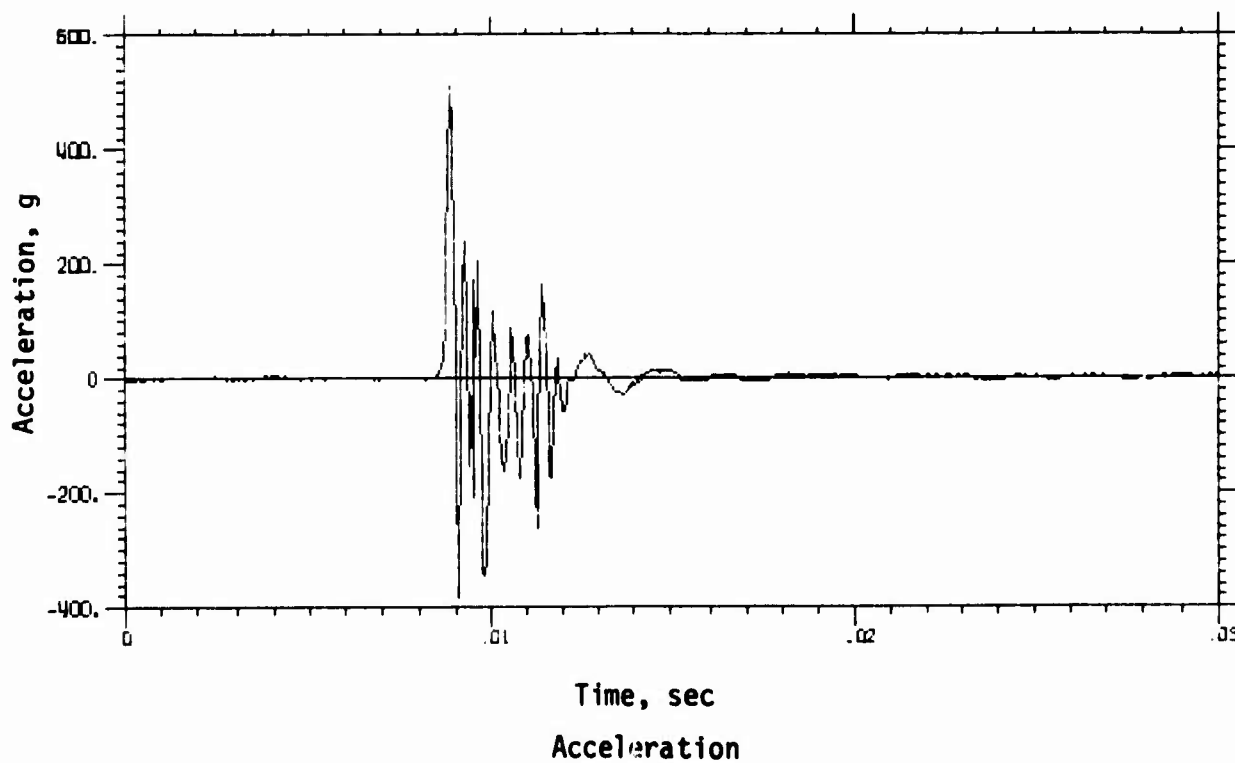
TEST 13 (1 of 3)

Time, sec

Vertical Shear Stress

Time, sec

Inferred Vertical Shear Stress

TEST 13 (2 of 3)
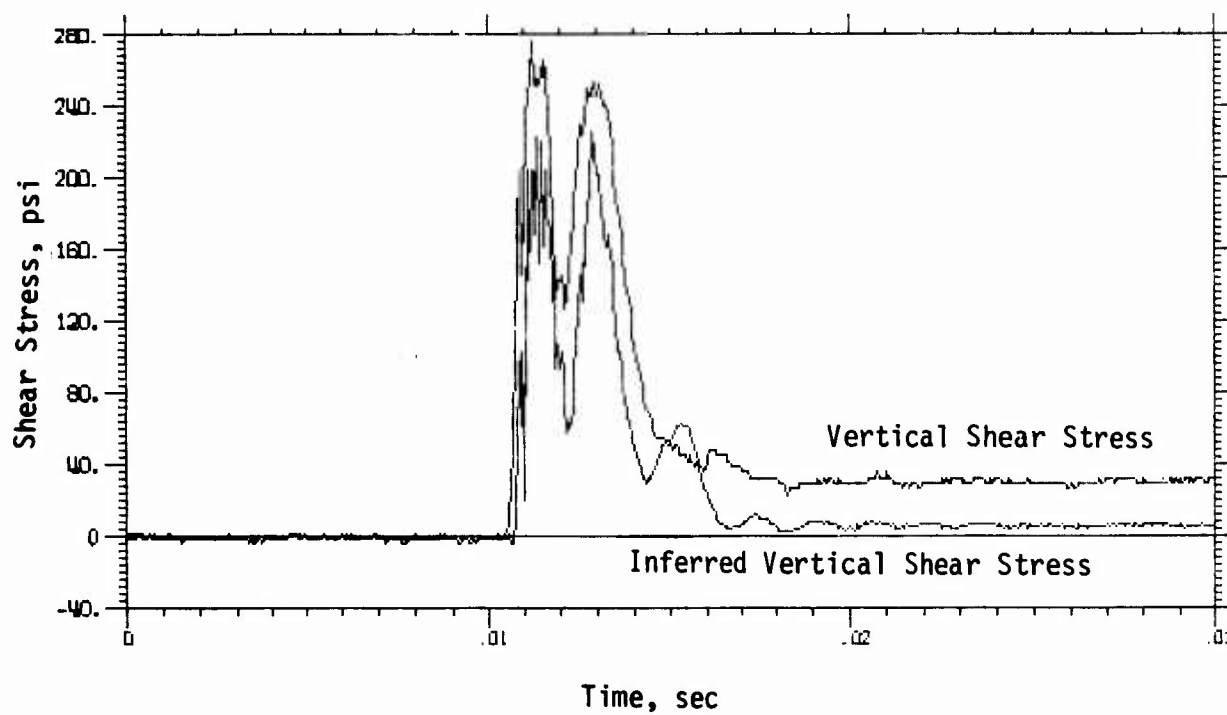
Vertical Shear Stresses (Comparison)

Acceleration

TEST 13 (3 of 3)
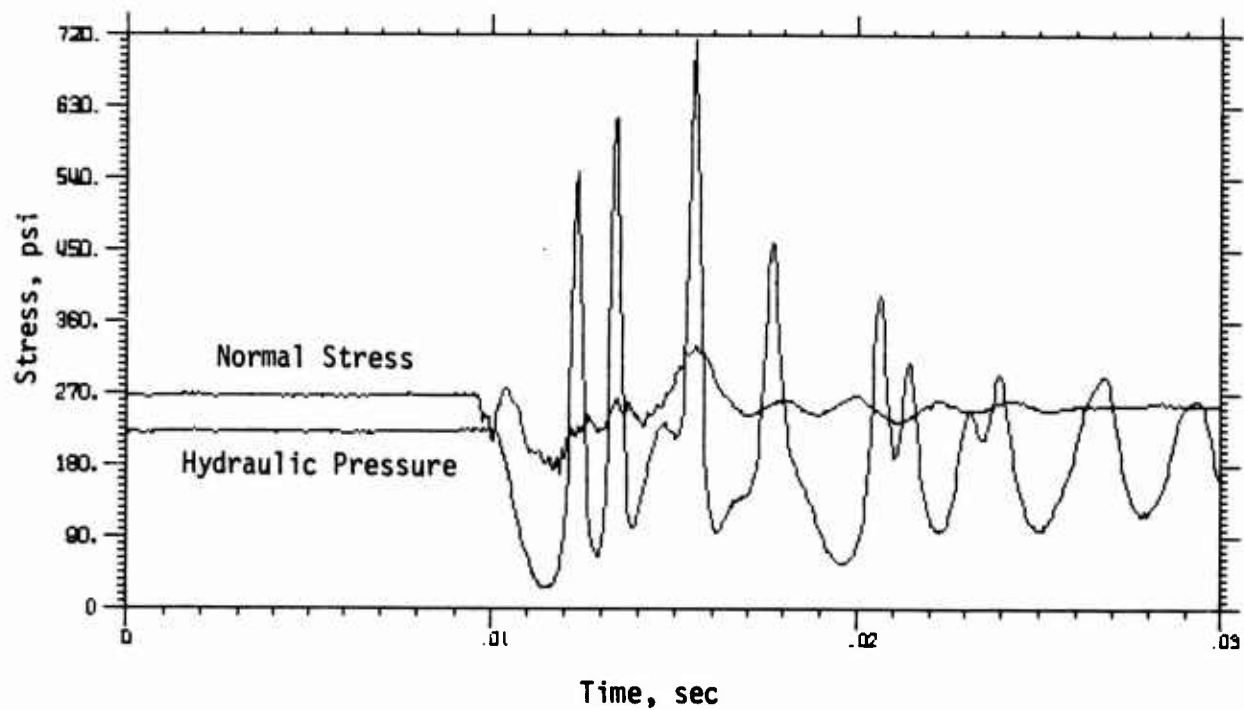
Hydraulic Pressure and Normal Stress

Horizontal Shear Stress

TEST 14 (1 of 3)
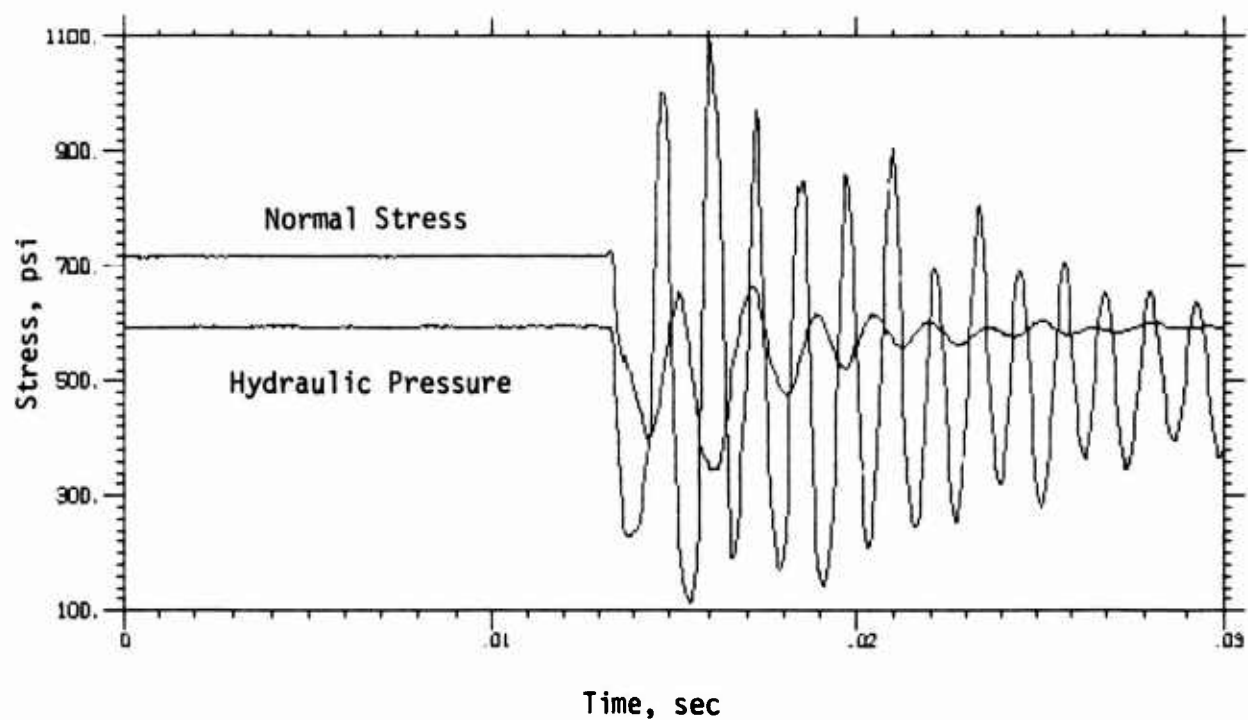
Vertical Shear Stress

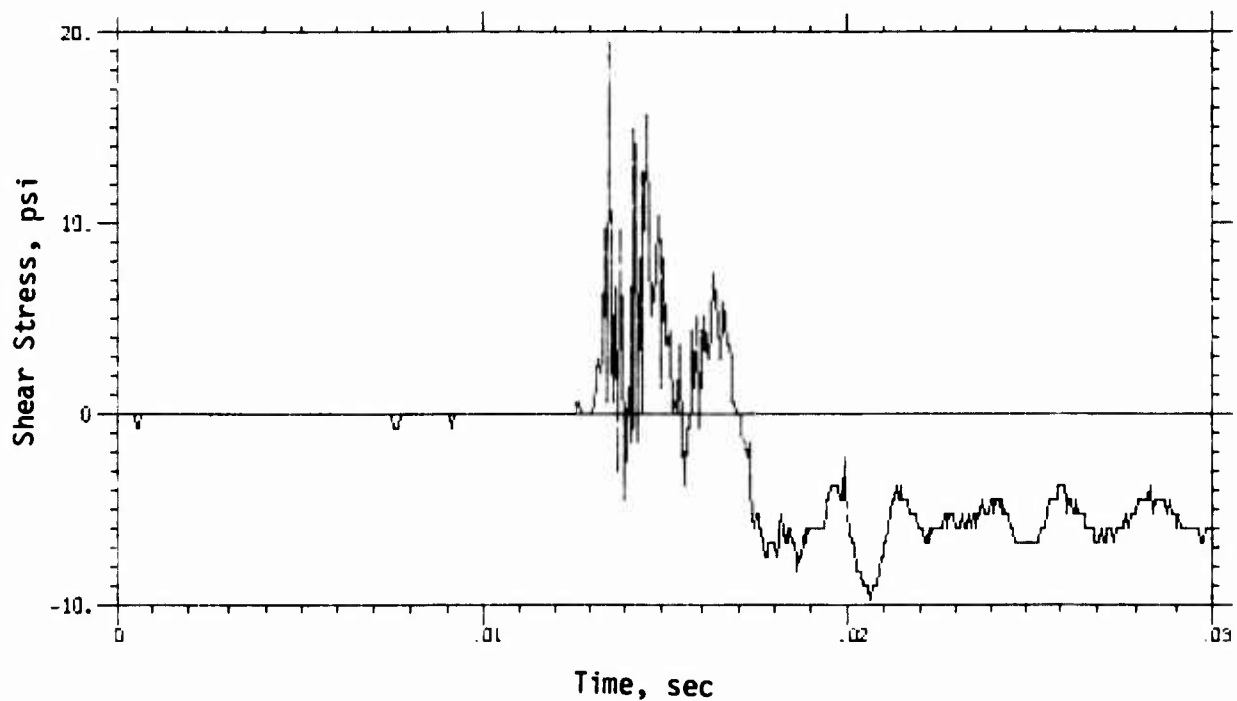Inferred Vertical Shear Stress

TEST 14 (2 of 3)
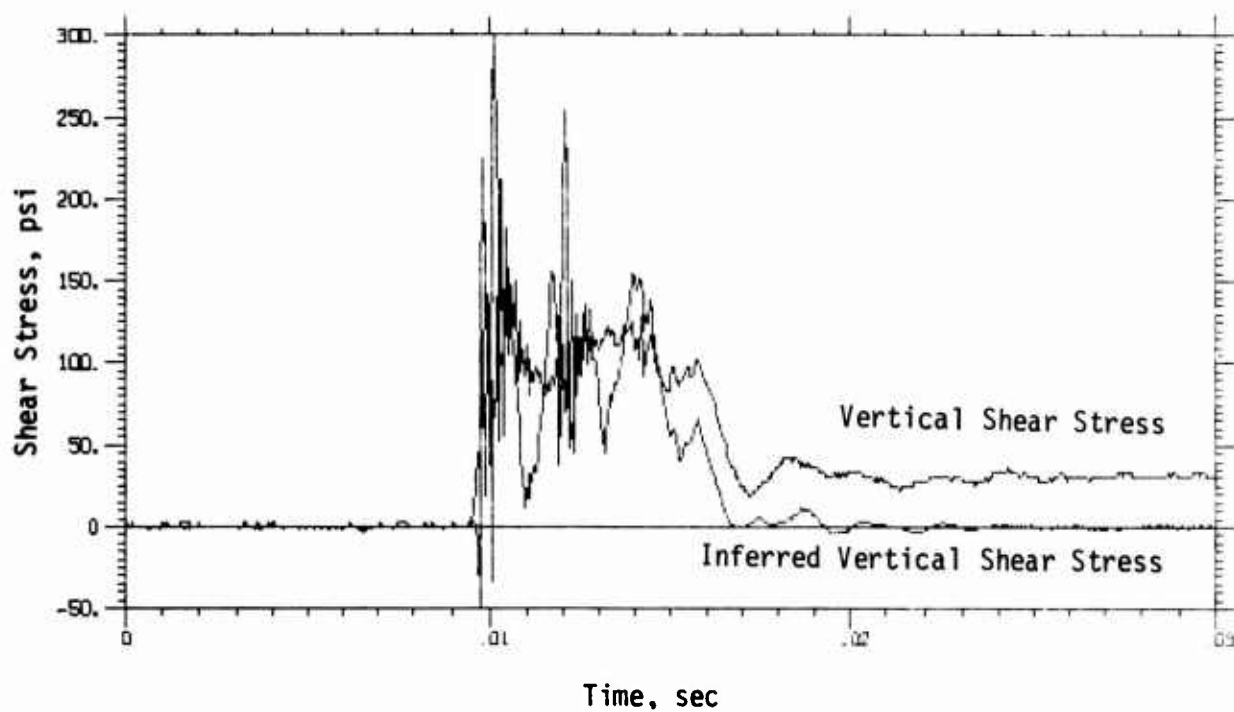
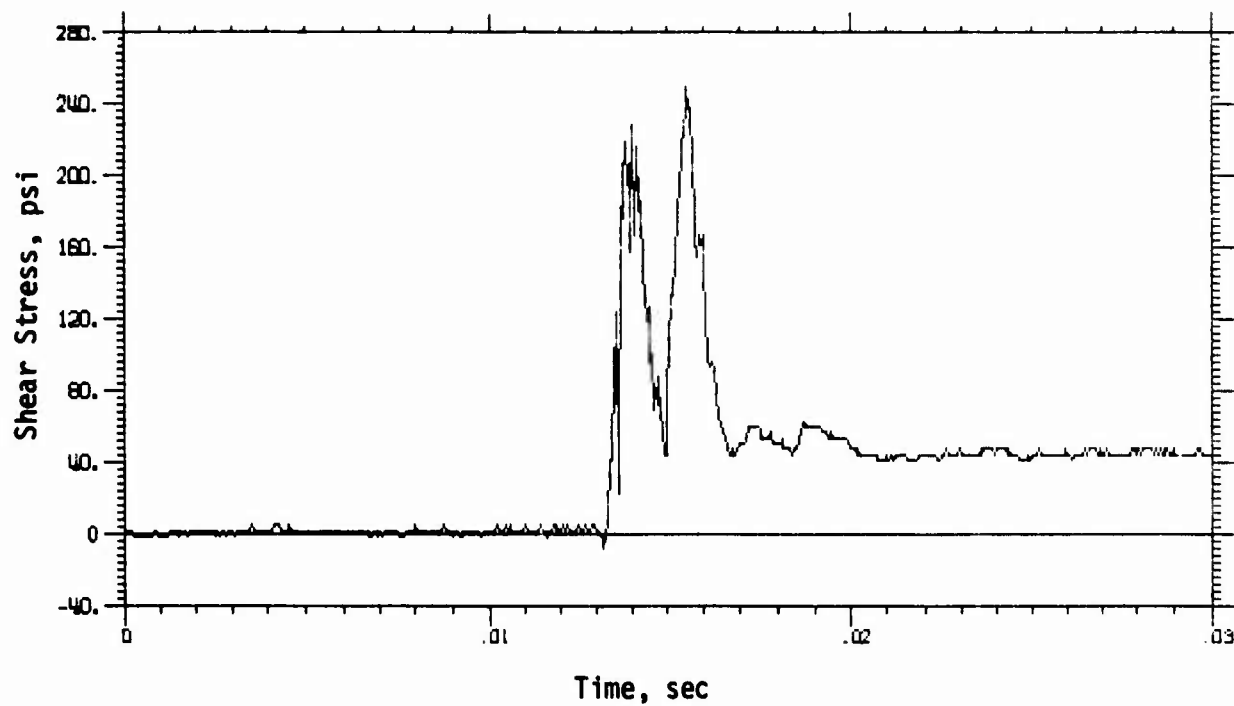Vertical Shear Stresses (Comparison)

Acceleration

TEST 14 (3 of 3)

84

Hydraulic Pressure and Normal Stress

Horizontal Shear Stress

TEST 17 (1 of 3)

85

Vertical Shear Stress

Inferred Vertical Shear Stress

TEST 17 (2 of 3)
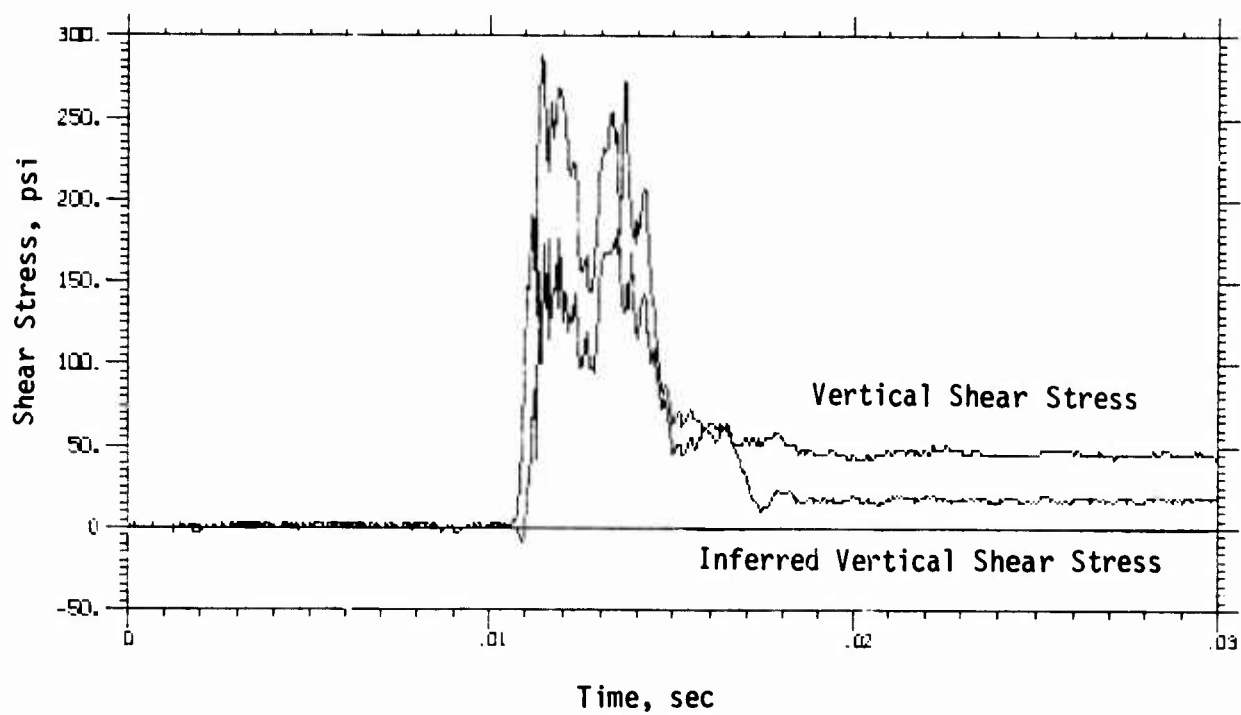
Vertical Shear Stresses (Comparison)

Acceleration

TEST 17 (3 of 3)

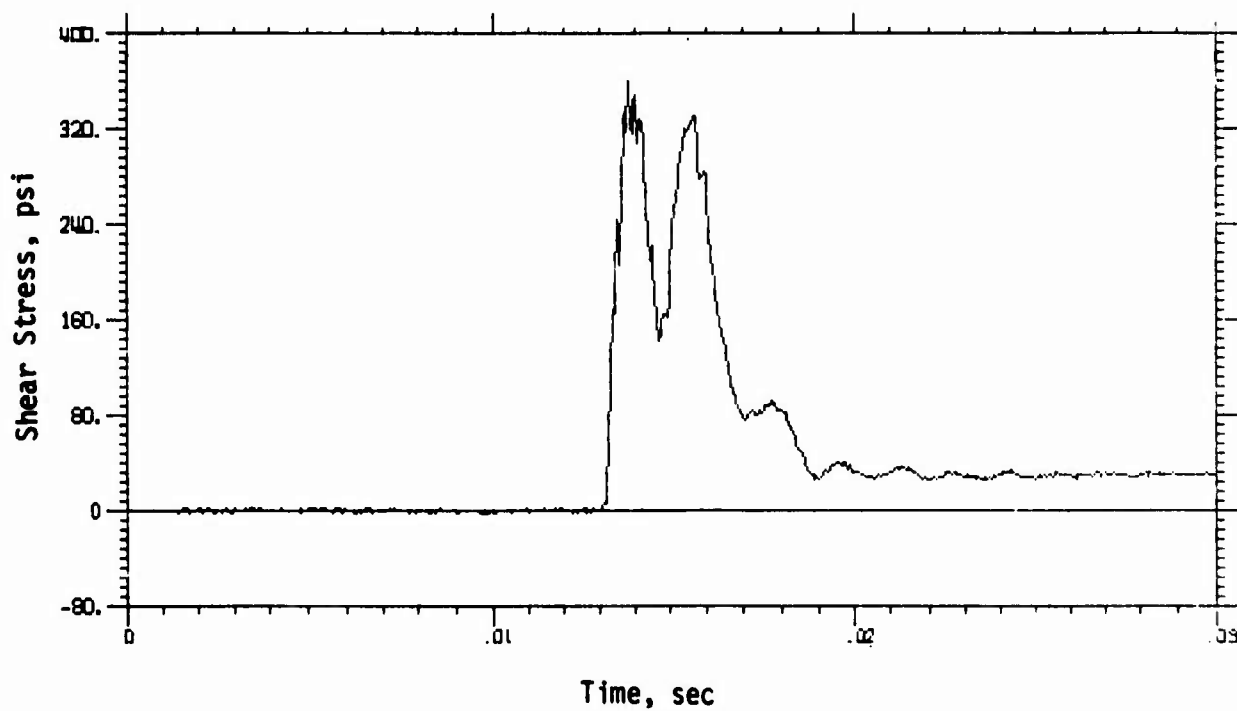Hydraulic Pressure and Normal Stress
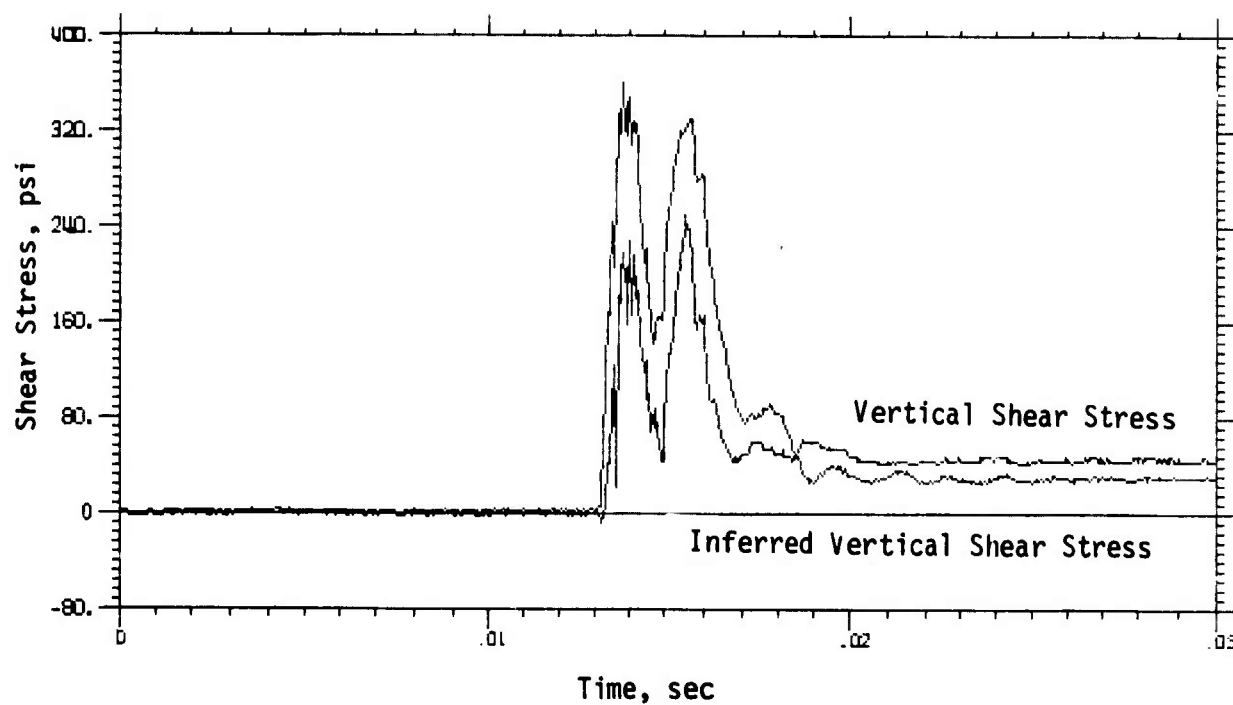

Horizontal Shear Stress

TEST 18 (1 of 3)

Vertical Shear Stress

Inferred Vertical Shear Stress

TEST 18 (2 of 3)

89

Vertical Shear Stresses (Comparison)

Acceleration

TEST 18 (3 of 3)

90

Hydraulic Pressure and Normal Stress

Horizontal Shear Stress

TEST 19 (1 of 3)

91

Vertical Shear Stress
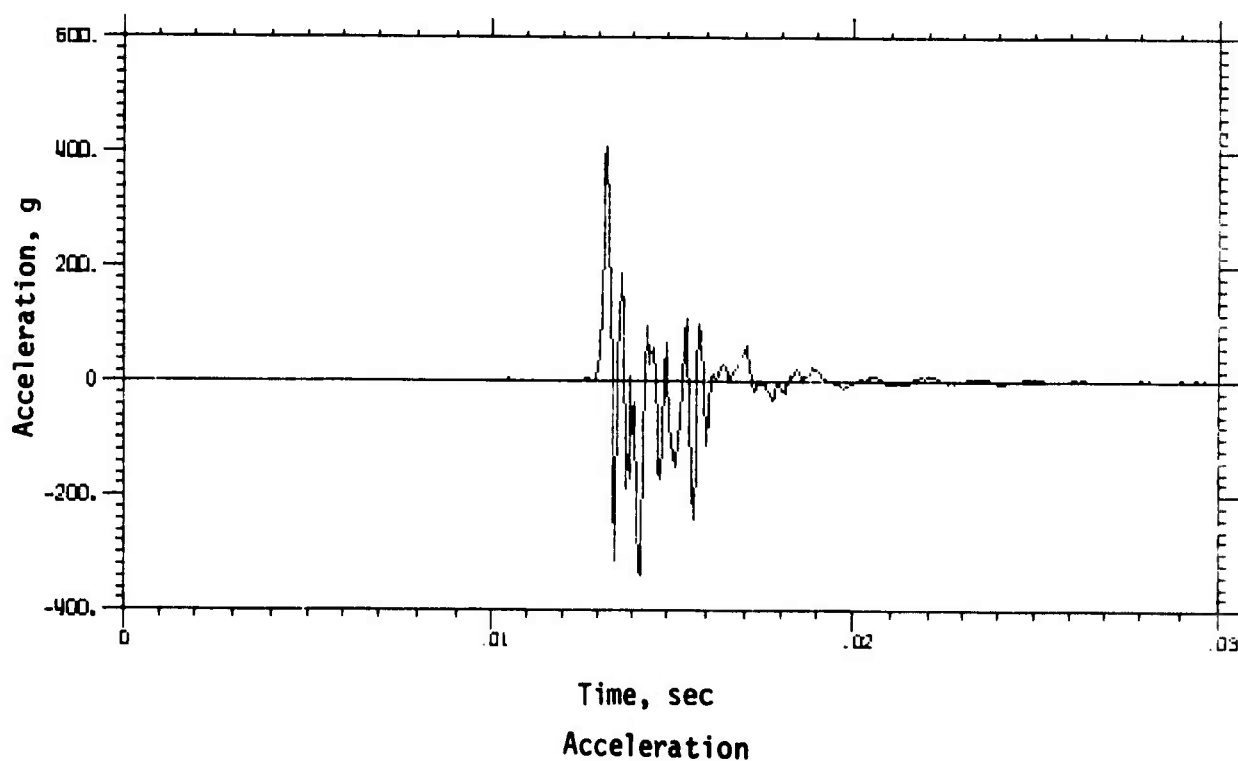

Inferred Vertical Shear Stress

TEST 19 (2 of 3)

92

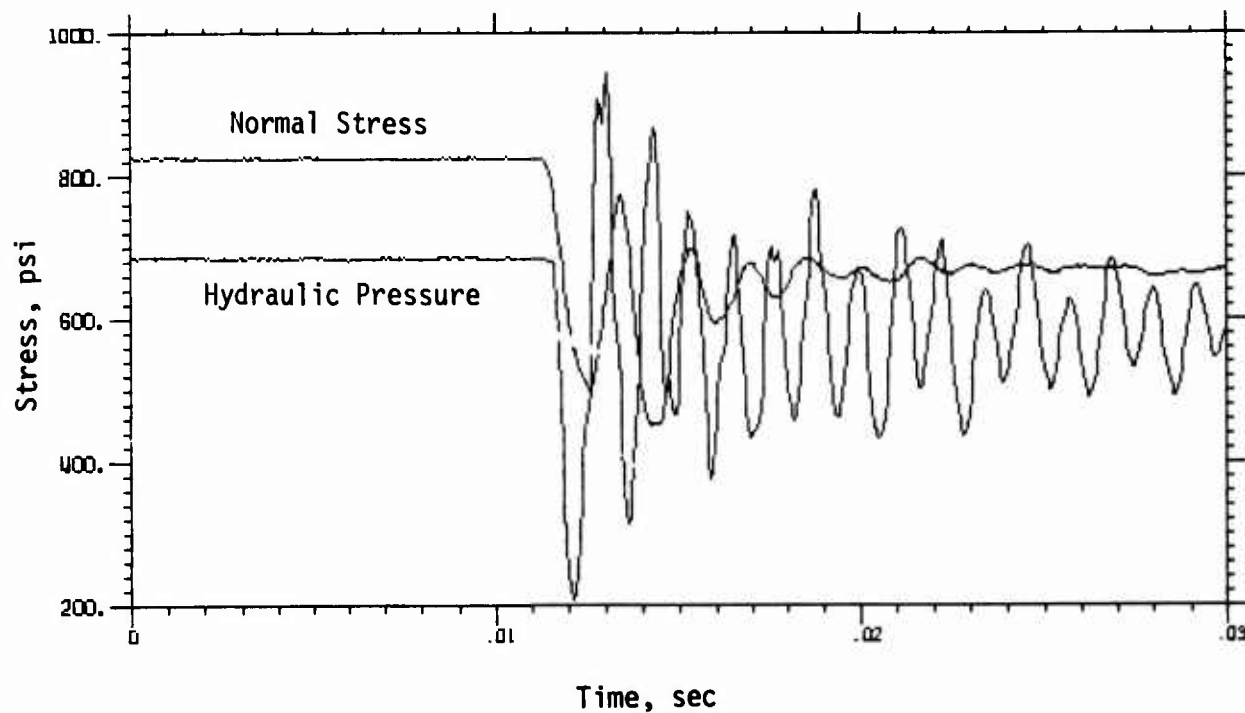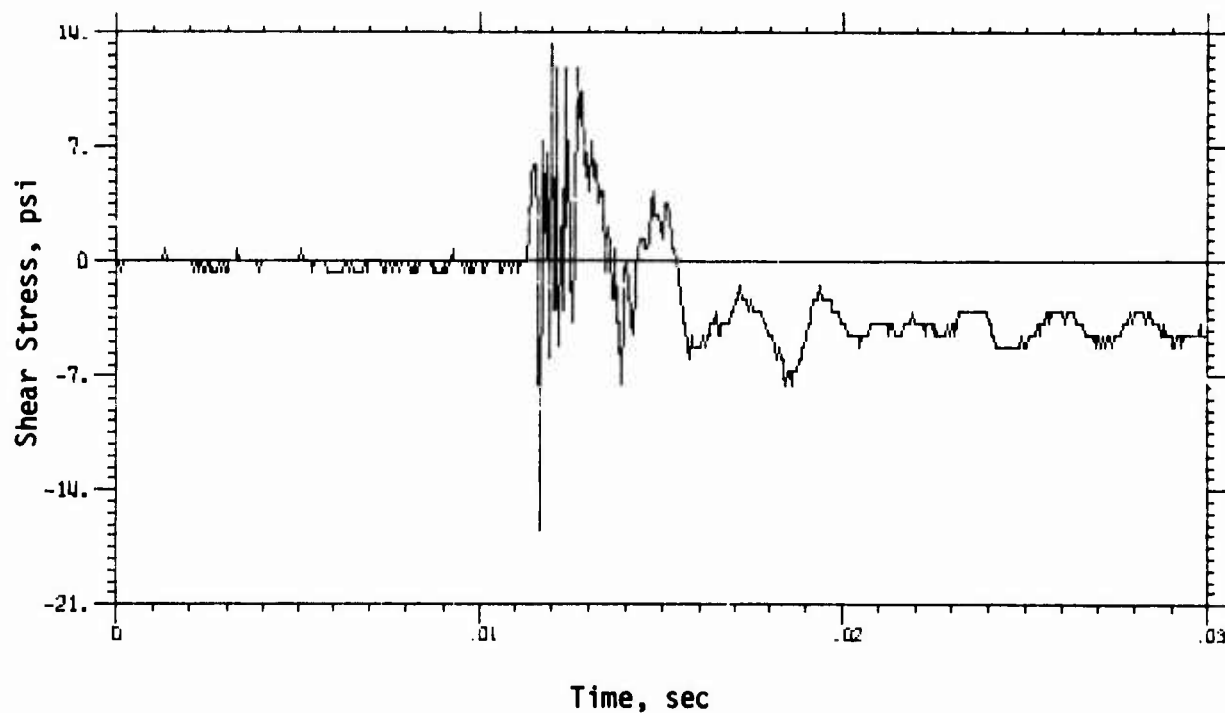Vertical Shear Stresses (Comparison)

Acceleration

TEST 19 (3 of 3)

93

THIS REPORT HAS BEEN DELIMITED
AND CLEARED FOR PUBLIC RELEASE
UNDER DOD DIRECTIVE 5200.20 AND
NO RESTRICTIONS ARE IMPOSED UPON
ITS USE AND DISCLOSURE.

DISTRIBUTION STATEMENT A
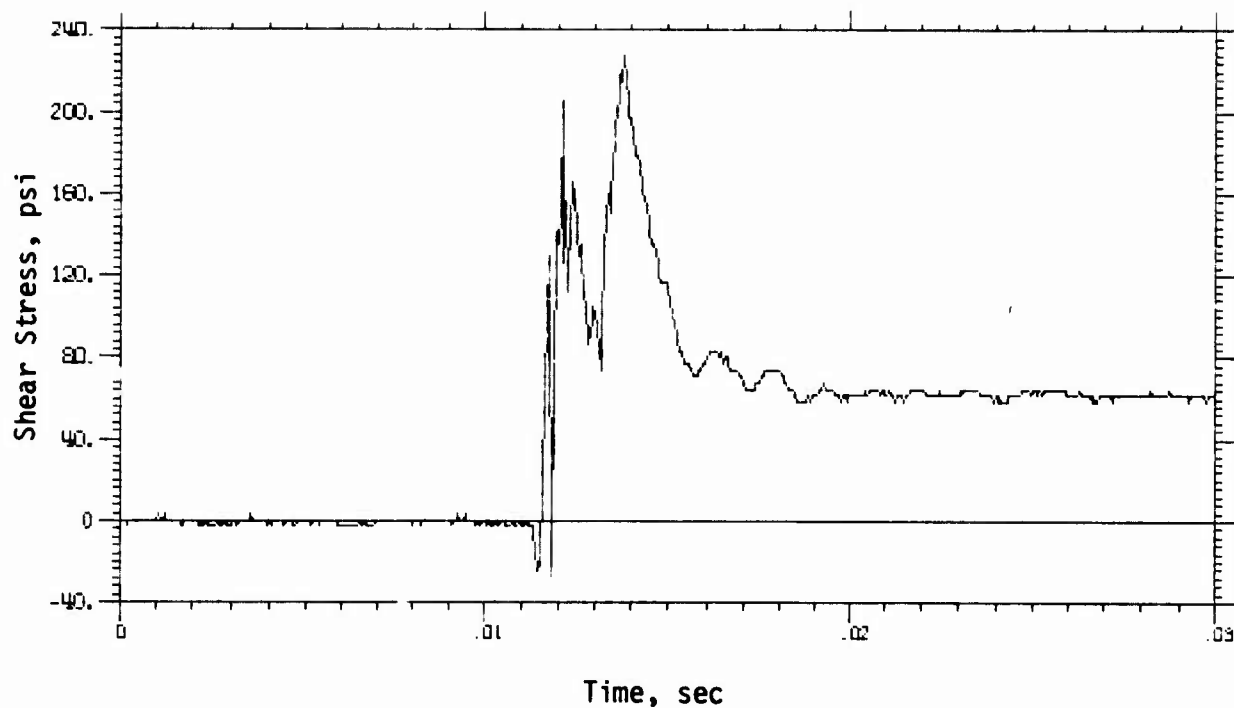
APPROVED FOR PUBLIC RELEASE;
DISTRIBUTION UNLIMITED.

Time, sec

Hydraulic Pressure and Normal Stress

Time, sec

Horizontal Shear Stress

TEST 20 (1 of 3)

94

Vertical Shear Stress

Inferred Vertical Shear Stress

TEST 20 (2 of 3)

95

Vertical Shear Stresses (Comparison)

Acceleration

TEST 20 (3 of 3)

96

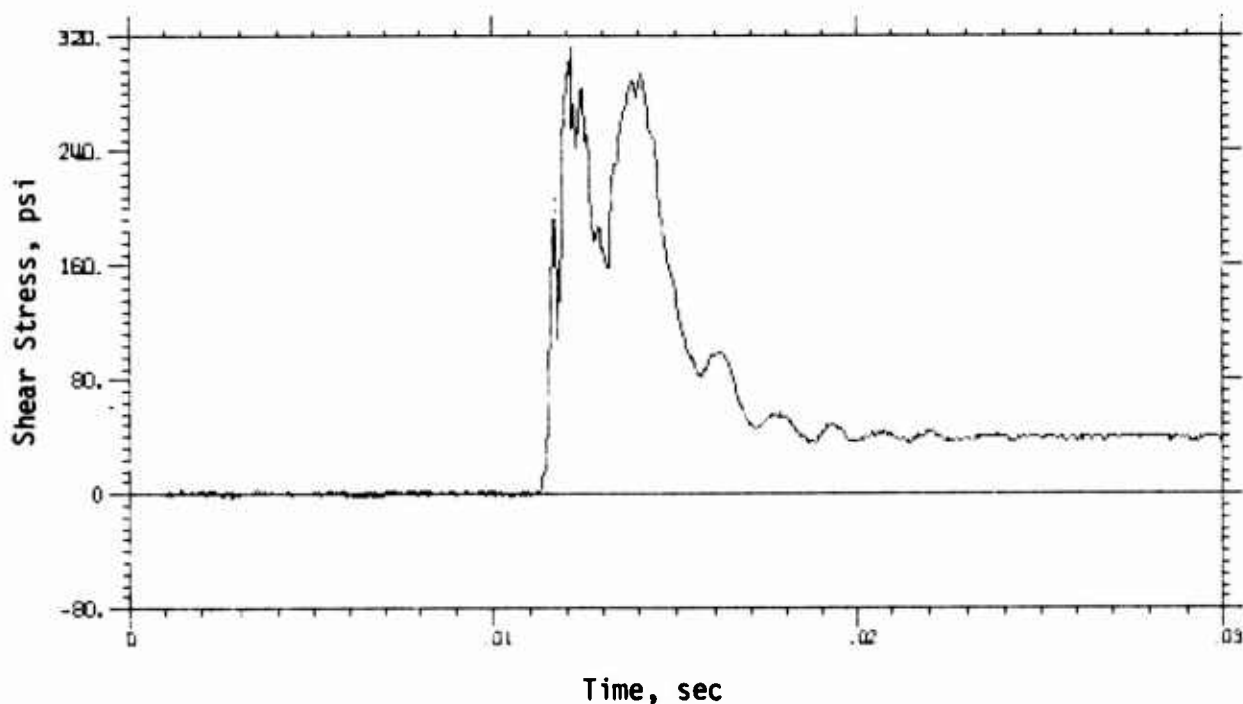Hydraulic Pressure and Normal Stress

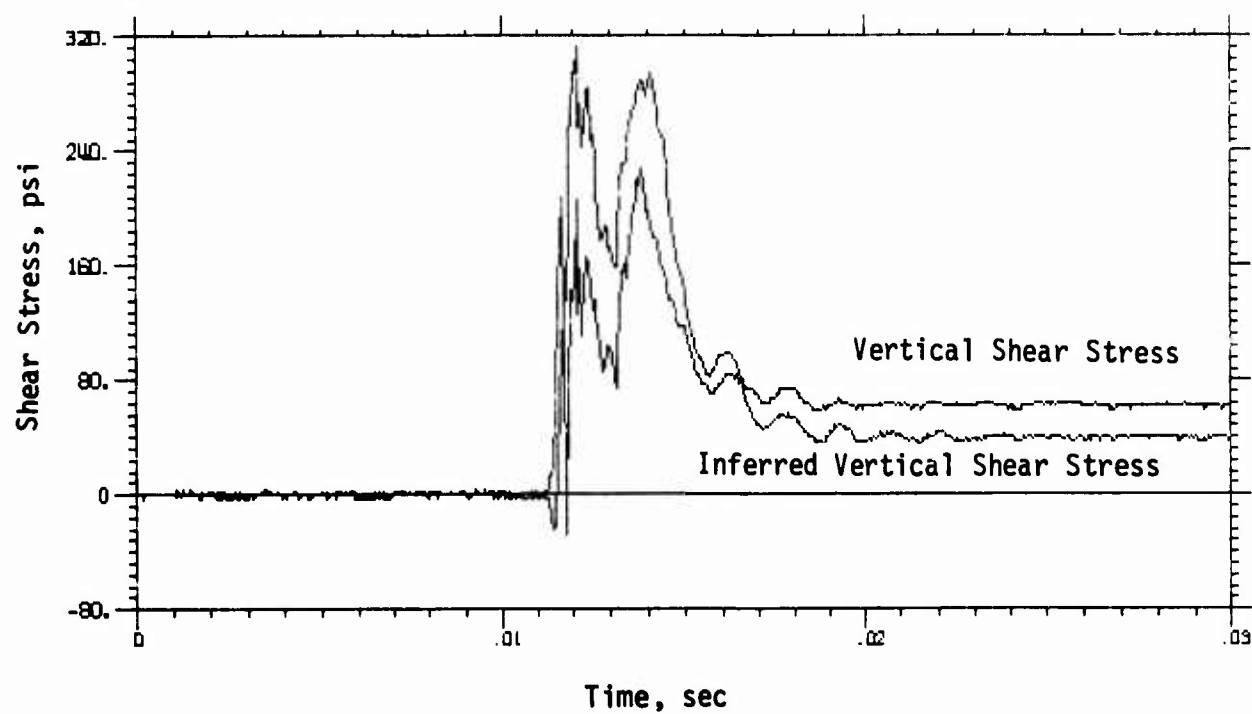
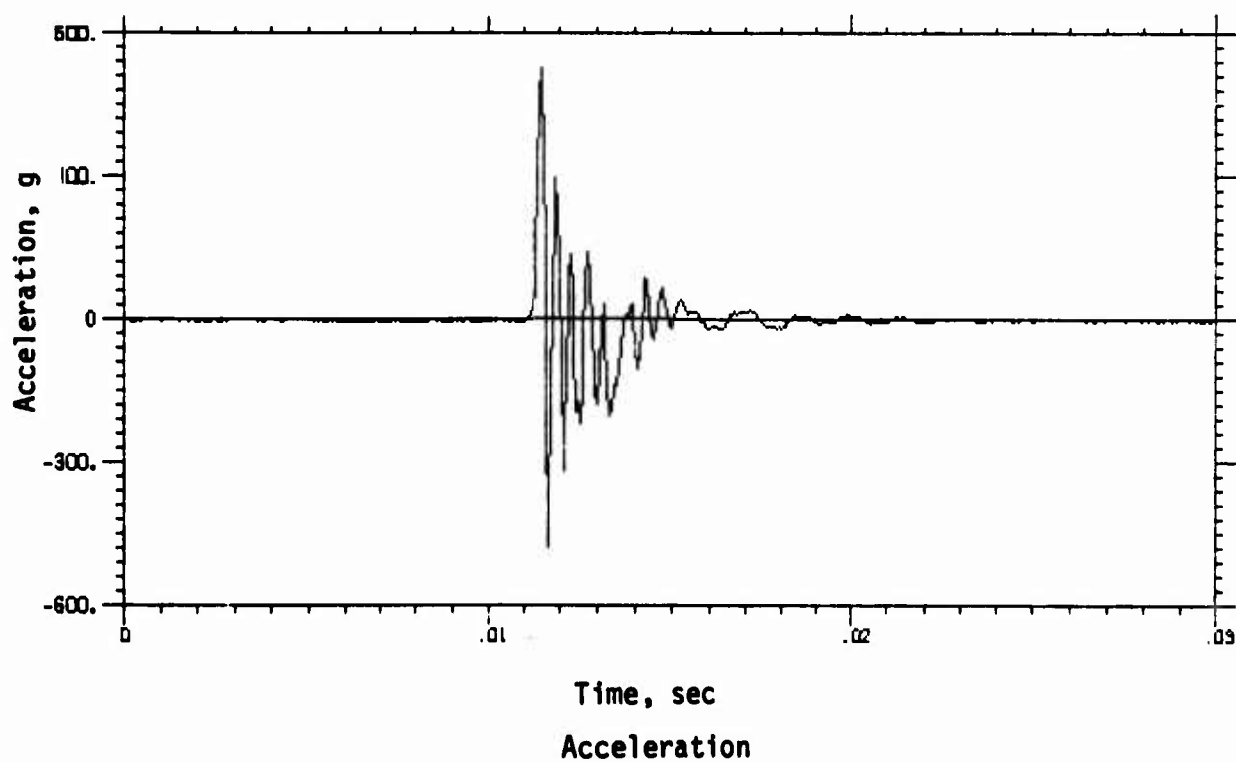Horizontal Shear Stress

TEST 21 (1 of 3)

Vertical Shear Stress
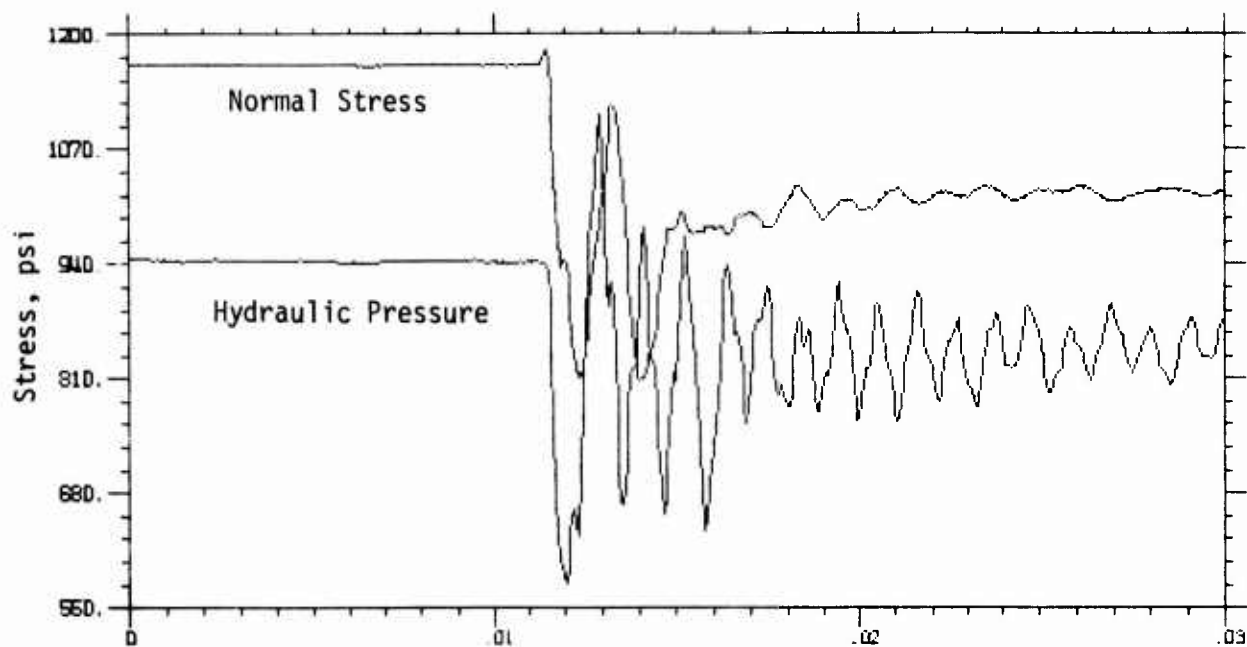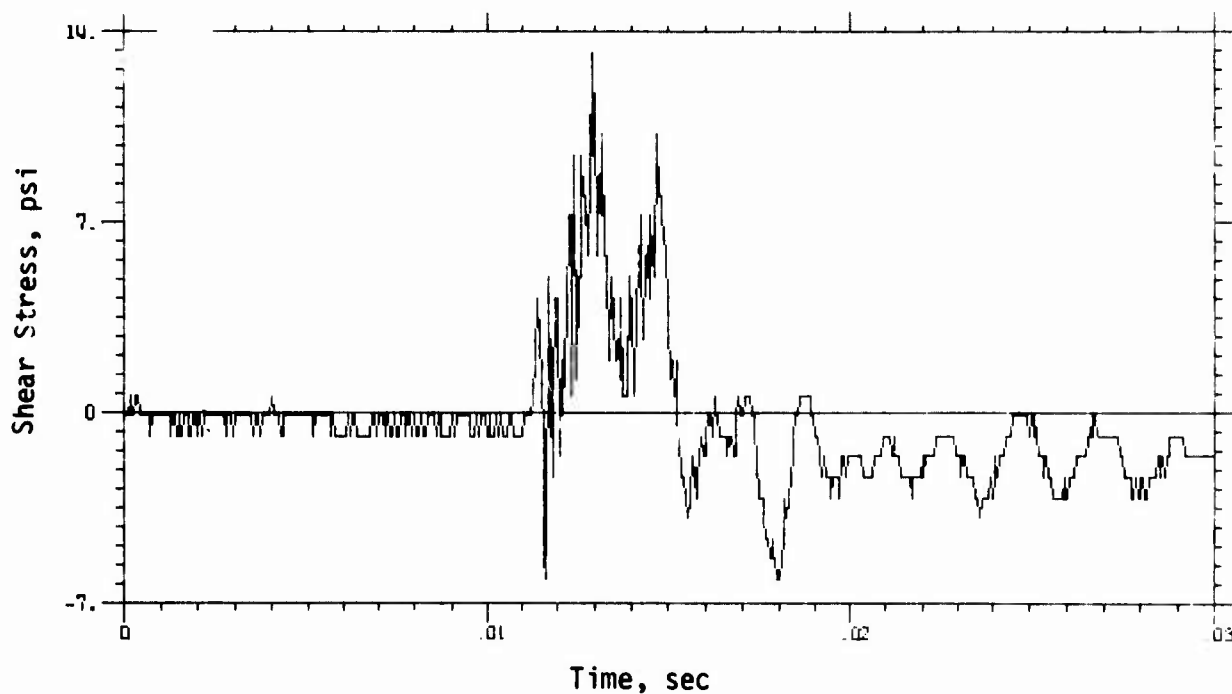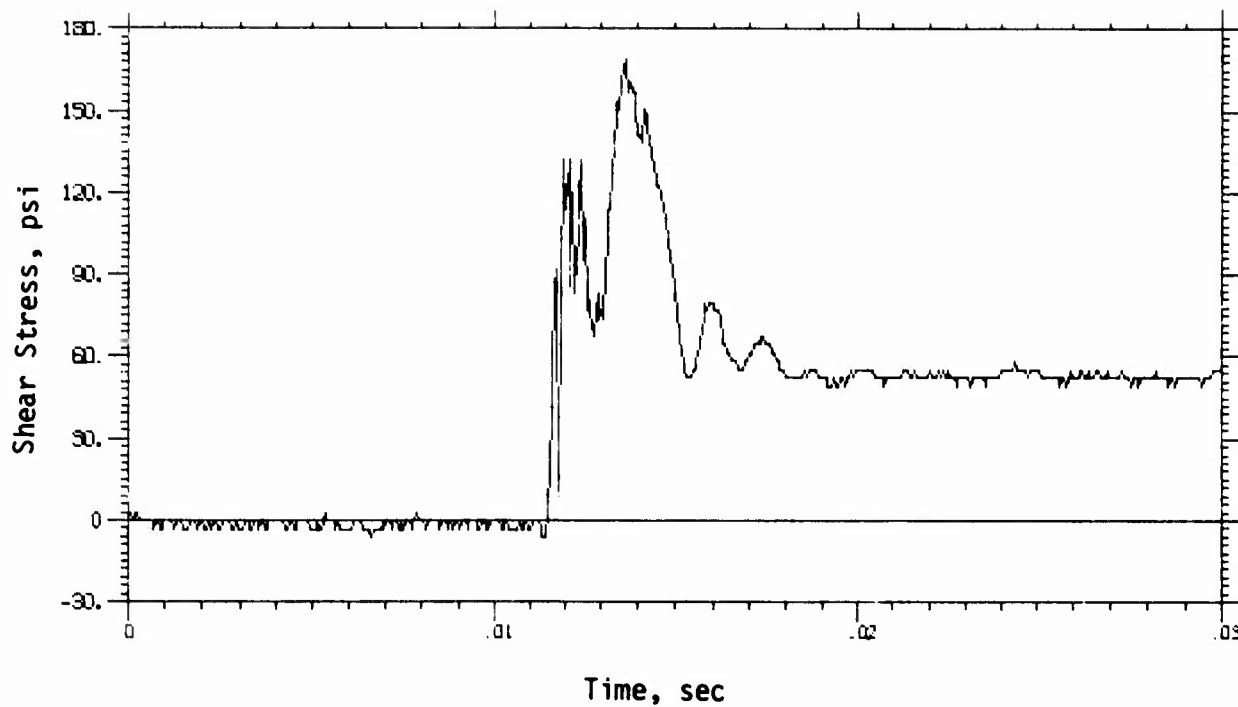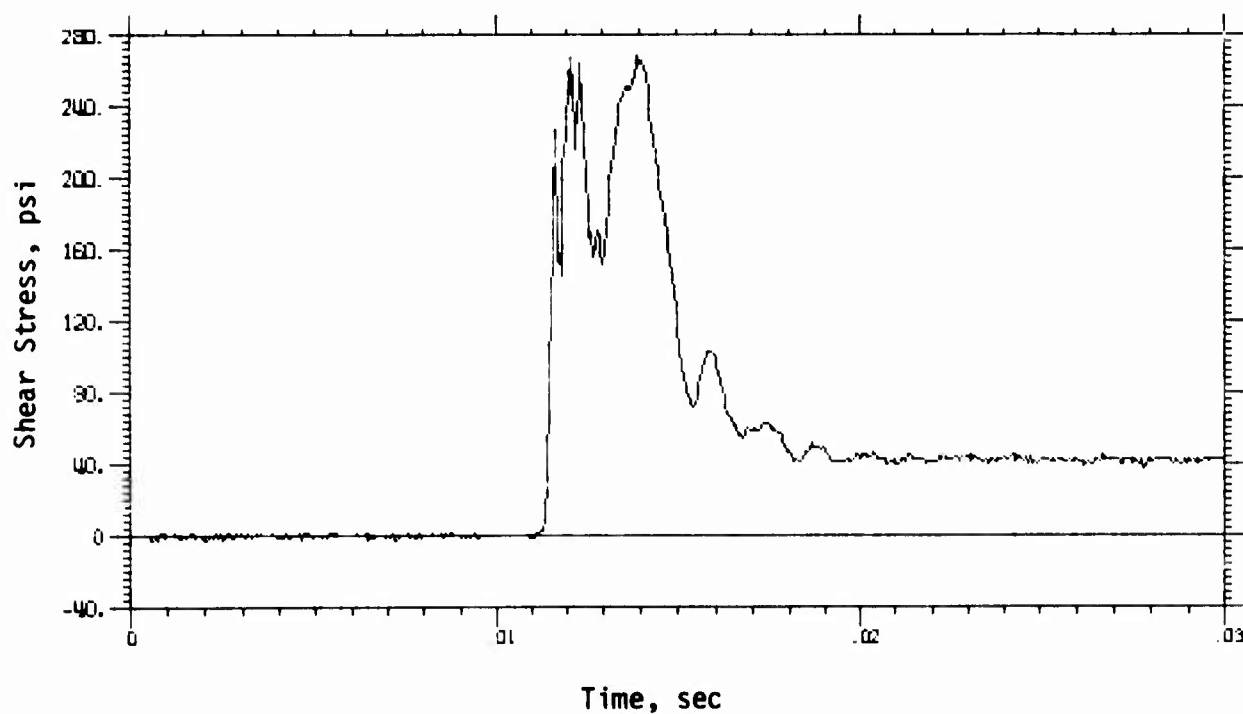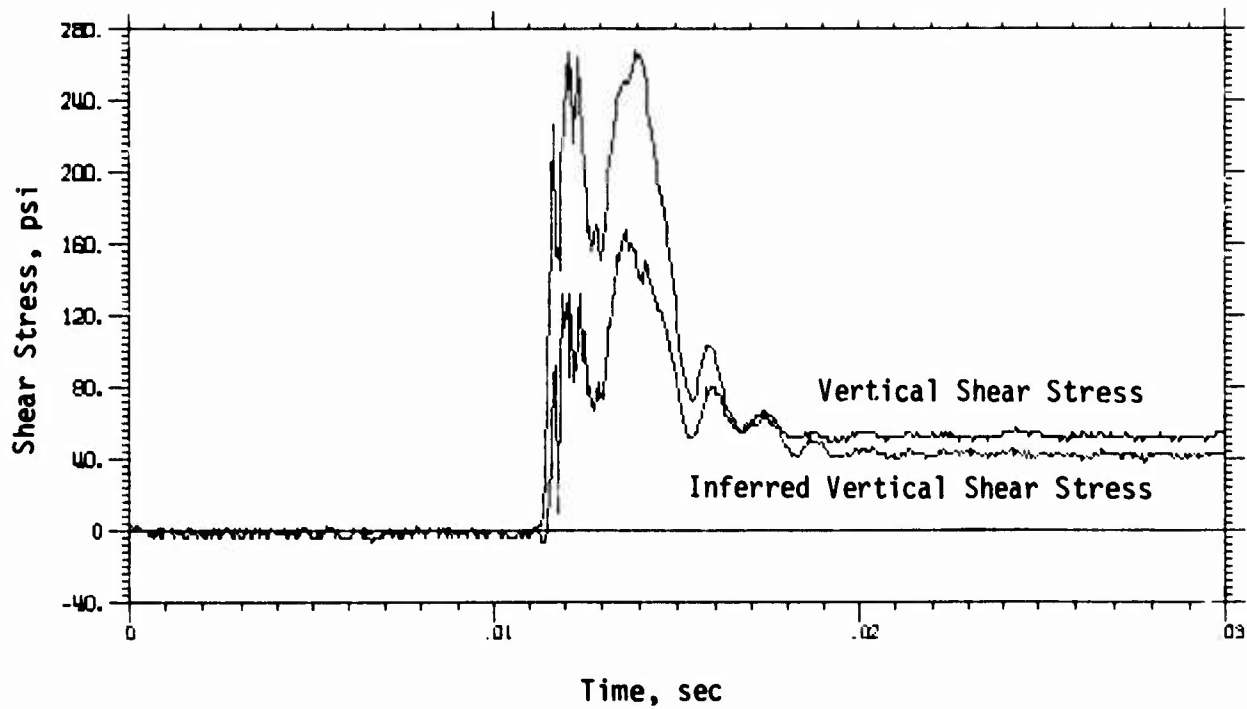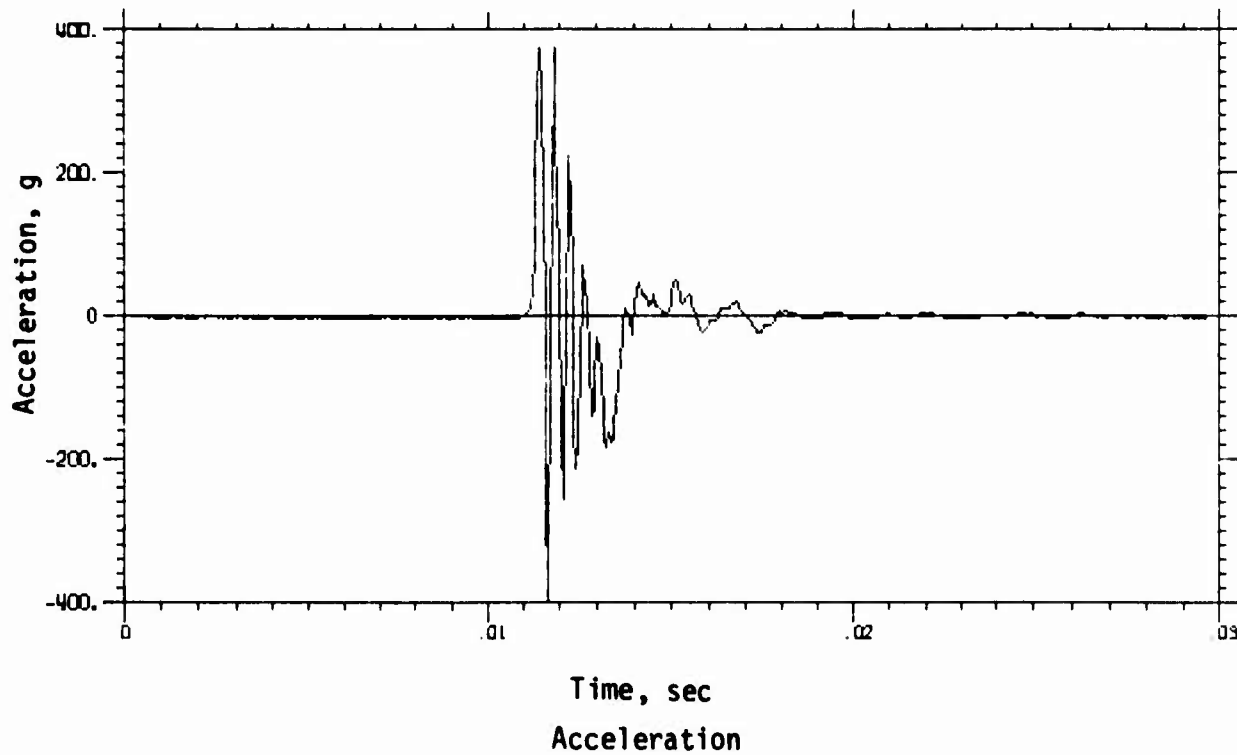

Inferred Vertical Shear Stress

TEST 21 (2 of 3)

Vertical Shear Stresses (Comparison)

Acceleration

TEST 21 (3 of 3)

LIST OF SYMBOLS

A	effective force-collecting area
E	elastic modulus
E_i	bridge input voltage
E_o	bridge output voltage
E_{oh}	horizontal-axis output voltage
E_{on}	normal-axis output voltage
E_{ov}	vertical-axis output voltage
F_L	lower load-cell force
F_s	total shear force on concrete sample
F_u	upper load-cell force
I	moment of inertia
M_x	bending moment
N	negative type semiconductor material
P	positive type semiconductor material
R	resistance
a	acceleration of sample
a, a'	points of location for active beam upper and lower strain gage, respectively
b, b'	points of location for dummy beam upper and lower strain gage, respectively
c	distance from neutral axis to surface of beam at points a and a'
ℓ	total length of beam
m	mass of sample
x	distance from free end of beam to points a and a'
α	vertical-axis output scale factor with vertical shear input only
α'	horizontal-axis output scale factor with vertical shear input only
α''	normal-axis output scale factor with vertical shear input only
β	vertical-axis output scale factor with horizontal shear input only
β'	horizontal-axis output scale factor with horizontal shear input only
β''	normal-axis output scale factor with horizontal shear input only
γ	vertical-axis output scale factor with normal stress input only
γ'	horizontal-axis output scale factor with normal stress input only
γ''	normal-axis output scale factor with normal stress input only
ζ	strain

σ_n	normal stress
σ_s	shear stress
σ_{sh}	horizontal shear stress
σ_{sv}	vertical shear stress

DISTRIBUTION LIST

DEPARTMENT OF DEFENSE

Director
Defense Advanced Research Project Agency
    ATTN: Technical Library
    ATTN: STO
    ATTN: NMRO
    ATTN: PMO

Defense Documentation Center
2 cy ATTN: TC

Director
Defense Nuclear Agency
    ATTN: DDST
2 cy ATTN: SPSS
2 cy ATTN: TITL, Tech. Lib.

Commander
Field Command
Defense Nuclear Agency
    ATTN: FCTMOF
    ATTN: FCPR
    ATTN: FCT

DEPARTMENT OF THE ARMY

Chief of Research, Development & Acquisition
    ATTN: Technical Library

Commander
Harry Diamond Laboratories
    ATTN: DRXDO-NP
    ATTN: DRXDO-TI

Director
U. S. Army Ballistic Research Laboratories
    ATTN: Tech. Lib., Edward Baicy

Director
U.S. Army Engr. Waterways Experiment Station
    ATTN: Leo Ingram
    ATTN: Technical Library
    ATTN: Francis Hanes
    ATTN: J. K. Ingram
    ATTN: J. Balsara

Commander
U.S. Army Materiel Dev. & Readiness Command
    ATTN: Technical Library

DEPARTMENT OF THE NAVY

Chief of Naval Research
    ATTN: Technical Library

Officer-In-Charge
Civil Engineering Laboratory
Naval Construction Battalion Center
    ATTN: Technical Library
    ATTN: W. Shaw
    ATTN: R. J. Odello

Commander
Naval Facilities Engineering Command
    ATTN: Technical Library

DEPARTMENT OF THE NAVY (Continued)

Commander
Naval Surface Weapons Center
    ATTN: Code 730, Tech. Lib.
    ATTN: Code 241, J. Petes
    ATTN: Code 1224, Navy Nuc. Prgms. Off.

DEPARTMENT OF THE AIR FORCE

AF Cambridge Research Labs., AFSC
    ATTN: SUOL, AFCRL Research Library

AF Institute of Technology, AU
    ATTN: Library, AFIT, Bldg. 640, Area B

AF Weapons Laboratory, AFSC
    ATTN: SUL
    ATTN: DES, M. A. Plamondon
    ATTN: DED
    ATTN: DED, J. D. Renick
5 cy ATTN: S. J. Ayala

Hq, USAF/IN
    ATTN: INATA

DEPARTMENT OF ENERGY

Sandia Laboratories
    ATTN: Doc. Control for Tech. Library

Sandia Laboratories
    ATTN: Doc. Control for Luke J. Vortman
    ATTN: Doc. Control for A. J. Chabai
    ATTN: Doc. Control for 3141, Sandia Rpt. Coll.

Department of Energy
Albuquerque Operations Office
    ATTN: Doc. Control for Tech. Library

Department of Energy
Division of Headquarters Services
Library Branch, G-043
    ATTN: Doc. Con. for Class. Tech. Lib.

Department of Energy
Nevada Operations Office
    ATTN: Doc. Con. for Tech. Lib.

University of California
Lawrence Livermore Laboratory
    ATTN: Technical Library

DEPARTMENT OF DEFENSE CONTRACTORS

Agbabian Associates
    ATTN: M. Agbabian

Artec Associates, Inc.
    ATTN: N. Baum

Civil/Nuclear Systems Corp.
    ATTN: Robert Crawford

EG&G, Inc.
Albuquerque Division
    ATTN: Technical Library

DEPARTMENT OF DEFENSE CONTRACTORS (Continued)

Electromechanical Sys. of New Mexico
      ATTN: R. A. Shunk

General Electric Company
TEMPO-Center for Advanced Studies
      ATTN: DASIAC

H-Tech. Laboratories
      ATTN: Bruce Hartenbaum

Merritt CASES, Inc.
      ATTN: J. L. Merritt
      ATTN: Technical Library

Kaman Sciences Corporation
      ATTN: Don Sachs
      ATTN: Library

Nathan M. Newmark
Consulting Engineering Services
      ATTN: Nathan M. Newmark

Physics International Company
      ATTN: Doc. Con. for Coye Vincent
      ATTN: Doc. Con. for Tech. Lib.

DEPARTMENT OF DEFENSE CONTRACTORS (Continued)

R & D Associates
      ATTN: Tech. Lib.
      ATTN: J. G. Lewis

Stanford Research Institute
      ATTN: George R. Abrahamson
      ATTN: Burt R. Gasten
      ATTN: P. De Carli

Systems, Science and Software, Inc.
      ATTN: Tech. Lib.
      ATTN: Donald R. Grine

TRW Systems Group
      ATTN: Tech. Info. Center, S-1930
      ATTN: Paul Lieberman

The Eric H. Wang
Civil Engineering Research Facility
      ATTN: Neal Baum
      ATTN: Steve Pickett